The Pennsylvania State University

The Graduate School

SPATIOTEMPORAL INFECTION PATTERNS AND INTERPATCH MOVEMENT IN *NOTOPHTHALMUS VIRIDESCENS* POPULATIONS

A Thesis in

Ecology

by

Doua Jim Lor

Submitted in Partial Fulfillment

of the Requirements

for the Degree of

Master of Science

May 2022

The thesis of Doua Jim Lor was reviewed by and approved by the following:

David A. W. Miller

Associate Professor of Wildlife Population Ecology

Thesis Advisor

Julian Avery

Assistant Research Professor of Wildlife Ecology and Conservation

David Kennedy

Assistant Professor of Biology

Jason Kaye

Professor of Soil Biogeochemistry

Chair of Ecology Intercollege Graduate Degree Program

ABSTRACT

Infectious diseases have been associated with the decline of wildlife populations and the extinction of species worldwide. Amphibians are an especially vulnerable taxa to multiple threats including infectious diseases. Chytridiomycosis is an amphibian disease caused by the fungal pathogen, *Batrachochytrium dendrobatidis* (*Bd*), that has a wide host-range with varying impacts on its hosts. Individuals and environmental conditions can vary in time and space. When these dynamics factors interact, they can affect disease risk and result in heterogeneity with disease impact and transmission. This variation occurs at and has consequences for individuals, populations, and species. To improve our understanding of disease dynamics, we examined how host and environmental factors can affect population-level infection patterns and explored how such dynamics can interact with host movement patterns. We investigated how patterns in *Bd* infections changed spatiotemporally in populations of the adult eastern red-spotted newt, *Notophthalmus viridescens*, from 2018 to 2021. Using extensive capture-mark-recapture data, we investigated how infection levels (infection prevalence and infection intensity) fluctuated in response to temporal and spatial covariates (i.e., temperature, host density, and hydroperiod) and individual characteristics (i.e., sex and size) in central Pennsylvania, and compared the observed temporal patterns to two other newt populations in Wisconsin and Massachusetts (Chapter 1). Additionally, we examined the connectivity of the Pennsylvanian ponds through adult newt interpatch movements and determined how infection state and movement related to one another (Chapter 2).

Our results show that infection levels in adult newt populations vary spatiotemporally and such patterns in infection dynamics can interact with and affect the movements of newts between the ponds. Quadratic relationships between environmental temperature and infection levels were present in all of our study areas and show peak infection levels occurring in early-summer when other species are metamorphosing. This pattern in newt infection dynamics could have larger impacts for more vulnerable species as they expend energy to metamorphose and affect their response to *Bd* infection. Additionally, larger individuals were more likely to have lower *Bd* infection intensities compared to smaller individuals, and this result could indicate potential age or size specific immunity or resistance to disease. From our movement and infection analyses,

we found that 10% of a pond's adult newt population made interpatch movements. Even though we observed a trend where infected newts were less likely to move between ponds in a breeding season compared to healthy conspecifics, this connectivity between the ponds suggest that there is potential for disease transmission between different habitats. Still, regardless of starting infection state, newts that moved to a different pond within a breeding season were more likely to have lower infection levels. Our study is one of the first to intensively sample adult *N. viridescens* populations for spatiotemporal patterns of *Bd* infections and to investigate the relationship between interpatch movements and *Bd* infection. We demonstrate that *Bd* infections are common, persistent, and cyclical in newt populations and that newts have the potential to be a reservoir species that spread *Bd* through interpatch movements between aquatic habitats.

TABLE OF CONTENTS

List of Tables

Chapter 1. Spatiotemporal dynamics of *Batrachochytrium dendrobatidis* infection levels in Eastern red-spotted newt populations

Chapter 2. Connectivity of ponds through movement of a host species and its implications for disease spread

List of Figures

Chapter 1. Spatiotemporal dynamics of *Batrachochytrium dendrobatidis* infection levels in Eastern red-spotted newt populations

Chapter 2. Connectivity of Ponds through Movement of a Host Species and its Implications for Disease Spread

ACKNOWLEDGEMENTS

I would like to express my sincerest gratitude to my advisor and mentor, Dr. Dave Miller, for his supervision and support of my Master's study and research, for his enthusiasm and drive for big data and small newts, and for his patience in fostering the scientist in me. His guidance helped me in all parts of my thesis, from data collection to writing up the last bit of the manuscript. Thank you for seeing the potential in me and encouraging me along the way.

Besides my advisor, I would also like to thank my committee: Dr. Julian Avery and Dr. David Kennedy, for their patience and wealth of knowledge that helped improve this thesis.

I am also thankful for the collaborators of this research project: Dr. Evan Grant, Jill Fleming, and Dr. Dan Grear for their assistance with data collection, analysis, and processing the thousands of swab samples.

In addition, I would like to thank the Applied Population Ecology lab for helping me with data collection, proofreading my chapter drafts, and providing valuable feedback on my presentations.

My research would have been much more difficult without the help of my field crews. Thank you, Katie Reese, Hunter Kauffman, Rysa Thomas, and Destini Acosta, for spending your spring and summer days out in the field and dipping for newts with me.

To my family, I am thankful to have your unconditional support. You all believed in me and always welcomed me with open arms when I needed "home" the most.

To my friends, I am deeply grateful for all the ways you all have supported me on this journey: Carli Dinsmore, you were my senior graduate student mentor and helped me find my sense of belonging amongst all the talented and intelligent people in graduate school; Devyn McPheeters, we shared many writing Tuesdays that helped shape this thesis and I appreciate your unwavering emotional support; Taryn Garew, although you were far, you always believed in me and provided the voice of reasoning in times of need; and Maisie MacKnight, for our café work sessions, for all the time you reviewed my writing and bounced ideas with me, and for the unconditional support you offered selflessly...you are the better half of Jimaising. Lastly, I would like to sincerely thank Rodrigo Cruz for supporting my decisions despite the hardships it brought, for reminding me that self-growth is important, and for teaching me to appreciate the time we have with each other. Without these people, my time in graduate school and my thesis would have been much diminished.

This work was funded by the USGS PA Cooperative Wildlife Fish and Wildlife Research Unit Work Order 93. The findings and conclusions of this research do not necessarily reflect the views of this funding agency. Any use of trade, product or firm names in this publication is for descriptive purposes only and does not imply endorsement by the U.S. government.

Chapter 1: Spatiotemporal dynamics of *Batrachochytrium dendrobatidis* infection levels in Eastern red-spotted newt populations

Abstract

Batrachochytrium dendrobatidis (*Bd*) is a fungal pathogen responsible for declines in amphibian populations worldwide. Although previous studies have shown that there is seasonality in overall infection patterns, few have extensively tracked *Bd* infection in the same populations throughout time and space. Lab studies show that growth of *Bd* is highly sensitive to temperature and may explain seasonal fluctuations in temperate ecosystems, which see large fluctuations in temperature across the annual cycle. We present results of *Bd* infection dynamics across multiple years for three widely dispersed population of the Eastern red-spotted newt (*Notophthalmus viridescens*). The species is locally common, geographically widespread, and present for long durations in aquatic habitats – making it a potentially key species in maintenance and transmission of *Bd* in amphibian communities where it occurs. We used capture-mark-recapture sampling methods and swabbed individual newts across three years to determine how infection levels (prevalence and intensity) relate to temperature, among-pond covariates, and individual characteristics. We then compared the patterns between three study areas across the newt's longitudinal range. We found a quadratic relationship between infection levels and temperature, a negative relationship between infection levels and newt size, and a positive relationship between infection prevalence and host density. Our results suggest newts are reservoirs of *Bd* because they tend to be infected with low intensity but persistent infections across their range, and their long duration in these aquatic habitats have implications for multiple host species across different life stages. If newts are important in *Bd* transmission and persistence, it is important to understand the spatiotemporal dynamics of infection within our study system. Our results demonstrate that seasonal dynamics are correlated with changes in environmental temperature and peak potential for transmission occurs in early-summer when other vernal pool amphibians are metamorphosing and leaving ponds.

Keywords: Seasonality, *Batrachochytrium dendrobatidis*, temperature, host density, infection intensity, infection prevalence

INTRODUCTION

Emerging infectious diseases are a threat to the conservation of many species and have resulted in population declines and biodiversity loss (Daszak *et al.*, 2000; Lips *et al.*, 2006; Vredenburg *et al.*, 2010). Wildlife diseases such as White nose syndrome in bats (Blehert *et al.*, 2009), West Nile virus in birds (McLean *et al.*, 2001), and chytridiomycosis in amphibians (Berger *et al.*, 1998) have been responsible for mass mortality events, leading to population declines across multiple species locally and globally. Chytridiomycosis, a skin disease caused by the fungal pathogen *Batrachochytrium dendrobatidis* (hereafter, *Bd*), has been recognized as the "biggest threat to vertebrate biodiversity" (Skerratt *et al.*, 2007). Since its discovery in the late 1990s, *Bd* has been responsible for the decline of over 500 species and the extinction of at least 90 species (Ben C Scheele *et al.*, 2019). By disrupting food webs and extirpating amphibian that may have previously filled niches, *Bd* also has indirect impacts on non-amphibian species (Whiles *et al.*, 2006; Zipkin *et al.*, 2020). While the overall impacts of chytridiomycosis on biodiversity are apparent, heterogeneity in disease impacts among *Bd*'s broad host species range are still unclear. Different host species have varying responses to different *Bd* strains and can range from asymptomatic infected individuals to infected individuals with clinical symptoms and infected individuals that can either recover or result in mortality (Retallick and Miera, 2007; Gahl *et al.*, 2011; Voyles *et al.*, 2011; Van Rooij *et al.*, 2015). Because of the potential to decimate local populations and alter community composition, understanding drivers of heterogeneity in different species is crucial for predicting and controlling disease outbreaks. Heterogeneity in disease impacts can be addressed using an ecological framework, known as the disease triangle, that describes interactions between pathogen, host, and environmental factors (Scholthof, 2007).

Bd is a fungal pathogen that is dependent on temperature and water for growth and transmission. There are two distinct life stages: the motile zoospore that can infect susceptible individuals in the aquatic environment and the sessile, reproductive sporangium that infects keratinized skin tissue on hosts (Berger *et al.*, 2005). Because of the differences in the amount and location of keratinized cells and the resource-intensive costs of metamorphosis, *Bd* can have varying effects on the different life stages of amphibians (Berger *et al.*, 1998; Garner *et al.*,

2009). In cultures, *Bd* has a growth range between 4 and 27 °C with an optimal temperature range between 17 and 23 °C, while dying at temperatures above 30 °C (Piotrowski *et al.*, 2004). This pattern is also consistent with field studies where *Bd* infection levels are greater in cooler temperatures and higher elevations (Longcore *et al.*, 1999; Berger *et al.*, 2005; Sapsford *et al.*, 2013). In addition to temperature, *Bd* requires water to survive and spread to potential hosts (Piotrowski *et al.*, 2004; Berger *et al.*, 2005). Previous studies have shown that *Bd* has associations with water availability and may survive in ponds from seven weeks to several years without a host (Johnson and Speare, 2003; Mosher *et al.*, 2018; Ruggeri *et al.*, 2018). Furthermore, *Bd* zoospores in the aquatic environment can be predated on by species of *Daphnia* (Searle *et al.*, 2013). Because of *Bd*'s broad host-range, it is important to consider how host species may contribute to the persistence and transmission of *Bd* across the landscape and within populations.

Eastern red-spotted newts (*Notophthalmus viridescens*; hereafter, "newts") are an important species to consider in *Bd*-host interactions. Newts are a widespread, common species and found in habitats that range from ephemeral pools to more permanent bodies of water across the eastern United States (Gates and Thompson, 1982; Gabor and Nice, 2004). Newts are one of the few species that are present in these aquatic environments for the full duration of water inundation during which multiple other amphibian species come and go according to the timing of their breeding seasons. During this period, newts are important keystone predators of amphibian larvae via differential predation (Morin, 1981). Furthermore, newts are known to be susceptible to *Bd* infections, have high infection rates, and other studies suggest that direct mortality may be uncommon (Rothermel *et al.*, 2008, 2016; Groner and Relyea, 2010; Raffel *et al.*, 2010). For these reasons, newts are likely to be disproportionately important in determining among species transmission within ponds and understanding seasonal and spatial infection dynamics for this species will provide insights into when and which species are most susceptible to community transmission. In addition, individual characteristics such as age, size, and sex can affect susceptibility and resistance to disease (Casadevall and Pirofski, 2018).

Newts and other amphibian species can potentially deal with infections through physiological or behavioral mechanisms that may directly reduce *Bd* growth or indirectly reduce damage from *Bd* (VanderWaal and Ezenwa, 2016). Because newts are ectotherms, their immune

system is dependent on ambient temperatures and can affect immune function indirectly through thermal stress response or directly affecting immune cell activity (Terrell *et al.*, 2013). In addition, amphibians are also more susceptible to disease at lower temperatures (Maniero and Carey 1997, Raffel et al., 2006, Carey et al., 1999). *In vitro* studies can provide optimal growth conditions for *Bd*, but field conditions may be less ideal for *Bd* growth. Additionally, host behavior and physiology can add to the complexity of field conditions and we cannot expect lab optima to match observed peaks in the field. Among population differences in environmental conditions can alter host-pathogen relationships and seasonal changes in such conditions can result in cyclical outbreaks of disease (Altizer *et al.*, 2006; Grassly and Fraser, 2006). As temperature changes across a season, *Bd* abundance and growth may increase or decrease at different times. This variation in *Bd* abundance and growth combined with newts' temperature-dependent immune function can result in a dynamic relationship between pathogen and host. Understanding how disease varies in a population seasonally can give insight into when disease outbreaks are likely to happen, how control measures can be implanted, and how climate change and other factors could potentially alter such patterns.

The interaction between host and pathogen often occur in specific locations and spatial context is crucial in determining how infectious diseases are distributed across the landscape (Real and Biek, 2007). Heterogeneous landscapes can result in differences in environmental conditions that can affect host-pathogen interactions. Because *Bd* growth and survival is limited by moisture and temperature, we considered hydroperiod (the duration in which a location holds water) of ponds. Hydroperiod is also important in determining the community composition of a pond due to the time it takes for species to develop and undergo metamorphosis before ponds dry (Semlitsch, 2000; Snodgrass *et al.*, 2000). Furthermore, hydroperiod along with other factors such as size and shape can determine habitat quality and, consequently, host densities. Newts and other species respond to seasonal environmental conditions by having annual breeding migrations to breeding grounds (Hurlbert, 1963; Tøttrup *et al.*, 2008; Bailey and Muths, 2019). The mass congregation by both conspecifics and individuals of other species increase contact rates between infected and susceptible individuals with higher quality ponds having higher host densities (Denoël and Lehmann, 2006; Altizer *et al.*, 2011; Daversa *et al.*, 2017; Daversa, Monsalve-Carcaño, *et al.*, 2018). Knowing how infection patterns vary temporally and spatially

is important when considering how disease spreads and persists in populations and across the landscape.

Given the complexity of the interactions between pathogen, host, and environmental conditions and the widespread presence of newts, newts are an ideal system for understanding temporal and spatial variation in *Bd* infection patterns. In this study, we quantify within and among year variation in infection prevalence (proportion of positive individuals to total individuals) and infection intensity (severity of infection in a positive individual) of newts to better understand factors correlated with seasonal outbreaks of *Bd* in this key reservoir species. We measured *Bd* presence and load for more than 7,000 newt captures over a three-year period in three study areas in the northeastern United States to determine how infection prevalence and intensity change across seasons and years within newt populations. Our primary goals were to determine 1) how seasonal changes in infection levels (infection prevalence and intensity) relate to environmental temperature experienced by newts, 2) whether spatial differences in infection levels relate to hydroperiod and host density, 3) which individual traits relate to within-population variation in infection levels, and 4) whether these relationships are consistent across the three study areas that differ in average temperature and hydrological characteristics of ponds. We predicted that *Bd* infection prevalence and intensity in newt populations will increase as temperature reaches optimal growth temperature range and decrease above optimal growth temperature range. Additionally, we predicted that habitats with longer hydroperiods and higher host densities will have higher infection levels by prolonging growing conditions for *Bd* and increasing contact rate between infected and susceptible individuals, respectively. We also predicted that females would have higher infection levels via increased contact rate due to copulation with multiple males and that larger-older individuals would have lower infection levels. Finally, we predicted that the environmental and individual characteristics associated with infection levels would be consistent across different study areas.

METHODS

Study Areas

We collected data in three study areas across the northern ranges of our study species. The first study area in central Pennsylvania was compromised of a network of eleven ponds varying in size, hydrology, and amphibian community. Our PA study area consisted of three clusters of ponds with the shortest distance between ponds being forty meters and longest distance 582 meters. Maximum area at peak inundation of PA ponds ranged from 125 m^2 to 1869 m^2. Of the eleven ponds, seven are ephemeral ponds that completely dry in mid-to-late summer in every year while four are semi-permanent, drying in some years and not in others. Although our study species used all eleven ponds, the abundances of newts vary from pond to pond and changed throughout the season with newts becoming active in ponds soon after ice melted each spring and numbers declining as ponds began to approach drying out. Other amphibian species that occur in the ponds include *Ambystoma jeffersonianum*, *Ambystoma maculatum*, *Hyla chrysoscelis*, *Lithobathes clamitans*, *Lithobates sylvatica*, and *Pseudacris crucifer*. The second study area in Massachusetts included one semi-permanent beaver pond and two ephemeral pools. The third study area in Wisconsin consisted of two permanent ponds. Our most intensive data collection occurred in the PA study area, and for that reason we focus first on analysis of the PA data. We then ask whether patterns we observe in this study area are consistent with those observed in the two other areas, which are located in very disparate parts of the species' range. This general approach allowed us to test whether our results were repeatable and therefore likely to be representative across the species' range.

Data Collection

We repeatedly sampled each pond multiple times across a season from 2018 to 2020, with some minor differences in sampling protocols among our study areas. Adult newts become active in ponds soon after spring thaw, and are present in our study areas until ponds dry. In PA, we began sampling as soon as ponds cleared of ice and snow in March and continued until mid to late summer when most of the ponds are completely dry in August and newts were rare in

samples from ponds that still contained water. Alternatively, in WI and MA, we sampled for shorter time frames within a season. We attempted to visit ponds weekly and continued to do so if they were still inundated. To look at infection and how infection patterns change within a season, newts were intensively sampled for *Bd* during three to five separate week-long sessions each season (once per month). Some additional intermittent sampling occurred in between the intensive sessions in the PA study area to improve temporal and spatial coverage. Starting and ending dates for each study area varied according to weather, pond type, and availability. With the PA study area, three ponds were sampled for a total of thirteen days in 2018 and all eleven were sampled in 2019 for forty-nine days and 2020 for fifty-six days. WI ponds were sampled twenty-four days in 2018, twenty-three days in 2019, and twenty-three days in 2020 while MA ponds were sampled seventeen days in 2019 and twenty-four days in 2020.

We captured and processed newts individually to avoid cross-contamination. Newts were captured by dragging a dipnet along the edges of a pond and once captured were held individually in a plastic bag. We used ultraviolet flashlights while newts were in the plastic bags to identify unique individuals through Visual Implant Elastomer (VIE) marks. When identified as a recaptured individual, another researcher confirmed VIE marks to reduce identification error. Once identified as a recaptured or new individual, unique newts were then swabbed once using a sterile, rayon-tipped dry swab (MW-113). We used new gloves for each animal and swabbed newts five times each at the inner thigh region, inner arm region, alongside the stomach, under the chin, alongside the back, and on both sides of the tail for a total of thirty-five times. Unique newts caught a second time in the same week were not resampled but if the same animal was caught multiple times within a year on separate weeks, we collected samples during each encounter.

In addition to sampling newts for *Bd*, we also measured length, determined their sex, and gave newly caught individuals a unique mark. We measured both snout-vent-length (SVL; mm) and total length (TL; mm) for newts. Males were determined by assessing physical characteristics such as darker and swollen cloaca, larger tail fin and hindlegs, and nuptial pads on the hind legs that occur earlier in the breeding season (Figure 1.1). We also observed a coloration pattern where females had a lighter stripe that ran alongside the tail as a secondary method to confirm female individuals (Figure 1.2). Upon initial capture, newly caught newts were marked

with VIE, which have been shown to not affect individual survival or movements (Northwest Marine Technology, Shaw Island, Washington USA; Sapsford *et al.*, 2014). Each unique individual was given a unique six-color combination consisting of four colors (blue, orange, red, and yellow) immediately behind the front legs, immediately in front of the back legs, and immediately behind the back legs at the base of the tail. The colors used for the two tail marks were kept unique to a pond to clearly identify the pond an individual was first caught in as well as minimize the likelihood of misidentifying a movement among ponds. Animals were released at approximately the same capture location.

Bd Sampling

We used quantitative polymerase chain reaction (qPCR) to quantify *Bd* zoospores in our swab samples and determined individual infection status (positive if zoospore copies per swab were estimated to be > 0 or negative if estimated zoospore copies per swab = 0) and intensity (estimated *Bd* zoospore copies per swab given an individual was positive) (Boyle *et al.*, 2004; Hyatt *et al.*, 2007; Rebollar *et al.*, 2017). We extracted DNA from swabs as described by Hyatt et al. (2007) except that 125 µl of PrepMan® Ultra Sample Preparation Reagent (Applied Biosystems, Foster City, CA) and 100 mg of zirconium/silica beads (Biospec Products, Bartlesville, OK) were used so that the entire swab was immersed during the procedure and the bead-beating steps were conducted using a FastPrep®-24 homogenizer (MP Biomedicals, Santa Ana, CA). We ran reactions on the 7500 fast real-time PCR system (Applied Biosystems, Foster City, CA) using QuantiFast Probe RT-PCR mastermix kit with ROX dye (Qiagen, Valencia, CA) and BSA as per the kit instructions. We used five microliters of the PrepMan® solution containing the extracted DNA as template for the PCR. We included a negative extraction control and a standard curve run in duplicate on each PCR plate. The standard curve consisted of five different concentrations of the target sequence for *Bd* included from commercially synthesized single gene block (gBlock, Integrated DNA Technologies, Coralville, IA). The concentrations of the standards occurred at ten-fold dilutions ranging from 110-1,100,000 copies (0.5 fg – 5000 fg DNA) per reaction. The threshold for signal detection was set at 5% of the maximum fluorescence of the standards run for that assay. We calculated the efficiency of each run using standard curve amplification and repeated PCR plates with an efficiency of less than 90% or greater than 110%.

Temperature

To quantify environmental temperatures to which newts were exposed to at the PA study area, we equipped four ponds in 2019 and 2020 with Onset HOBO Temperature data loggers (# UA-002-08) at even intervals along the pool edge at the same water depth (20 cm below the water surface and 5 cm above the pond bottom; 4- 15 units per pond) to measure temperature every hour. Temperature loggers were regularly repositioned as pond levels fluctuated. In the PA study area, we limited our temperature loggers to the four ponds with the most consistent newt captures. We averaged the hourly-recorded temperatures to determine average daily water temperatures for the four ponds. Furthermore, weekly average water temperature for the one week previous and the two weeks previous were calculated to account for potential time lags between temperature and onset of infection. In addition to water temperature, we obtained daily maximum air temperature from the nearest weather station. Daily maximum air and daily average water temperature are highly correlated in our study areas from April to July (0.93; CI = 0.88 – 0.95), and thus air temperature is a good proxy for water temperature. We calculated weekly average daily maximum air temperature one week previous and two weeks previous to help determine the best temperature predictor for *Bd* infections. Water temperature data obtained at the MA study area were obtained similarly for all 3 ponds while the WI study area only had water temperature data recorded at specific times and days when surveys occurred. Air temperature data for both study areas were obtained in the same manner as PA. We calculated 5 different measurements of temperature: 1) average water temperature day of sampling, 2) average water temperature for the one week prior to sampling, 3) average water temperature for the two weeks prior to sampling, 4) weekly average air temperature one week prior to sampling, 5) and average air temperature for the two weeks prior to sampling (correlation among the five measures was high, ranging from 0.79 – 0.97; Figure 1.3).

Among-pond Covariates

For our analysis of among pond variation, we limited our data to the PA study area because of the limited spatial replicates within each of our two other study areas. Following the methods of Davis et al. (2018), we categorized the eleven ponds into “short” and “long” hydroperiod ponds. This was based on the length of the inundation period with long defined as

ponds that in an average year maintain water for the duration of larval *A. maculatum* development (mean time to drying = 47 days for short hydroperiod and 148 days for long hydroperiod; Table 1.1). Furthermore, we estimated newt abundance using a closed-population capture-recapture model. Encounter histories were generated from our individual capture records and were analyzed using R (R Core Team, 2021) and Rmark package (v2.2.7; Laake, Jeff), which runs analyses using the Program Mark (Version 9.0). Although newt abundance for each pond fluctuates across the season as environmental conditions change, we decided to use annual abundance estimations as we feel that these pond-level estimations are a good representation of the variation of susceptible host populations at our study area (Table 1.1). We used maximum pond width and length from a previous study to determine pond area and calculated newt densities of each pond by dividing abundance estimates by pond area (Davis *et al.*, 2018).

Statistical Analysis

We analyzed our data in sequential order, first fitting models for only the PA study area to fully explore patterns for this study area. We then examined whether patterns were consistent across study areas by fitting models with data from all three and determining whether there was an interaction between study area and the effect size of our different predictors. Our goal was to determine the factors that predicted two measures of infection levels. First, the probability an animal was infected with *Bd* (a measure of overall population prevalence) and second, the number of estimated copies of *Bd* on the swab for animals where *Bd* was detected (a measure of infection intensity). For each, we fit generalized linear mixed models to estimate relationships, using a logit-link function and binomial distribution for probability of infection and log-link and negative binomial distribution for *Bd* copies per swab. Our infection intensity analyses only included samples for individuals that were positive for *Bd* presence, and thus is limited to patterns within the infected portion of the population. In our models, we considered individual-level covariates (sex and SVL), pond-level covariates (host density, host abundance, hydroperiod, pond, and study area), and within and between season covariates (Julian date, year, and the 5 measures of temperature). The full set of model parameters considered across all analyses are defined in Table 1.2. For all analyses, we used AIC to select among a predefined set

of infection prevalence and infection intensity models. All analyses were conducted using R (R Core Team, 2021) with the package, lme4 (v.1.1-26, Bates, Douglas).

We first analyzed data to determine the best predictor of within-season variation and among-season variation for our PA dataset. We limited our dataset to year 2019 and 2020 when four of our PA ponds were equipped with HOBO temperature loggers. These ponds comprised the majority of our full dataset for the study area and were visited most frequently and consistently. This limited the potential for spurious patterns owing to irregular or imbalanced sampling. Our base model included SVL, year, and sex as fixed effects and pond as a random effect to account for multiple sampling from the same ponds. We then compared among models that included these effects and separately each of the five air and water temperature measurements we calculated from our field and weather station temperature measures and a null model with no temperature covariate. Our goal for the analysis was to determine, whether infection prevalence and infection intensity were related to temperature, whether the pattern was consistent among temperature measures, and which temperature measure fit best (Table 1.3). In addition, we fit a model using day of year as a covariate to determine how each changed temporally.

After determining the best covariate for incorporating temperature into analyses, we next determined which spatial factors could explain among pond variation in the eleven ponds at the PA study area in 2018, 2019, and 2020. We focused only on this study area for this question because it was the only study area where we had sufficient spatial replication to measure potential differences. Again, we examined responses in both infection prevalence and intensity and how differences in each related to hydroperiod length of a pond, the total abundance of newts in a pond, and the density of newts in a pond (abundance/area). We used the same base model with the addition of the best temperature predictor for of the infection parameters based on our previous analysis. For each temperature predictor, we calculated the mean temperature of the four ponds as a study area-level variable to be able to apply a temperature covariate for our eleven ponds. We used the best fit model for among pond covariates to examine SVL and sex effects since it is the largest dataset for our PA study area and encompasses all eleven ponds. We fit and compared six different models for spatial variation, 1) a null model without any spatial covariate, 2) three models exploring hydroperiod, host abundance, and host density separately

and 3) two models including a combination of hydroperiod with either host abundance or host density (Table 1.4).

Finally, we determined if the observed relationships of infection level to temperature and day of year differed among our three study areas. To do so, we applied the best temporal and individual covariates model to a combined dataset of all three study areas to determine how well variation in overall infection prevalence and intensity can be explained by our PA model. We combined all three study areas to be able to include study area as a fixed effect allowing us to test for an interaction between temperature and study area. We fit five models for each disease measurement comparing the base model, an additive model with temperature and study area, an additive model with Julian date and study area, an interactive model with temperature and study area, and an interactive model with Julian date and study area. We decided to use the best air temperature model and excluded SVL due to incomplete data collection from some study areas that would limit the number of observations.

RESULTS

We captured and swabbed 3,009 newts in the PA study area (543 in 2018, 1,259 in 2019, and 1,207 in 2021), 2,151 in the MA study area (576 in 2019 and 1,575 in 2020), and 1,867 in the WI study area (565 in 2018, 683 in 2019, and 619 in 2020; Table 1.5). We swabbed 7,027 newt captures and found that *Bd* infection was present in all study areas in all years sampled. The study areas had an overall infection prevalence of 0.74 (seventeen ponds that ranged from 0.13 to 0.95) with the average infection intensity of 172,052 copies per swab and maximum infection intensity of 196,000,000 copies per swab.

Temperature

Infection Prevalence – To determine the best temperature predictor of infection levels in the PA study area, we compared fit of six models all of which included sex, SVL, year, and pond

as predictors but differed in whether and how temperature was included. All five models that included one of our measures of temperature fit better than the null model with temperature not included. Likewise, we estimated a quadratic relationship between temperature and infection prevalence for all five temperature variables (Table 1.3). When selecting among our temperature variables, our best fitting model for prevalence included weekly average daily average water temperature for the prior two weeks (temperature: coef. = -0.85, $p < 0.001$; temperature^2: coef. = -1.89, $p < 0.001$). For the PA study area, infection prevalence peaked at 14.5 °C and remained above 90% when water temperatures were between 10 and 17 °C and was close to 0 below 5 °C and above 24 C (Figure 1.4a). When considering the difference between years, we estimated a log-odds ratio of 1.88 higher prevalence in 2020 compared to 2019 (CI: 1.13 – 2.62; p = < 0.001).

Infection Intensity – Average daily water temperature was the best temperature predictor for infection intensity (temperature: coef. = -0.08, $p < 0.001$; temperature^2: coef. = -0.06, $p < 0.001$). There was a quadratic relationship where *Bd* intensity was greatest at 15.1 °C at 18,034 copies per swab (Figure 1.4c). Our model indicated that there was not a significant difference in intensity between years (coef. = -0.028; CI: -0.07 – 0.01; p = 0.155).

Julian Date – Similar to the relationship we observed for temperature, we found that both infection prevalence and intensity were also quadratically related to Julian date (Julian day: coef. = -0.47, $p < 0.001$; Julian day^2: coef. = -0.94, $p < 0.001$ and Julian day: coef. = -0.07, $p < 0.001$; Julian day^2: coef. = -0.08, $p < 0.001$, respectively). Prevalence was under 10% in our earliest samples, increasing to 50% of individuals infected by day 109, peaking at closest to 100% infected on day 151, and decreased back to 50% by day 194 (Figure 1.4b). Average water temperature for the two weeks prior to these days were 10.2 ℃ (day 109), 14.2 ℃ (day 151), and 21.7 ℃ (day 194), respectively, in 2020. Greater than 90% of individuals sampled were positive for *Bd* from day 123 and 180, during which average two week prior temperatures ranged from 8.1 ℃ to 17.6 ℃ in 2020. Similarly, we estimated that infection intensity peaked on day 150 with an infection load of 18,215 copies per swab with an associated daily average water temperature of 18.9 ℃ in 2020 (Figure 1.4d). There was not a difference in infection prevalence or intensity between years (coef. = -0.37; CI: -0.82 – 0.08; p = 0.110 and coef. = -0.003; CI: -0.04 – 0.03; p = 0.867, respectively).

Among-pond Covariates

Infection Prevalence – When comparing results for all eleven sites in the PA study area, the models with the lowest AIC value for infection prevalence included a positive effect of host density on infection prevalence, although there was a small overlap with 0 for the 95% CI (coef. = 0.91, CI: -0.018 – 1.843; p = 0.054; Table 1.4). As with the previous analysis, the effect of temperature remained significant (temperature: coef. = -0.81, $p < 0.001$; temperature^2: coef. = -1.41, $p < 0.001$) and the relationship between host density and prevalence was more pronounced for the temperature range where prevalence was increasing or decreasing (Figure 1.5). 2020 had a 1.14 times higher infection prevalence than 2019 (CI: 0.52 – 1.80; $p < 0.001$), while there was no significant difference between males and females (coef.; -0.26; CI: -0.56 – 0.04; p = 0.089). Additionally, larger individuals had a lower probability of being infected compared to smaller individuals (coef. = -0.18, CI: -0.33 – -0.03; p = 0.020; Figure 1.6).

Infection Intensity – The best model for infection intensity included hydroperiod (Table 1.4). We found a small correlation in our PA study area between hydroperiod and infection intensity, with average infection intensity 6% higher in short rather than long hydroperiod ponds (CI: -0.01, 0.13; p = 0.079). Again, temperature was significant (temperature: coef. = -0.05, $p < 0.001$; temperature^2: coef. = -0.06, $p < 0.001$) and the relationship between intensity and temperature was similar in form. There were no significant differences in intensity between year 2019 and year 2020 (coef. = -0.02, CI: -0.05 – 0.01; p = 0.225). Males had lower infection intensities than females (coef. = -0.05, CI: -0.08 – -0.01; p = 0.005) and larger individuals had lower intensities, with a 75% decrease in infection intensity from the smallest individual to the largest (coef. = -0.05, CI: -0.06 – -0.03; $p < 0.001$; Figure 1.6).

Study Area Comparisons

Infection Prevalence – Our final goal was to determine whether the seasonal relationships we observed for the PA study area were repeatable across the three study areas (Table 1.6). As a base model, we included our best fitting air temperature model as an explanatory variable (the average max air temperature one week prior). Water temperature was unavailable for the WI study area and, as we demonstrate for the PA study area, correlation between air and water

temperature metrics is high and have similar predictive ability. Like our PA study area models, all three study areas had a significant quadratic relationship between infection prevalence and temperature (temperature: coef. = -0.04, p = 0.551; temperature^2: coef. = -0.36, p < 0.001). PA and MA shared similar patterns, but prevalence in the PA study area was lower to start and end and also peaked at higher values as compared to MA across all years (Figure 1.8a). WI infection prevalence increased more slowly throughout the season. Infection prevalence between 2018 and 2019 was different (coef. = 0.66; CI: 0.29 – 1.04; P < 0.001) but not between 2018 and 2020 (coef. = -0.10; CI: -0.46 – 0.26; p = 0.585). There was not a significant difference between males and females (coef. = 0.09; CI: -0.09 – 0.26; P = 0.322).

Infection Intensity – Similarly, we tested infection intensity with the average max air temperature one week prior with the combined study area set and found that temperature remained an important predictor. A quadratic relationship between infection intensity and temperature was present at all study areas ((temperature: coef. = -0.003, p = 0.76; temperature^2: coef. = -0.04, p < 0.001; Figure 1.8c). WI and PA peaked at similar temperatures (~15°C), while MA peaked at a higher temperature (20.3 °C). Year 2018 was not significantly different from 2019 but was from 2020 (coef. = -0.02; CI: -0.06 – 0.02; p = 0.345 and coef. = -0.059, CI: -0.10 – -0.02; P = 0.003). Although there were no differences between sexes for infection prevalence, males tended to have lower infection intensities than females once infected (coef. = -0.038, CI: -0.06 – -0.02; P < 0.001).

Julian Date – In addition to temperature, we fit a Julian date model to compare between temperature and Julian date at our study areas (Table 1.6 and Table 1.7, respectively). Interactive models performed better than additive models with Julian date and included an interaction between Julian date and the two infection measurements. Both infection prevalence and intensity had a quadratic relationship with Julian date (Julian day: coef. = 0.43, p < 0.001; Julian day^2: coef. = -0.43, p < 0.001 and Julian day: coef. = 0.03, p = 0.03; Julian day^2: coef. = -0.06, p < 0.001, respectively). PA prevalence was higher and peaked earlier on Julian day 155, MA prevalence peaked on Julian day 158, and WI prevalence was increasing throughout our sampling period (Figure 1.8b, d). Max air temperatures one week prior to these dates and at the study areas are 18.5° C (PA) and 15.8° C (MA). With infection intensity and Julian date, Julian date was significant with PA and MA, but not WI. Although PA intensities started and ended

lower than WI and MA, PA had a higher peak intensity of 13,359 copies per swab on day 151 compared to 4,447 copies per swab on day 153 for the MA study area (Figure 1.8d). Temperatures associated with these days and study areas are 20.5° C (PA) and 16.3° C (MA). Surprisingly, WI infection intensity was consistently near 2,980 copies per swab throughout the season, although there is a lot of uncertainty at the beginning and end of the season (Figure 1.8d). Sex was not a significant predictor for infection prevalence (coef. = 0.11; CI: -0.07 – 0.30; p = 0.218), but was important for infection intensity (coef. = -0.03; CI: -0.06 – -0.01; P = 0.001).

DISCUSSION

Seasonal variation in environmental conditions can alter host-pathogen relationships and create cyclic patterns of infectious disease dynamics (Altizer *et al.*, 2006). Our results indicate quadratic patterns of disease with both infection prevalence and intensity within a season and is present across years. This pattern in infection was explained largely by changes in temperature within a season and between seasons and highlight temperature as an important driver in understanding how *Bd* infections vary temporally within newt populations. Additionally, individual differences (i.e., SVL) in the newt population explained some variation in infection levels. Our findings suggest that newts are likely to act as reservoirs for *Bd* due to their high infection prevalence at low to moderate infection intensities.

Temperature is an essential regulator of the *Bd*'s lifecycle and strongly determines growth rates of the pathogen in lab settings (Piotrowski *et al.*, 2004; Berger *et al.*, 2005). Infection prevalence was best explained by average temperatures two weeks prior to sampling while average temperatures day of sampling explained variation in intensity best. Piotrowski et al. (2004) tested *in vitro* growth of *Bd* at different temperature ranges and found that *Bd* reached stationary growth phase in 12 days between 17-25 °C while Berger et al. (2005) found that the *Bd* lifecycle *in vitro* is 4 to 5 days at 22 °C. Our results suggest that our ability to detect infection may be best predicted by temperatures when transmission occurred rather than the current temperature at the time when samples were collected. Few studies investigate both infection

prevalence and intensity as a function of temperature. Within these studies, time delay between time of infection and minimum intensity for detection is usually considered by using air temperature 30 days prior. However, most studies only use one time period in their analyses rather than testing among lag times as we have in this study (Kriger *et al.*, 2007; Lenker *et al.*, 2014; Petersen *et al.*, 2016; Hudson *et al.*, 2019; but see Sonn *et al.*, 2019). In contrast to our results for prevalence, we found that infection intensity is best predicted by the current temperature when the sample was collected. This may be due to the time it takes for *Bd* to mature and reproduce more zoospores to be released onto the skin and detected during swabbing. Similarly, Kriger et al. (2007) found that sunset water temperature the day of sampling best explained their infection levels while in contrast Sonn et al. (2019) found that 15 days prior to sampling predicted prevalence best and 30 days prior to sampling for infection load. Our study better informs temperature relationships between prevalence and intensity since we sampled the same population of one species multiple times throughout a season and across multiple seasons.

Our results show that peak infection prevalence and intensity in the newt population in the PA study area occurred at lower temperatures than that of *in vitro Bd*. Optimal conditions for *in vitro Bd* are between 17 and 25 °C (Piotrowski *et al.*, 2004). However, *in vitro* conditions may exclude additional factors that can affect *Bd* growth. Optimal temperature for peak infection levels for *Bd* has been reported as between 18 and 19 °C in central Virginia (Pullen *et al.*, 2010) and 15.9 °C in adult *Litoria wilcoxii* (Kerry M. Kriger and Hero, 2007); yet, our PA newt population had peak infection levels at 15 °C. These differences can be explained by 1) physiological differences between newts and other species 2) behavioral responses to combat infections or 3) the chosen environmental metrics of our study. The majority of chytrid studies with newts support the idea that *Bd* infection is common in this species (Rothermel *et al.*, 2008; Groner and Relyea, 2010; Lenker *et al.*, 2014). Regardless of infection levels, comparatively lower threshold of 15 °C may be enough for newts to combat and recover from *Bd* infection. Another explanation for differences in peak infection temperatures may be behavioral responses. Ectotherms utilize warmer areas of their habitat to help combat infections by directly affecting pathogen growth or increasing immune system function (Terrell *et al.*, 2013; Rakus *et al.*, 2017). Lastly, our study used average daily temperatures and therefore cannot rule out the possibility that daily maximum temperatures may be a more important regulator of *Bd* growth in the wild populations.

We observed cyclic patterns of seasonal *Bd* infection in all of our newt populations and in every year sampled. The strong quadratic relationship between temperature and *Bd* prevalence and intensity suggests the seasonal dynamics are driven in large part by changes in environmental temperatures. At the latitude where we study populations, this leads to low infection prevalence and intensity in newts at the beginning of the active season when other wetland breeding amphibians such as wood frog, spotted salamander, and Jefferson salamander adults visit ponds to breed and deposit eggs. In contrast, newts are most likely to transmit *Bd* to other species at the time that the larval stages of these species metamorphose and become more vulnerable to infection (Rollins-Smith, 1998; Garner *et al.*, 2009). Finally, we observed declines in infection during mid-summer, when most ponds are drying – perhaps allowing newts to reduce or clear infection loads prior to leaving ponds. Our results add to the evidence from previous studies covering different latitudinal and longitudinal study areas showing that seasonality in *Bd* infections are common and present in multiple host species (Berger *et al.*, 2004; Kerry M. Kriger and Hero, 2007; Rothermel *et al.*, 2008; Pullen *et al.*, 2010; Kinney *et al.*, 2011; Lenker *et al.*, 2014; Petersen *et al.*, 2016; Hudson *et al.*, 2019; Sonn *et al.*, 2019). We found cyclic seasonality in infection intensity to occur in population across all 3 study areas, across ponds within study areas, and across the years of our study.

Although our results suggest temperature as the driver of infection when hosts are in aquatic habitats, our results are correlative and other drivers could potentially explain the patterns we observed. Breeding migrations can result in seasonality of disease by influencing the number of individuals (both conspecifics and other species) available for disease transmission (Altizer *et al.*, 2011). In our system, there are fewer individuals early in the season as individuals are migrating into the ponds and later as individuals return to terrestrial habitats that may affect the number of susceptible individuals available. The rise, peak, and fall of infection levels are consistent with other studies on breeding migrations (Kinney *et al.*, 2011; Brannelly *et al.*, 2015). We were only able to observe infection levels while newts are in the ponds, but low infection levels earlier in the season may also be explained by recovery from infections when migrating back to terrestrial habitats (Kinney *et al.*, 2011; Daversa, Monsalve-Carcaño, *et al.*, 2018). In addition, the rise and fall in infection levels can be affected by the increased direct contact from breeding interactions. The majority of courtship between newts happens from March to June where males attach to females to copulate as well as compete with other males and the number of

direct contacts may reduce and affect the decrease in infection levels as well (Grayson *et al.*, 2012). Another alternative explanation may be the decrease in environmental *Bd* abundance through *Daphnia* predation, which can also vary as *Daphnia* populations within the ponds can change as a result of abiotic and biotic conditions (Steiner, 2004; Searle *et al.*, 2013). Finally, it is important to differentiate the effects of seasonal conditions on *Bd* infections and the newts' ability to recover from infection. While temperature can affect both *Bd* growth and newt immune response, other factors such as innate immune defenses, adaptive immune components, and the skin microbiome may explain some of the variation in infection patterns (Grogan *et al.*, 2018). Further investigations on how *Bd* affects newt survival and recovery will help determine how temperature affects *Bd* growth versus the newt's ability to deal with infection.

Our results suggest that *Bd* infection is nearly ubiquitous at peak infection cycle in all but one of the 19 populations that was sampled across our three study areas. Although overall prevalence across the duration of our study was 74% (5,198 out of 7,012), our models indicate that, when temperatures were between 12 and 18 °C, nearly all individuals were positive for *Bd*. Previous studies with multiple species generally had a lower overall prevalence around 12 – 27 % (Kerry M. Kriger and Hero, 2007; Pullen *et al.*, 2010; Sonn *et al.*, 2019). Our results showed a higher prevalence than other studies with *N. virisdescens*, where overall infection prevalence ranged from 26.8% (11 out of 41) from April to August (Lenker *et al.*, 2014), 34.8% (16 out of 46) from April to May (Groner and Relyea, 2010), and 39.2% (60 out of 153) from May to June (Raffel *et al.*, 2010). However, we did not analyze individual infection histories to determine if recovery and re-infections occurred within a season or between years. Additionally, the timing at which the majority of newts are infected also coincide with the presence of multiple amphibian species, some of which are developing and undergoing metamorphosis. While tadpoles are generally more resistant to *Bd* infection, metamorphosis can increase disease risk for recent metamorphs due to increased keratin and less-developed immune systems (Rollins-Smith, 1998; Garner *et al.*, 2009; Kilpatrick *et al.*, 2009). Wood frogs (*L. sylvaticus*) are a common species in our ponds and have been found to be susceptible and fatal to *Bd* infections when undergoing metamorphosis in lab exposure trials (Gahl *et al.*, 2011).

Although *Bd* is present in the newt population throughout a season, we did not observe mortality events and few clinical symptoms of chytridiomycosis on individuals. During peak

infection, the average infection intensity was still lower than the critical threshold (ZE) reported for host mortality and population decline (Vredenburg *et al.*, 2010). Average infection intensity was approximately 172,052 copies per swab and can range from 956 ZE to 8,603 ZE depending on the number of copies per zoospore (20 – 180 in North American strains). *Litoria lesueuri* had a maximum of 235,287 zoospores (Kerry M. Kriger and Hero, 2007), *L. wilcoxii* had a max mean intensity of 4,377 ZE (Van Sluys and Hero, 2009), and *L. clamitans* had a maximum of 190,755 GE (Korfel and Hetherington, 2014). Another study using Eastern red-spotted newts had a maximum of about 3,162 ZE (Raffel *et al.*, 2010). Given the different strains of *Bd* with varying copies of DNA per zoospore, there remains some uncertainty with standardizing infection intensity across studies (Rebollar *et al.*, 2017). While infection intensity is low in newt populations, eliciting an immune response towards infection may still accrue energetic costs for newts and reduce overall fitness (Lochmiller and Deerenberg, 2000; Retallick and Miera, 2007) . If newts are commonly infected with *Bd* at relatively low intensities at the same time as more vulnerable species are developing, they are potentially important reservoirs for *Bd*.

Our among-pond analyses showed that differences in host density and hydroperiods can affect the infection levels of newts. Habitats with varying host densities can affect infection levels when increasing host densities also increase pathogen abundance and contact rates between infected and susceptible individuals (Beldomenico and Begon, 2010; Roche *et al.*, 2012). Our results indicate that ponds with higher host densities had higher infection prevalence. This pattern is supported by other studies that also investigated density effects on infection levels (Brannelly *et al.*, 2015; Adams *et al.*, 2017). Additionally, although not quite significant, ponds with shorter hydroperiods had higher infection levels, which is similar to the trend that Peterson and McKenzie (2014) reported in their study. Conversely, others have reported no patterns or the opposite trend where more permanent ponds had higher infection levels (Kerry M Kriger and Hero, 2007; Ocock *et al.*, 2013). Although the majority of studies on hydroperiod focuses on developmental stress of larvae, ponds with shorter hydroperiods may be poorer habitat quality and increase stress on individuals and affect their immune function (Kiesecker and Skelly, 2001; Brannelly *et al.*, 2019).

The infection patterns of *Bd* infection were present in all three study areas; however, the temperatures at which infection rises, peaks, and falls varied among newt populations. This

variation in infection patterns could be attributed to habitat differences. PA sites are composed of ephemeral vernal pools and semi-permanent ponds, many of which have closed canopies. WI ponds and MA's most productive pond (1997 out of 2151) were larger more permanent bodies of water. The differences in size, permanence, and canopy coverage of ponds can result in differences in microhabitat temperature variation that can affect how newts deal with infection. Raffel et al. (2010) found that substrate complexity could indicate shade coverage that could potentially cool down temperature of shallow water and increase newt susceptibility to infections. Furthermore, MA's most productive pond is a beaver pond with a stream flowing through, which can affect pond temperatures as well as increase pathogen transmission from upstream habitats. Kriger and Hero (2007) found that permanent, free-flowing aquatic habitats had higher infection prevalence than ephemeral pools in Queensland, Australia; however, Padgett-Flohr and Hopkins (2010) found *Bd* to be widely present in both ephemeral and more permanent ponds. In addition, WI had higher variation and peaked later than PA and MA with regards to prevalence. WI's dataset consists of two ponds that are a 48.5 km distance from each other and show significant differences in infection patterns. WI had the most different results and may have differences in optimal temperatures, but the results should be interpreted with caution because sampling was not as intense in all years sampled. Regardless of the differences in peak infection levels, the general seasonal patterns of high prevalence and low intensity in newt populations apply across the longitudinal gradient of newt's geographic range.

Our study shows that variation in infection prevalence and intensity can be partially explained with individual size. There was a negative correlation where larger individuals tend to have lower probability of infection and lower infection intensities than smaller individuals. A potential explanation for this trend is a size-related effect where size can determine infection intensity or body condition can influence how individuals deal with infection (Searle *et al.*, 2011). SVL can also be a proxy for age and is relevant when considering age-related effects where older individuals have acquired immunity through repeated exposure or increased resistance with age; however, size and age can have interactive effects as well (Boots and Bowers, 2004). Size and age are well-studied effects on disease and is ubiquitous across host-pathogen systems including fish (Ryce *et al.*, 2005), plants (Ando *et al.*, 2009), and corals (Dube *et al.*, 2002). Our findings on a negative correlation between size and infection levels in newts are supported with studies on other newt populations (Raffel *et al.*, 2010), *Rhinella marina*

(Brannelly *et al.*, 2018), *L. lesueuri* (Kriger *et al.*, 2007), and *Anaxyrus americanus* (Burrow *et al.*, 2017). Conversely, Bradley et al. (2019) found opposite trends with age and infection in experiments with *Pseudacris regilla* and *Rana aurora*. The increase in disease risk for smaller and younger individuals can have population-level effects, especially for more vulnerable species or smaller populations.

We found strong seasonal *Bd* infection dynamics driven by temperature within newt populations across its longitudinal range. The infection dynamics at all three study areas (PA, MA, and WI) show a quadratic relationship between infection levels (prevalence and intensity) and temperature; however, peak infection occurs at different temperatures for each study area. Although there is support in the literature for seasonal variation in *Bd* infection, this is the first study to observe such a pattern in the same species across different longitudes and included intensive sampling across multiple populations within study areas and multiple years of sampling. Additionally, our study suggest that newts are a likely reservoir species for *Bd*. Newts are a widespread species that are highly infected at low to moderate infection intensity and are present in ponds when other more transient species are present and susceptible to transmission. It will be important to assess how newt infection dynamics correlate with community infection levels and determine how newts are spreading and maintaining *Bd* within these habitats.

REFERENCES

Adams, A.J., Kupferberg, S.J., Wilber, M.Q., Pessier, A.P., Grefsrud, M., Bobzie, S., *et al.* 2017. Extreme drought, host density, sex, and bullfrogs influence fungal pathogen infection in a declining lotic amphibian. *Ecosphere*, **8**.

Adams, M.J., Miller, D.A.W., Muths, E., Corn, P.S., Grant, E.H.C., Bailey, L.L., *et al.* 2013. Trends in Amphibian Occupancy in the United States. *PLoS One*, **8**: 6–10.

Altizer, S., Bartel, R., Han, B.A., Altizer, S., Bartel, R. and Han, B.A. 2011. Animal Migration and Infectious Disease Risk. *Science (80-.).*, **331**: 296–302.

Altizer, S., Dobson, A., Hosseini, P., Hudson, P. and Pascual, M. 2006. Seasonality and the dynamics of infectious diseases. 467–484.

Ando, K., Hammar, S. and Grumet, R. 2009. Age-related resistance of diverse Cucurbit fruit to infection by phytophthora capsici. *J. Am. Soc. Hortic. Sci.*, **134**: 176–182.

Bailey, L.L. and Muths, E. 2019. Integrating amphibian movement studies across scales better informs conservation decisions. *Biol. Conserv.*, **236**: 261–268. Elsevier.

Baines, C.B., Diab, S. and McCauley, S.J. 2020. Parasitism risk and infection alter host dispersal. *Am. Nat.*, **196**: 119–131.

Bar-David, S., Segev, O., Peleg, N., Hill, N., Templeton, A.R., Schultz, C.B., *et al.* 2007. Long-distance movements by fire salamanders (Salamandra infraimmaculata) and implications for habitat fragmentation. *Isr. J. Ecol. Evol.*, **53**: 143–159.

Barrile, G.M., Walters, A., Webster, M. and Chalfoun, A.D. 2021. Informed breeding dispersal following stochastic changes to patch quality in a pond-breeding amphibian. *J. Anim. Ecol.*, **90**: 1878–1890.

Behringer, D.C., Butler, M.J. and Shields, J.D. 2008. Ecological and physiological effects of PaV1 infection on the Caribbean spiny lobster (Panulirus argus Latreille). *J. Experiemental Mar. Biol. Ecol.*, **359**: 26–33.

Beldomenico, P.M. and Begon, M. 2010. Disease spread, susceptibility and infection intensity: vicious circles? *Trends Ecol. Evol.*, **25**: 21–27.

Berger, L., Hyatt, A.D., Speare, R. and Longcore, J.E. 2005. Life cycle stages of the amphibian chytrid Batrachochytrium dendrobatidis. *Dis. Aquat. Organ.*, **68**: 51–63.

Berger, L., Speare, R., Daszak, P., Green, D.E., Cunningham, A.A., Goggin, C.L., *et al.* 1998. Chytridiomycosis causes amphibian mortality associated with population declines in the rain forests of Australia and Central America. *Proc. Natl. Acad. Sci. U. S. A.*, **95**: 9031–9036.

Berger, L., Speare, R., Hines, H.B., Marantelli, G., Hyatt, A.D., Donald, K.R.M.C., *et al.* 2004. Effect of season and temperature on mortality in amphibians due to chytridiomycosis. *Aust. Vet. J.*, **82**: 434–439.

Binning, S.A., Shaw, A.K. and Roche, D.G. 2017. Parasites and host performance: Incorporating infection into our understanding of animal movement. *Integr. Comp. Biol.*, **57**: 267–280.

Blehert, D.S., Hicks, A.C., Behr, M., Meteyer, C.U., Brenda, M., Buckles, E.L., *et al.* 2009. Bat White-Nose Syndrome: An Emerging Fungal Pathogen? *Science (80-.).*, **323**: 227.

Bloch, A.M. and Grayson, K.L. 2010. Reproductive costs of migration for males in a partially migrating, pond-breeding amphibian. *Can. J. Zool.*, **88**: 1113–1120.

Boots, M. and Bowers, R.G. 2004. The evolution of resistance through costly acquired immunity. *Proc. R. Soc. B Biol. Sci.*, **271**: 715–723.

Borg, N.J., Mitchell, M.S., Lukacs, P.M., Mack, C.M., Waits, L.P. and Krausman, P.R. 2017. Behavioral connectivity among bighorn sheep suggests potential for disease spread. *J. Wildl. Manage.*, **81**: 38–45.

Boulinier, T., Kada, S., Ponchon, A., Dupraz, M., Dietrich, M., Gamble, A., *et al.* 2016. Migration, Prospecting, Dispersal? What Host Movement Matters for Infectious Agent Circulation? *Integr. Comp. Biol.*, **56**: 330–342.

Bowne, D.R., Bowers, M.A. and Hines, J.E. 2006. Connectivity in an agricultural landscape as reflected by interpond movements of a freshwater turtle. *Conserv. Biol.*, **20**: 780–791.

Boyle, D.G., Boyle, D.B., Olsen, V., Morgan, J.A.T. and Hyatt, A.D. 2004. Rapid quantitative detection of chytridiomycosis (Batrachochytrium dendrobatidis) in amphibian samples using real-time Taqman PCR assay. *Dis. Aquat. Organ.*, **60**: 141–148.

Brannelly, L.A., Hunter, D.A., Lenger, D., Scheele, B.C., Skerratt, L.F. and Berger, L. 2015. Dynamics of Chytridiomycosis during the Breeding Season in an Australian Alpine Amphibian. *PLoS One*, **10**: 1–15.

Brannelly, L.A., Martin, G., Llewelyn, J., Skerratt, L.F. and Berger, L. 2018. Age- and size-dependent resistance to chytridiomycosis in the invasive cane toad Rhinella marina. *Dis. Aquat. Organ.*, **131**: 107–120.

Brannelly, L.A., Ohmer, M.E.B., Saenz, V. and Richards-Zawacki, C.L. 2019. Effects of hydroperiod on growth, development, survival and immune defences in a temperate amphibian. *Funct. Ecol.*, **33**: 1952–1961.

Burrow, A.K., Rumschlag, S.L. and Boone, M.D. 2017. Host size influences the effects of four isolates of an amphibian chytrid fungus. *Ecol. Evol.*, **7**: 9196–9202.

Casadevall, A. and Pirofski, L. anne. 2018. What is a host? Attributes of individual susceptibility. *Infect. Immun.*, **86**: 1–12.

Cayuela, H., Schmidt, B.R., Weinbach, A., Besnard, A. and Joly, P. 2019. Multiple density- -dependent processes shape the dynamics of a spatially structured amphibian population. *J. Anim. Ecol.*, 164–177.

Chatfield, M.W.H., Brannelly, L.A., Robak, M.J., Freeborn, L., Lailvaux, S.P. and Richards-Zawacki, C.L. 2013. Fitness consequences of infection by batrachochytrium dendrobatidis in northern leopard frogs (Lithobates pipiens). *Ecohealth*, **10**: 90–98.

Daszak, P., Cunningham, A.A. and Hyatt, A.D. 2000. Emerging infectious diseases of wildlife - Threats to biodiversity and human health. *Science (80-.).*, **287**: 443–449.

Daversa, D.R., Fenton, A., Dell, A.I., Garner, T.W.J. and Manica, A. 2017. Infections on the move: How transient phases of host movement influence disease spread. *Proc. R. Soc. B Biol. Sci.*, **284**.

Daversa, D.R., Manica, A., Bosch, J., Jolles, J.W. and Garner, T.W.J. 2018. Routine habitat switching alters the likelihood and persistence of infection with a pathogenic parasite. *Funct. Ecol.*, **32**: 1262–1270.

Daversa, D.R., Monsalve-Carcaño, C., Carrascal, L.M. and Bosch, J. 2018. Seasonal migrations, body temperature fluctuations, and infection dynamics in adult amphibians. *PeerJ*, **2018**: 1–17.

Davis, C.L., Teitsworth, E.W. and Miller, D.A.W. 2018. Combining Data Sources to Understand Drivers of Spotted Salamander (Ambystoma maculatum) Population Abundance. *J. Herpetol.*, **52**: 116–126.

Denoël, M., Dalleur, S., Langrand, E., Besnard, A. and Cayuela, H. 2018. Dispersal and alternative breeding site fidelity strategies in an amphibian. *Ecography (Cop.).*, **41**: 1543–1555.

Denoël, M. and Lehmann, A. 2006. Multi-scale effect of landscape processes and habitat quality on newt abundance: Implications for conservation. *Biol. Conserv.*, **130**: 495–504.

Dougherty, E.R., Seidel, D.P., Carlson, C.J., Spiegel, O. and Getz, W.M. 2018. Going through the motions: incorporating movement analyses into disease research. *Ecol. Lett.*, **21**: 588–604.

Dube, D., Kim, K., Alker, A.P. and Harvell, C.D. 2002. Size structure and geographic variation in chemical resistance of sea fan corals Gorgonia ventalina to a fungal pathogen. *Mar. Ecol. Prog. Ser.*, **231**: 139–150.

Fujiwara, M., Anderson, K.E., Neubert, M.G. and Caswell, H. 2006. On the estimation of dispersal kernels from individual mark-recapture data. *Environ. Ecol. Stat.*, **13**: 183–197.

Gabor, C.R. and Nice, C.C. 2004. Genetic Variation among Populations of Eastern Newts , Notophthalmus viridescens : A Preliminary Analysis Based on Allozymes. *Her*, **60**: 373–386.

Gahl, M.K., Longcore, J.E. and Houlahan, J.E. 2011. Varying Responses of Northeastern North American Amphibians to the Chytrid Pathogen Batrachochytrium dendrobatidis. *Conserv. Biol.*, **26**: 135–141.

Garner, T.W.J., Walker, S., Bosch, J., Leech, S., Rowcliffe, J.M., Cunningham, A.A., *et al.* 2009. Life history tradeoffs influence mortality associated with the amphibian pathogen Batrachochytrium dendrobatidis. *Oikos*, **118**: 783–791.

Gates, J.E. and Thompson, E.L. 1982. Small Pool Habitat Selection by Red-Spotted Newts in Western Maryland. *J. Herpetol.*, **16**: 7–15.

Gill, D.E. 1978a. Effective Population Size and Interdemic Migration Rates in a Metapopulation of the Red-Spotted Newt, Notophthalmus viridescens (Rafinesque). *Evolution (N. Y).*, **32**: 839.

Gill, D.E. 1978b. The Metapopulation Ecology of the Red-Spotted Newt, Notophthalmus viridescens (Rafinesque). *Ecol. Monogr.*, **48**: 145–166.

Grant, E.H.C., Miller, D.A.W., Schmidt, B.R., Adams, M.J., Amburgey, S.M., Chambert, T., *et al.* 2016. Quantitative evidence for the effects of multiple drivers on continental-scale amphibian declines. *Sci. Rep.*, **6**: 1–9.

Grassly, N.C. and Fraser, C. 2006. Seasonal infectious disease epidemiology. *Proc. R. Soc. B Biol. Sci.*, **273**: 2541–2550.

Grayson, K.L., De Lisle, S.P., Jackson, J.E., Black, S.J. and Crespi, E.J. 2012. Behavioral and physiological female responses to male sex ratio bias in a pond-breeding amphibian. *Front. Zool.*, **9**.

Grayson, K.L. and Wilbur, H.M. 2009. Sex- and context-dependent migration in a pond-breeding amphibian. *Ecology*, **90**: 306–312.

Grogan, L.F., Robert, J., Berger, L., Skerratt, L.F., Scheele, B.C., Castley, J.G., *et al.* 2018. Review of the amphibian immune response to chytridiomycosis, and future directions. *Front. Immunol.*, **9**: 1–20.

Groner, M.L. and Relyea, R.A. 2010. Batrachochytrium dendrobatidis is Present in Northwest Pennsylvania , USA , with High Prevalence in Notophthalmus viridescens. *Herpetol. Rev.*, **41**: 462–465.

Heard, G.W., Scroggie, M.P. and Malone, B.S. 2012. Classical metapopulation theory as a useful paradigm for the conservation of an endangered amphibian. *Biol. Conserv.*, **148**: 156–166. Elsevier Ltd.

Hudson, M.A., Griffiths, R.A., Martin, L., Fenton, C., Adams, S.L., Blackman, A., *et al.* 2019. Reservoir frogs: Seasonality of Batrachochytrium dendrobatidis infection in robber frogs in Dominica and Montserrat. *PeerJ*, **2019**: 1–21.

Hurlbert, S.H. 1963. The Breeding Migrations and Interhabitat Wandering of the Vermilion-spotted Newt Notophthalmus Viridescens (Rafinesque). *Ecol. Monogr.*, **39**: 465–488.

Hyatt, A.D., Boyle, D.G., Olsen, V., Boyle, D.B., Berger, L., Obendorf, D., *et al.* 2007. Diagnostic assays and sampling protocols for the detection of Batrachochytrium dendrobatidis. *Dis. Aquat. Organ.*, **73**: 175–192.

John, R.R., Gitzen, R.A. and Guyer, C. 2019. Overnight Movements of Green Salamanders (Aneides aeneus) in Northern Alabama. *J. Herpetol.*, **53**: 158–164.

Johnson, J.R., Knouft, J.H. and Semlitsch, R.D. 2007. Sex and seasonal differences in the spatial terrestrial distribution of gray treefrog (Hyla versicolor) populations. *Biol. Conserv.*, **140**: 250–258.

Johnson, M.L. and Speare, R. 2003. Survival of Batrachochytrium dendrobatidis in water:

Quarantine and disease control implications. *Emerg. Infect. Dis.*, **9**: 922–925.

Joly, P. 2019. Behavior in a Changing Landscape: Using Movement Ecology to Inform the Conservation of Pond-Breeding Amphibians. *Front. Ecol. Evol.*, **7**: 1–17.

Kärvemo, S., Wikström, G., Widenfalk, L.A., Höglund, J. and Laurila, A. 2020. Chytrid fungus dynamics and infections associated with movement distances in a red-listed amphibian. *J. Zool.*, **311**: 164–174.

Kiesecker, J.M. and Skelly, D.K. 2001. Effects of disease and pond drying on gray tree frog growth, development, and survival. *Ecology*, **82**: 1956–1963.

Kilpatrick, A.M., Briggs, C.J. and Daszak, P. 2009. The ecology and impact of chytridiomycosis : an emerging disease of amphibians. *Trends Ecol. Evol.*, **25**: 109–118.

Kinney, V.C., Heemeyer, J.L., Pessier, A.P. and Lannoo, M.J. 2011. Seasonal pattern of batrachochytrium dendrobatidis infection and mortality in lithobates areolatus: Affirmation of vredenburg's "10,000 zoospore rule." *PLoS One*, **6**: 0–10.

Kopecký, O., Vojar, J. and Denoël, M. 2010. Movements of Alpine newts (Mesotriton alpestris) between small aquatic habitats (ruts) during the breeding season. *Amphib. Reptil.*, **31**: 109–116.

Korfel, C.A. and Hetherington, T.E. 2014. Temperature alone does not explain patterns of Batrachochytrium dendrobatidis infections in the green frog Lithobates clamitans. *Dis. Aquat. Organ.*, **109**: 177–185.

Kriger, Kerry M and Hero, J. 2007. The chytrid fungus Batrachochytrium dendrobatidis is non-randomly distributed across amphibian breeding habitats. *Divers. Distrib.*, **13**: 781–788.

Kriger, Kerry M. and Hero, J.M. 2007. Large-scale seasonal variation in the prevalence and severity of chytridiomycosis. *J. Zool.*, **271**: 352–359.

Kriger, K.M., Pereoglou, F. and Hero, J.M. 2007. Latitudinal variation in the prevalence and intensity of chytrid (Batrachochytrium dendrobatidis) infection in eastern Australia. *Conserv. Biol.*, **21**: 1280–1290.

Lafferty, K.D. and Shaw, J.C. 2013. Comparing mechanisms of host manipulation across host and parasite taxa. *J. Exp. Biol.*, **216**: 56–66.

Lenker, M.A., Savage, A.E., Becker, C.G., Rodriguez, D. and Zamudio, K.R. 2014. Batrachochytrium dendrobatidis infection dynamics vary seasonally in upstate New York, USA. *Dis. Aquat. Organ.*, **111**: 51–60.

Lips, K.R., Brem, F., Brenes, R., Reeve, J.D., Alford, R.A., Voyles, J., *et al.* 2006. Emerging infectious disease and the loss of biodiversity in a Neotropical amphibian community. *Proc. Natl. Acad. Sci. U. S. A.*, **103**: 3165–3170.

Lochmiller, R.L. and Deerenberg, C. 2000. Trade-Offs in Evolutionary Immunology : Just What Is the Cost of Immunity? *Oikos*, **88**: 87–98.

Longcore, J.E., Pessier, A.P., Nichols, D.K., Longcore, J.E., Pessier, A.P., Nichols, D.K., *et al.* 1999. Batrachochytrium dendrobatidis gen. et sp. nov., a chytrid pathogenic to amphibians.

Mycologia, **91**: 219–227.

Mazerolle, M.J. 2001. Amphibian Activity , Movement Patterns , and Body Size in Fragmented Peat Bogs. *J. Herpetol.*, **35**: 13–20.

McKenzie, J.M., Price, S.J., Connette, G.M., Bonner, S.J. and Lorch, J.M. 2021. Effects of snake fungal disease on short-term survival, behavior, and movement in free-ranging snakes. *Ecol. Appl.*, **31**: 1–11.

McLean, R.G., Ubico, S.R., Docherty, D.E., Hansen, W.R., Sileo, L. and McNamara, T.S. 2001. West Nile virus transmission and ecology in birds. *Ann. N. Y. Acad. Sci.*, **951**: 54–57.

Morin, P.J. 1981. Predatory salamanders reverse the outcome of competition among three species of anuran tadpoles. *Science (80-.).*, **212**: 1286–1288.

Mosher, B.A., Huyvaert, K.P. and Bailey, L.L. 2018. Beyond the swab: ecosystem sampling to understand the persistence of an amphibian pathogen. *Oecologia*, **188**: 319–330. Springer Berlin Heidelberg.

Muths, E., Bailey, L.L., Lambert, B.A. and Schneider, S.C. 2018. Estimating the probability of movement and partitioning seasonal survival in an amphibian metapopulation. *Ecosphere*, **9**: 1–15.

Nathan, R., Getz, W.M., Revilla, E., Holyoak, M., Kadmon, R., Saltz, D., *et al.* 2008. A movement ecology paradigm for unifying organismal movement research. *Proc. Natl. Acad. Sci. U. S. A.*, **105**: 19052–19059.

Ocock, J.F., Rowley, J.J.L., Penman, T.D., Rayner, T.S. and Kingsford, R.T. 2013. Amphibian chytrid prevalence in an amphibian community in arid Australia. *Ecohealth*, **10**: 77–81.

Park, A.W. 2012. Infectious disease in animal metapopulations: The importance of environmental transmission. *Ecol. Evol.*, **2**: 1398–1407.

Perrin, N. and Mazalov, V. 2000. Local competition, inbreeding, and the evolution of sex-biased dispersal. *Am. Nat.*, **155**: 116–127.

Petersen, C.E., Lovich, R.E., Phillips, C.A., Dreslik, M.J. and Lannoo, M.J. 2016. Prevalence and Seasonality of the Amphibian Chytrid Fungus Batrachochytrium dendrobatidis Along Widely Separated Longitudes Across the United States. *Ecohealth*, **13**: 368–382. Springer US.

Piotrowski, J.S., Annis, S.L. and Longcore, J.E. 2004. Physiology of Batrachochytrium dendrobatidis, a chytrid pathogen of amphibians. *Mycologia*, **96**: 9–15.

Pittman, S.E., Osbourn, M.S. and Semlitsch, R.D. 2014. Movement ecology of amphibians: A missing component for understanding population declines. *Biol. Conserv.*, **169**: 44–53. Elsevier Ltd.

Pullen, K.D., Best, A.M. and Ware, J.L. 2010. Amphibian pathogen Batrachochytrium dendrobatidis prevalence is correlated with season and not urbanization in central Virginia. *Dis. Aquat. Organ.*, **91**: 9–16.

Raffel, T.R., Michel, P.J., Sites, E.W. and Rohr, J.R. 2010. What Drives Chytrid Infections in

Newt Populations ? Associations with Substrate , Temperature , and Shade. *Ecohealth*, **7**: 526–536.

Rakus, K., Ronsmans, M. and Vanderplasschen, A. 2017. Behavioral fever in ectothermic vertebrates. *Dev. Comp. Immunol.*, **66**: 84–91. Elsevier Ltd.

Real, L.A. and Biek, R. 2007. Spatial dynamics and genetics of infectious diseases on heterogeneous landscapes. *J. R. Soc. Interface*, **4**: 935–948.

Rebollar, E.A., Woodhams, D.C., LaBumbard, B., Kielgast, J. and Harris, R.N. 2017. Prevalence and pathogen load estimates for the fungus Batrachochytrium dendrobatidis are impacted by ITS DNA copy number variation. *Dis. Aquat. Organ.*, **123**: 213–226.

Retallick, R.W.R. and Miera, V. 2007. Strain differences in the amphibian chytrid Batrachochytrium dendrobatidis and non-permanent, sub-lethal effects of infection. *Dis. Aquat. Organ.*, **75**: 201–207.

Rittenhouse, T.A.G., Semlitsch, R.D. and Thompson, F.R. 2015. Survival Costs Associated with Wood Frog Breeding Migrations : Effects of Timber Harvest and Drought Published by : Ecological Society of America Linked references are available on JSTOR for this article : You may need to log in to JSTOR to access the lin. *Ecology*, **90**: 1620–1630.

Roche, B., Dobson, A.P., Guégan, J.F. and Rohani, P. 2012. Linking community and disease ecology: The impact of biodiversity on pathogen transmission. *Philos. Trans. R. Soc. B Biol. Sci.*, **367**: 2807–2813.

Rollins-Smith, L.A. 1998. Metamorphosis and the amphibian immune system. *Immunol. Rev.*, **166**: 221–230.

Rothermel, B.B., Miller, D.L., Travis, E.R., McGuire, J.L.G., Jensen, J.B. and Yabsley, M.J. 2016. Disease dynamics of red-spotted newts and their anuran prey in a montane pond community. *Dis. Aquat. Organ.*, **118**: 113–127.

Rothermel, B.B., Walls, S.C., Mitchell, J.C., Jr, C.K.D., Irwin, L.K., Green, D.E., *et al.* 2008. Widespread occurrence of the amphibian chytrid fungus Batrachochytrium dendrobatidis in the southeastern USA. *Dis. Aquat. Organ.*, **82**: 3–18.

Ruggeri, J., De Carvalho-E-silva, S.P., James, T.Y. and Toledo, L.F. 2018. Amphibian chytrid infection is influenced by rainfall seasonality and water availability. *Dis. Aquat. Organ.*, **127**: 107–115.

Ryce, E.K.N., Zale, A. V., MacConnell, E. and Nelson, M. 2005. Effects of fish age versus size on the development of whirling disease in rainbow trout. *Dis. Aquat. Organ.*, **63**: 69–76.

Sapsford, S.J., Alford, R.A. and Schwarzkopf, L. 2013. Elevation , Temperature , and Aquatic Connectivity All Influence the Infection Dynamics of the Amphibian Chytrid Fungus in Adult Frogs. *PLoS One*, **8**: 1–13.

Sapsford, S.J., Roznik, E.A., Alford, R.A. and Schwarzkopf, L. 2014. Visible implant elastomer marking does not affect short-term movements or survival rates of the treefrog litoria rheocola. *Herpetologica*, **70**: 23–33.

Scheele, Ben C, Pasmans, F., Skerratt, L.F., Berger, L., Martel, A., Beukema, W., *et al.* 2019. Amphibian fungal panzootic causes catastrophic and ongoing loss of biodiversity. **1463**: 1459–1463.

Scheele, Ben C., Pasmans, F., Skerratt, L.F., Berger, L., Martel, A., Beukema, W., *et al.* 2019. Amphibian fungal panzootic causes catastrophic and ongoing loss of biodiversity. *Science (80-.).*, **1463**: 1459–1463.

Scholthof, K.G. 2007. The disease triangle : pathogens , the environment and society. **5**: 152–156.

Searcy, C.A., Gilbert, B., Krkošek, M., Rowe, L. and McCauley, S.J. 2018. Positive correlation between dispersal and body size in green frogs (Rana clamitans) naturally colonizing an experimental landscape. *Can. J. Zool.*, **96**: 1378–1384.

Searle, C.L., Gervasi, S.S., Hua, J., Hammond, J.I., Relyea, R.A., Olson, D.H., *et al.* 2011. Differential Host Susceptibility toBatrachochytrium dendrobatidis, an Emerging Amphibian Pathogen. *Conserv. Biol.*, **25**: 965–974.

Searle, C.L., Mendelson, J.R., Green, L.E. and Duffy, M.A. 2013. Daphnia predation on the amphibian chytrid fungus and its impacts on disease risk in tadpoles. *Ecol. Evol.*, **3**: 4129–4138.

Semlitsch, R.D. 2008. Differentiating Migration and Dispersal Processes for Pond-Breeding Amphibians. *J. Wildl. Manage.*, **72**: 260–267.

Semlitsch, R.D. 2000. Principles for Management of Aquatic-Breeding Amphibians. *J. Wildl. Manage.*, **64**: 615–631.

Shepard, E.L.C., Wilson, R.P., Rees, W.G., Grundy, E., Lambertucci, S.A. and Vosper, S.B. 2013. Energy landscapes shape animal movement ecology. *Am. Nat.*, **182**: 298–312.

Sinsch, U. 2014. Movement ecology of amphibians: From individual migratory behaviour to spatially structured populations in heterogeneous landscapes1,2. *Can. J. Zool.*, **92**: 491–502.

Skerratt, L.F., Berger, L., Speare, R., Cashins, S., McDonald, K.R., Phillott, A.D., *et al.* 2007. Spread of chytridiomycosis has caused the rapid global decline and extinction of frogs. *Ecohealth*, **4**: 125–134.

Smith, M.A. and Green, D.M. 2005. Dispersal and the metapopulation paradigm in amphibian ecology and conservation: Are all amphibian populations metapopulations? *Ecography (Cop.).*, **28**: 110–128.

Snodgrass, J.W., Komoroski, M.J., Bryan, A.L. and Burger, J. 2000. Relationships among isolated wetland size, hydroperiod, and amphibian species richness: Implications for wetland regulations. *Conserv. Biol.*, **14**: 414–419.

Sonn, J.M., Utz, R.M. and Richards-Zawacki, C.L. 2019. Effects of latitudinal, seasonal, and daily temperature variations on chytrid fungal infections in a North American frog. *Ecosphere*, **10**.

Steiner, C.F. 2004. Daphnia dominance and zooplankton community structure in fishless ponds.

J. Plankton Res., **26**: 799–810.

Stuart, S.N., Chanson, J.S., Cox, N.A., Young, B.E., Rodrigues, A.S.L., Fischman, D.L., *et al.* 2004. Status and trends of amphibian declines and extinctions worldwide. *Science (80-.).*, **306**: 1783–1786.

Tardy, O., Massé, A., Pelletier, F. and Fortin, D. 2018. Interplay between contact risk, conspecific density, and landscape connectivity: An individual-based modeling framework. *Ecol. Modell.*, **373**: 25–38. Elsevier.

Terrell, K.A., Quintero, R.P., Murray, S., Kleopfer, J.D., Murphy, J.B., Evans, M.J., *et al.* 2013. Cryptic impacts of temperature variability on amphibian immune function. *J. Exp. Biol.*, **216**: 4204–4211.

Tøttrup, A.P., Thorup, K., Rainio, K., Yosef, R. and Lehikoinen, E. 2008. Avian migrants adjust migration in response to environmental conditions en route. 685–688.

Tournier, E., Besnard, A., Tournier, V. and Cayuela, H. 2017. Manipulating waterbody hydroperiod affects movement behaviour and occupancy dynamics in an amphibian. *Freshw. Biol.*, **62**: 1768–1782.

Tracey, J.A., Bevins, S.N., Vandewoude, S. and Crooks, K.R. 2014. An agent-based movement model to assess the impact of landscape fragmentation on disease transmission. *Ecosphere*, **5**: 1–24.

Trenham, P.C., Koenig, W.D. and Shaffer, H.B. 2001. Spatially Autocorrelated Demography and Interpond Dispersal in the Salamander Ambystoma californiense. *Ecology*, **82**: 3519–3530.

van Dijk, J.G.B., Kleyheeg, E., Soons, M.B., Nolet, B.A., Fouchier, R.A.M. and Klaassen, M. 2015. Weak negative associations between avian influenza virus infection and movement behaviour in a key host species, the mallard Anas platyrhynchos. *Oikos*, **124**: 1293–1303.

Van Rooij, P., Martel, A., Haesebrouck, F. and Pasmans, F. 2015. Amphibian chytridiomycosis: A review with focus on fungus-host interactions. *Vet. Res.*, **46**: 1–22. BioMed Central.

Van Sluys, M. and Hero, J.M. 2009. How does chytrid infection vary among habitats? the case of Litoria wilcoxii (Anura, Hylidae) in SE Queensland, Australia. *Ecohealth*, **6**: 576–583.

VanderWaal, K.L. and Ezenwa, V.O. 2016. Heterogeneity in pathogen transmission: mechanisms and methodology. *Funct. Ecol.*, **30**: 1606–1622.

Vasconcelos, D. and Calhoun, A. 2004. Movement Patterns of Adult and Juvenile Rana sylvatica (LeConte) and Ambystoma maculatum (Shaw) in Three Restored Seasonal Pools in Maine. *J. Herpetol.*, **38**: 551–561.

Voyles, J., Rosenblum, E.B. and Berger, L. 2011. Interactions between Batrachochytrium dendrobatidis and its amphibian hosts : a review of pathogenesis and immunity. *Microbes Infect.*, **13**: 25–32. Elsevier Masson SAS.

Vredenburg, V.T., Knapp, R.A., Tunstall, T.S. and Briggs, C.J. 2010. Dynamics of an emerging disease drive large-scale amphibian population extinctions. *Proc. Natl. Acad. Sci. U. S. A.*, **107**: 9689–9694.

Watling, J.I. and Braga, L. 2015. Desiccation resistance explains amphibian distributions in a fragmented tropical forest landscape. *Landsc. Ecol.*, 1449–1459. Springer Netherlands.

Welicky, R.L. and Sikkel, P.C. 2015. Decreased movement related to parasite infection in a diel migratory coral reef fish. *Behav. Ecol. Sociobiol.*, **69**: 1437–1446.

Whiles, M.R., Lips, K.R., Pringle, C.M., Kilham, S.S., Bixby, R.J., Brenes, R., *et al.* 2006. The effects of amphibian population declines on the structure and function of neotropical stream ecosystems. *Front. Ecol. Environ.*, **4**: 27–34.

Worthington, H., McCrea, R., King, R. and Griffiths, R. 2019. Estimating abundance from multiple sampling capture-recapture data via a multi-state multi-period stopover model. *Ann. Appl. Stat.*, **13**: 2043–2064.

Zipkin, E.F., DiRenzo, G. V., Ray, J.M., Rossman, S. and Lips, K.R. 2020. Tropical snake diversity collapses after widespread amphibian loss. *Science (80-.).*, **367**: 814–816.

Chapter 1 Tables

Table 1.1. Summary table of ponds at the PA study area. Description of the 11 ponds sampled at the PA study area. Includes hydroperiod categorization, pond size, estimated newt abundance, and calculated newt density.

Site	Hydroperiod	Area (m^2)	Year	Abundance	Density
A04	Short	155	2019	19	0.125
			2020	15	0.098
A05	Short	152	2019	17	0.111
			2020	29	0.196
A10	Short	527	2019	43	0.082
			2020	9	0.016
A11	Short	269	2018	82	0.305
			2019	92	0.342
			2020	44	0.163
P1	Long	561	2018	658	1.174
			2019	435	0.776
			2020	442	0.788
P2	Long	1196	2019	228	0.190
			2020	206	0.172
P3	Short	249	2019	92	0.367
			2020	64	0.258
SC36	Long	1759	2019	476	0.270
			2020	65	0.037
SC37	Long	1869	2019	2539	1.358
			2020	1920	1.027
SC38	Short	141	2018	54	0.379
			2019	65	0.463
			2020	19	0.136
SC47	Short	302	2019	96	0.319
			2020	45	0.150

Table 1.2. Parameter definitions. Definitions for individual, temporal, and spatial parameters used in the temporal and spatial model sets.

Type	Parameter	Model Term	Definition
Individual	Sex	Sex	Male or female
	Snout-Vent-Length	SVL	Measurement from tip of snout to posterior opening of cloaca (mm)
Temporal	Julian date	Julian	Continuous count of the number of days beginning at Jan 1 each year
	Year	Year	Year sampled: 2018, 2019, or 2020
	Water temperature	Temp	24 hour daily average water temperature day of sampling event
	Water temperature 1 week prior	Temp1w	Weekly average water temperature one week before sampling event
	Water temperature 2 weeks prior	Temp2w	Weekly average water temperature two weeks before sampling event
	Air temperature 1 week prior	AirMax1w	Weekly average maximum air temperature one week before sampling event
	Air temperature 2 weeks prior	AirMax2w	Weekly average maximum air temperature two weeks before sampling event
Spatial	Host abundance	Abundance	Estimated abundance for each pond for 2019 and 2020
	Host density	Density	Calculated density by dividing abundance by pond area
	Hydroperiod	HP	Categorized as short or long based on inundation period and duration of larval development
	Pond	Site	Individual ponds at each study area
	Study area	Study Area	Locations where newt sampling occurred: MA, PA, or WI

Table 1.3. Temperature-related models for infection prevalence and intensity. Total of 6 models for each response variable. The best fit model was selected by comparing models using AIC values.

Response		Model	df	Log likelihood	AICc	ΔAICc	Akaike weight
Infection status		**Temp2w + Temp2w² + SVL + Sex + Year**	**7**	**-448.3**	**910.6**	**0**	**0.696**
		Temp + Temp² + SVL + Sex + Year	7	-449.4	913.0	2.34	0.216
		Temp1w + Temp1w² + SVL + Sex + Year	7	-450.3	914.8	4.13	0.088
		AirMax1w + AirMax1w² + SVL + Sex + Year	7	-494.5	1003.0	92.41	0
		AirMax2w + AirMax2w² + SVL + Sex + Year	7	-522.4	1058.9	148.31	0
	Null:	SVL + Sex + Year	5	-555.5	1120.9	210.32	0
Infection intensity		**Temp + Temp² + SVL + Sex + Year**	**8**	**-2920.6**	**5857.4**	**0**	**0.975**
		Temp1w + Temp1w² + SVL + Sex + Year	8	-2924.3	5864.7	7.33	0.025
		AirMax1w + AirMax1w² + SVL + Sex + Year	8	-2929.5	5875.2	17.79	0
		Temp2w + Temp2w² + SVL + Sex + Year	8	-2942.7	5901.5	44.10	0
		AirMax2w + AirMax2w² + SVL + Sex + Year	8	-2948.0	5912.1	54.71	0
	Null:	SVL + Sex + Year	6	-2978.0	5968.0	110.63	0

Table 1.4. Spatial-related models for infection prevalence and intensity. Total of 6 models for each response variable. The best fit model was selected by comparing models using AIC values.

Response		Model	df	Log likelihood	AICc	ΔAICc	Akaike weight
Infection status		**Density + SVL + Sex + Year + Temp2w + Temp2w²**	**8**	**-633.0**	**1282.1**	**0.00**	**0.448**
		HP + Density + SVL + Sex + Year + Temp2w + Temp2w²	9	-632.0	1282.2	0.05	0.438
		Abundance + SVL + Sex + Year + Temp2w + Temp2w²	8	-635.4	1286.8	4.66	0.043
	Null:	SVL + Sex + Year + Temp2w + Temp2w²	7	-636.6	1287.3	5.19	0.033
		HP + Abundance + SVL + Sex + Year + Temp2w + Temp2w²	9	-634.9	1287.9	5.79	0.025
		HP + SVL + Sex + Year + Temp2w + Temp2w²	8	-636.6	1289.2	7.04	0.013
Infection intensity		**HP + SVL + Sex + Year + Temp + Temp²**	**9**	**-4109.3**	**8236.7**	**0.00**	**0.205**
		Density + SVL + Sex + Year + Temp + Temp²	9	-4109.4	8236.9	0.21	0.184
		HP + Density + SVL + Sex + Year + Temp + Temp²	10	-4108.4	8236.9	0.27	0.179
		Abundance + SVL + Sex + Year + Temp + Temp²	9	-4109.5	8237.0	0.34	0.173
	Null:	SVL + Sex + Year + Temp + Temp²	8	-4110.6	8237.2	0.57	0.154
		Abundance + HP + SVL + Sex + Year + Temp + Temp²	10	-4105.0	8238.0	1.35	0.104

Table 1.5. Summary table of study areas for *N. viridescens* populations. Summary of number of observations, unique individuals, and captures swabbed categorized by pond and years sampled.

Study Area	Site ID	Years Sampled	Days Individuals Were Found	Unique Individuals	Total Captures	Total Swabbed
PA	SC37	2019	23	1117	1531	386
		2020	25	1188	1595	388
	P1	2018	12	343	474	326
		2019	22	421	869	317
		2020	31	467	1117	389
	A11	2018	11	65	94	86
		2019	20	110	298	143
		2020	25	69	246	110
	SC38	2018	10	108	152	131
		2019	20	92	254	120
		2020	24	90	190	86
	P2	2019	13	176	296	89
		2020	11	162	257	145
	SC47	2019	7	79	146	60
		2020	10	32	50	16
	SC36	2019	6	79	85	36
		2020	5	36	48	34
	P3	2019	7	55	77	55
		2020	9	24	29	18
	A10	2019	5	30	39	25
		2020	4	5	9	4
	A05	2019	4	12	12	5
		2020	6	22	23	11
	A04	2019	2	7	7	7
		2020	7	12	15	4
MA	SPR1	2019	16	389	445	434
		2020	24	1219	1694	1563
	SPR2	2019	12	77	100	93
		2020	6	11	12	12
	SPR3	2019	5	40	54	49
WI	EC	2018	12	214	322	320
		2019	12	-	466	466
		2020	12	-	434	434
	ML	2018	12	168	266	245
		2019	12	-	217	217
		2020	11	-	185	185

Table 1.6. Study area temperature-related models for infection prevalence and intensity. A total of three models were fitted to our combined dataset: an additive model, an interactive model, and a null model. The best fit model was selected by comparing models using AIC values.

Response		Model	df	Log likelihood	AICc	ΔAICc	Akaike weight
Infection		**AirMax1w + AirMax1w² + SA + (AirMax1w + AirMax1w²)*SA + Sex + Year**	**13**	**-1951.4**	**3928.9**	**0.00**	**1**
status		AirMax1w + AirMax1w² + SA + Sex + Year	9	-1978.9	3975.8	46.91	0
	Null:	SA + Sex + Year	7	-2116.2	4246.3	635.71	0
Infection		**AirMax1w + AirMax1w² + SA + (AirMax1w + AirMax1w²)*SA + Sex + Year**	**14**	**-10199.8**	**20427.6**	**0.00**	**1**
intensity		AirMax1w + AirMax1w² + SA + Sex + Year	10	-10217.5	20455.1	27.49	0
	Null:	SA + Sex + Year	8	-10240.6	20497.3	69.66	0

Table 1.7. Study area Julian day-related models for infection prevalence and intensity. A total of three models were fitted to our combined dataset: an additive model, an interactive model, and a null model. The best fit model was selected by comparing models using AIC values.

Response		Model	df	Log likelihood	AICc	ΔAICc	Akaike weight
Infection		**Julian + Julian² + SA + (Julian + Julian²)*SA + Sex + Year**	**13**	**-1792.8**	**3611.6**	**0.00**	**1**
status		Julian + Julian² + + SA + Sex + Year	9	-1821.7	3661.5	49.86	0
	Null:	SA + Sex + Year	7	-2116.2	4246.3	634.71	0
Infection		**Julian + Julian² + SA + (Julian + Julian²)*SA + Sex + Year**	**14**	**-10137.0**	**20302.2**	**0.00**	**0.994**
intensity		Julian + Julian² + SA + Sex + Year	10	-10146.1	20312.3	10.13	0.006
	Null:	SA + Sex + Year	8	-10242.3	20496.7	194.52	0

Chapter 2 Figures

Figure 1.1. Physiological characteristics of a male newt: We visually determined the sex of individuals by identifying males with characteristics such as larger hind legs, larger and darker cloaca, nuptial pads behind the hind legs, and larger and broader tail fins.

Figure 1.2. Female newt coloration pattern: Top: Female newt with a lighter band along her tail. Bottom: Male newt without a lighter band and a larger tailfin.

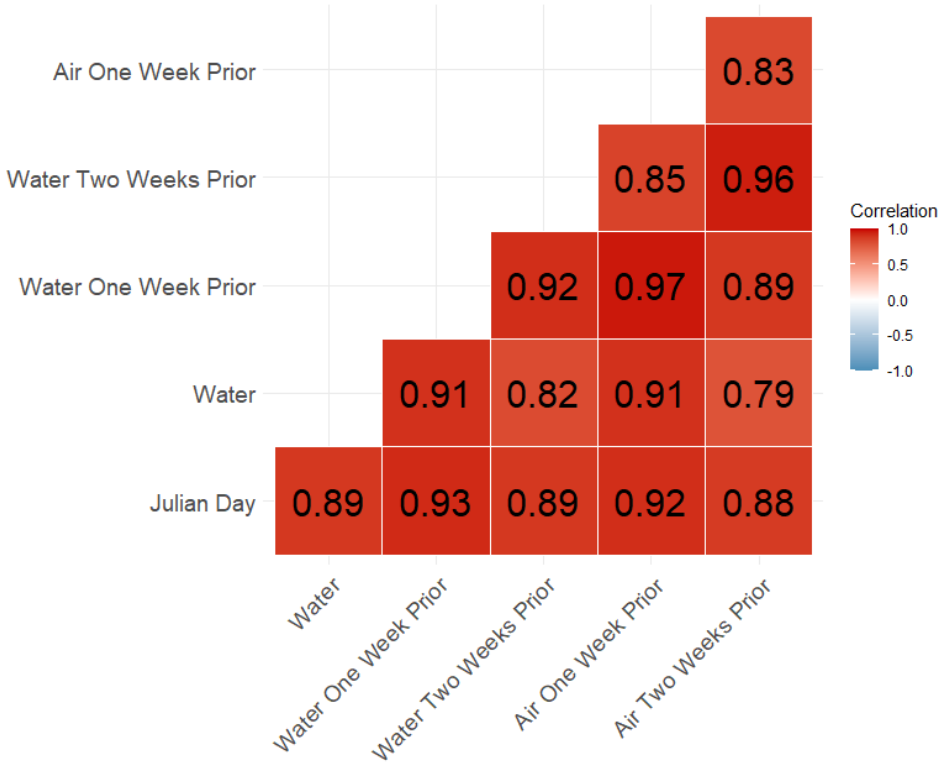

Figure 1.3. Correlations for temperatures and Julian day: Correlation plot of the temperatures from the four ponds equipped with temperature probes in the PA study area for a total of 52 unique Julian days from 2019 to 2020.

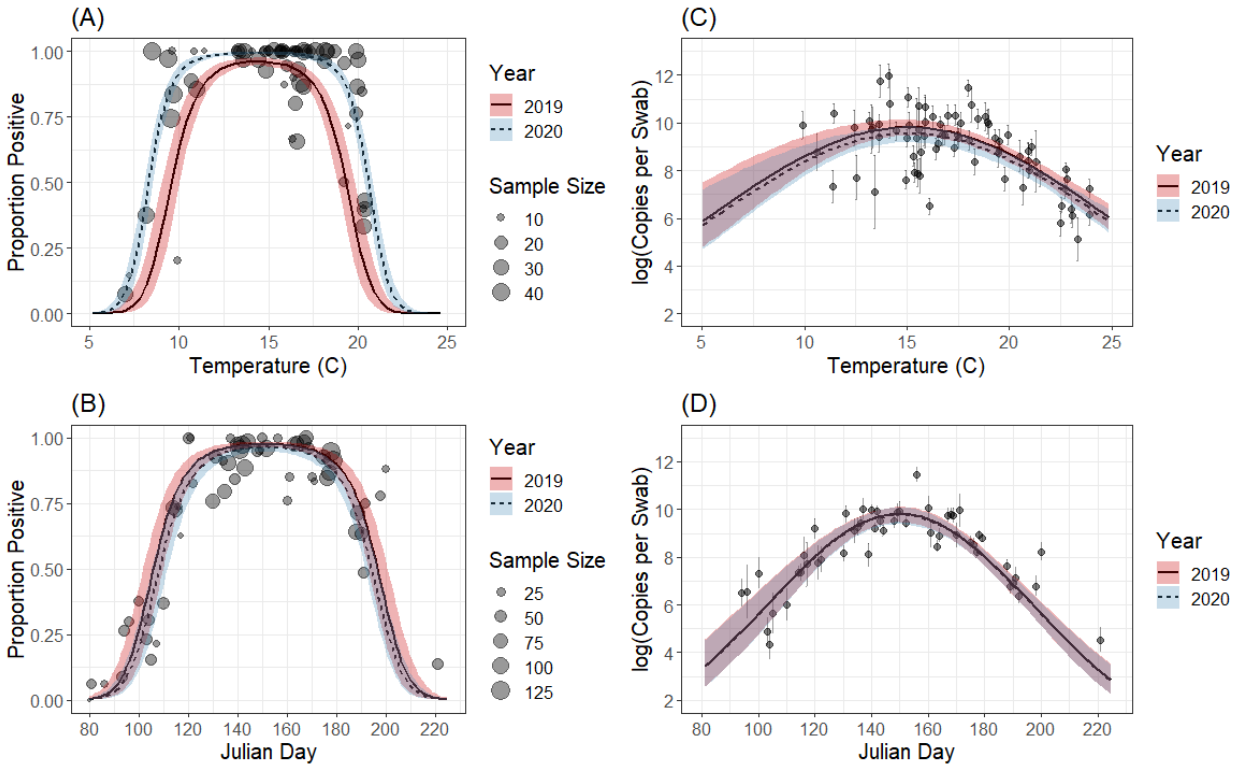

Figure 1.4. Infection prevalence and intensity by temperature and Julian date for the PA study area: (A) Infection prevalence by temperature. Each point represents the total number of swabs collected at that temperature. (B) Infection prevalence by julian day. Each point represents the total number of swabs collect on that julian day. (C) Infection intensity by temperature. Each point represents mean intensity at that temperature with standard error. (D) Infection intensity by julian day. Each point represents mean intensity at that julian day with standard error. We used the same dataset for (A) and (B) as well as for (C) and (D). The datasets only included observations from the four ponds equipped with temperature probes. The color fill represents the 95% confidence interval calculated after 10,000 iterations.

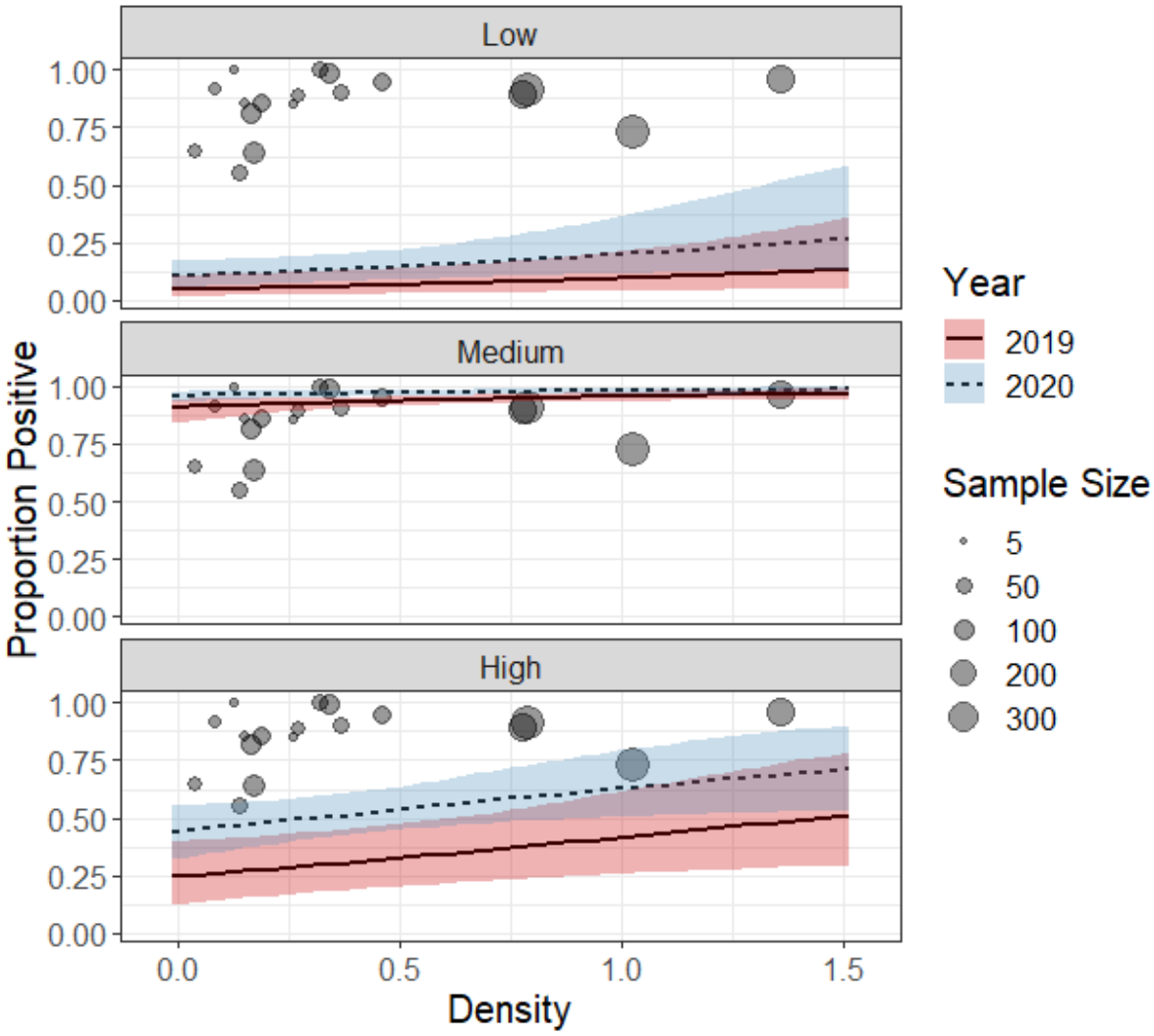

Figure 1.5. Prevalence and host density: The dataset included all 11 ponds at the PA study area. Because temperature influenced prevalence greatly, we have three different temperatures: 1) Low: 7.3 C, the minimum temperature, 2) Medium: 16.5 C, the median temperature, 3) and High: 20.3, the maximum temperature. Although non-significant (coef. = 0.91, CI: -0.018 – 1.843; p = 0.054), infection prevalence is increasing as host density increases. The color fill represents the 95% confidence interval calculated after 10,000 iterations. Each point represents the total number of swabs collect at that density.

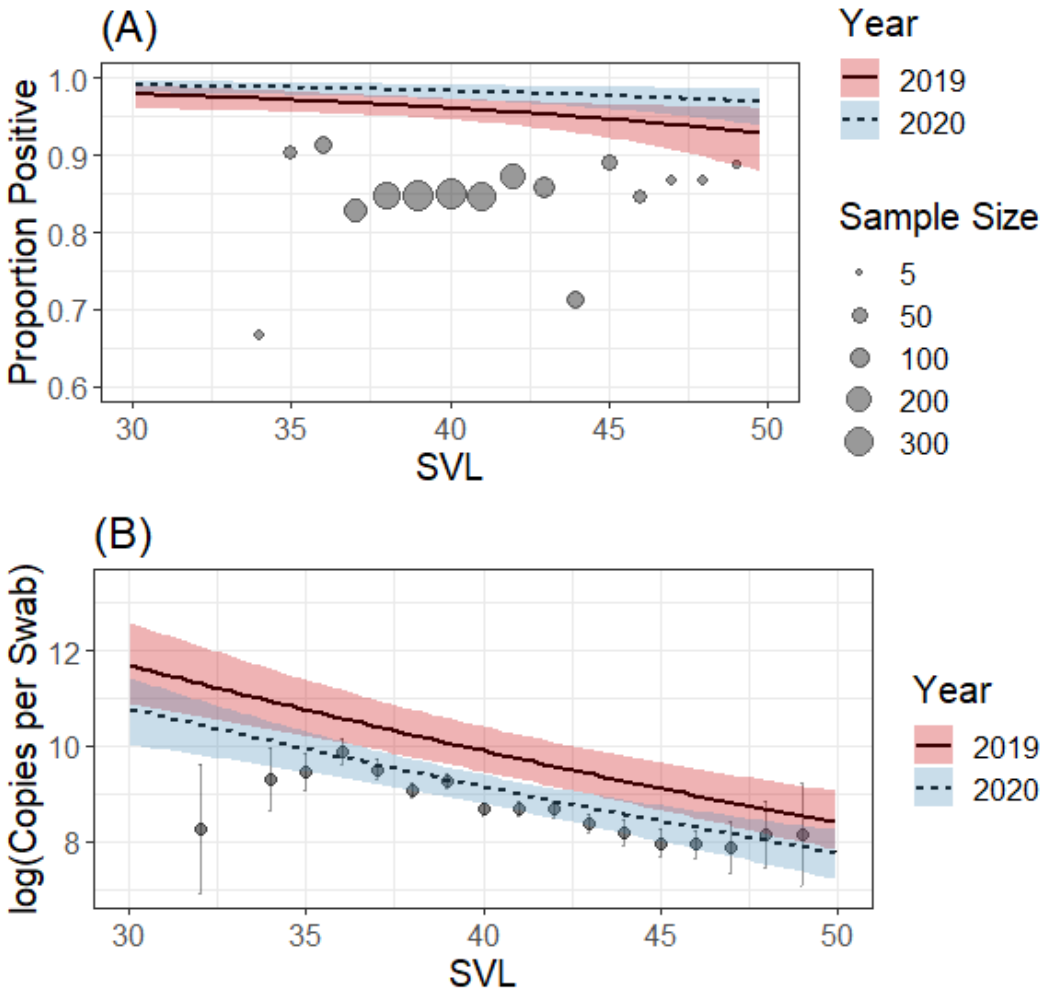

Figure 1.6. Infection trends with SVL: (A) Infection prevalence and (B) intensity patterns by SVL. The dataset included all eleven ponds in PA. We used the among-pond covariate models to construct this figure due to having more observations and including individuals from all our ponds. Although SVL was non-significant for infection prevalence (coef. = -0.15; CI: -0.33 – 0.03; $p = 0.095$), it was significant for infection intensity (coef. = -0.05; CI: -0.07 – -0.03; $p < 0.001$). The color fill represents the 95% confidence interval calculated after 10,000 iterations. Each point represents (A) the total number of swabs collected at that SVL and (B) mean intensity at that SVL with standard error.

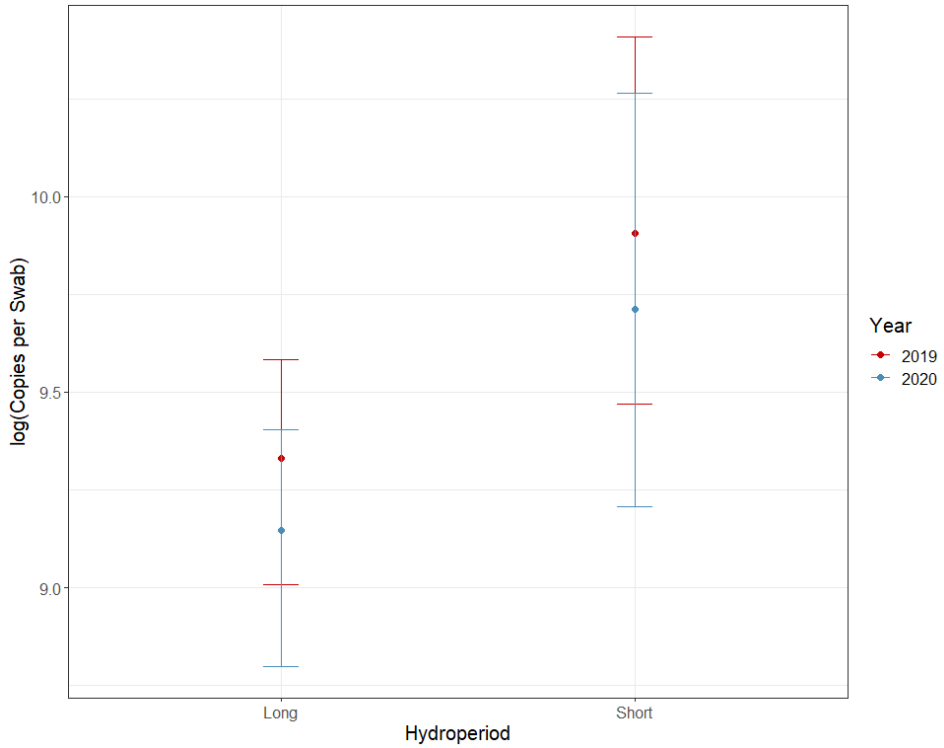

Figure 1.7. Intensity and hydroperiod: Hydroperiod of the ponds were categorized as either long or short. We used observations from all eleven ponds at our PA study area with seven short hydroperiods and four long hydroperiods. Hydroperiod was not significant (coef. = 0.06; CI: -0.01, 0.13; p = 0.079). The bars represent the 95% confidence interval calculated after 10,000 iterations.

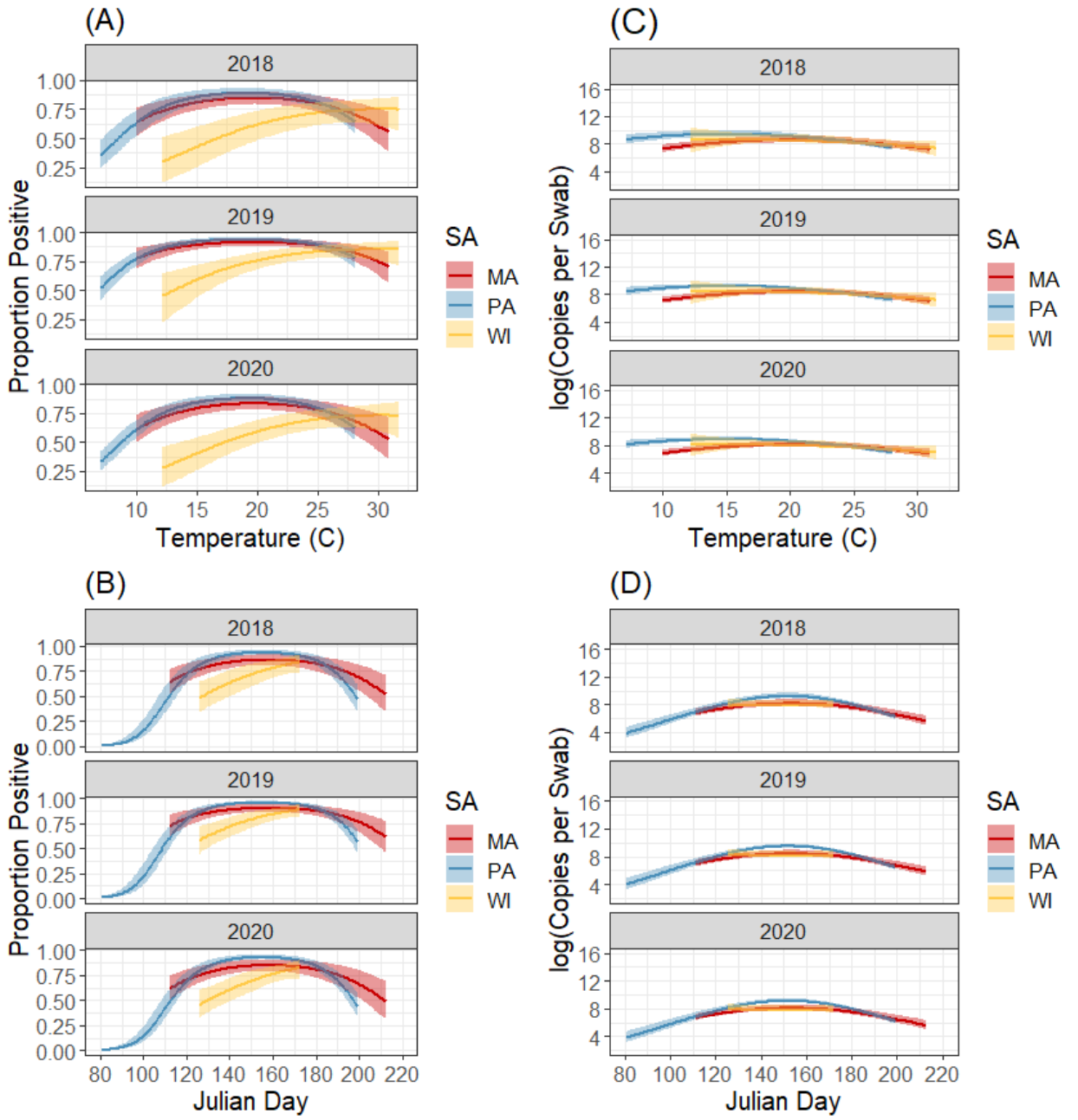

Figure 1.8. Study areas – infection, temperature, and Julian date: We used the same dataset for Julian day and temperature for infection prevalence as well as for Julian day and temperature for infection intensity. The datasets used combined observations from all three study areas. (A) Infection prevalence by temperature for the three study areas. (B) Infection prevalence by Julian day for the three study areas. (C) Infection intensity by temperature for the three study areas. (D) Infection intensity by Julian day for the three study areas.

Chapter Two: Connectivity of ponds through movement of a host species and its implications for disease spread

ABSTRACT

Movement of individuals across the landscape and between populations are crucial for determining pathogen dynamics and disease risk in wild populations. While the importance of movement on disease transmission has been recognized, the challenges of simultaneously measuring movement and infection state for many species makes it difficult to characterize connectivity and transmission networks in many host-pathogen systems. Doing this requires not only quantifying overall rates of movement and connectivity, but also understanding how infection state affects movement and how movement affects infection state. In pond-breeding amphibians, the connectivity between ponds is determined by rates of interpatch movements and such movements can potentially influence the disease dynamics of the amphibian fungal pathogen, *Batrachochytrium dendrobatidis*. We sought to answer (1) how connected twelve ponds in central Pennsylvania were through the interpatch movements of adult *Notophthalmus viridescens*, (2) how the probability of movements related to individual infection state (infection intensity and infection status), and (3) how infection state was affected by the choice to move. We used capture-mark-recapture sampling methods to track individuals across four years and modeled transition probabilities between the ponds as well as the relationship between within- and between-year movements and infection state. We found that 10% of a pond's adult newt population emigrated to other ponds with higher movement rates between closer proximity ponds. Additionally, we observed a trend where infected individuals were less likely to move compared to healthy conspecifics. Lastly, our results demonstrate that within-year movements were important for seasonal disease dynamics and resulted in lowered infections for individuals that moved. Our study is one of the first to examine the relationship between movement and *Bd* infection state of newts in the field.

Keywords: *Batrachochytrium dendrobatidis*, connectivity, interpatch movement, dispersal, *Notophthalmus viridescens*

INTRODUCTION

The movement of individuals across space and time can have important implications for the conservation of wildlife, specifically when considering disease spread and persistence in populations (Semlitsch, 2008; Altizer *et al.*, 2011; Dougherty *et al.*, 2018; Muths *et al.*, 2018). Movements from one location to another can alter transmission risk for susceptible individuals and infection severity for infected individuals as they interact with different abiotic and biotic factors (Watling and Braga, 2015; Daversa *et al.*, 2017). Susceptible individuals can become infected either through 1) indirect transmission when they encounter pathogens that were shed by infected individuals along their movement paths or when they move through environmental disease hotspots, and 2) direct transmission when susceptible individuals come into contact with infected individuals while moving or after relocating to a disease hot spot (Park, 2012; Dougherty *et al.*, 2018). Conversely, migratory escape can occur when an individual leaves a habitat before becoming infected or recover (migratory recovery) when infections are reduced and cleared by moving away from ideal conditions for the pathogen (Altizer *et al.*, 2011; Daversa, Manica, *et al.*, 2018; Daversa, Monsalve-Carcaño, *et al.*, 2018). To understand infectious disease dynamics among populations, it is important to investigate the relationship between host movements and infections.

Different types of host movements can have impacts on disease within (meta-) populations of wildlife (Boulinier *et al.*, 2016). Individual movements can determine the connectivity of different populations as well as habitats and the rate at which these movements occur can affect disease dynamics. Migratory movements are seasonal and involve large numbers of individuals that concentrate at high densities, and pathogen transmission can occur when infected and susceptible individuals interact (Altizer *et al.*, 2011; Boulinier *et al.*, 2016). Dispersal movements occur when individuals relocate from natal habitat to novel locations to breed, and these type of movements can lead to interpatch colonization for diseases (Sinsch, 2014; Boulinier *et al.*, 2016). While the majority of dispersal studies focus on juvenile dispersal, adult breeding dispersal does occur (Trenham *et al.*, 2001; Joly, 2019). Additionally, the movement between patches (interpatch movements), can determine the connectivity of habitats and the persistence of populations across the landscape (Bowne *et al.*, 2006; Sinsch, 2014).

These interpatch movements are important to consider when investigating pathogen transmission and persistence (Muths *et al.*, 2018).

The internal state of individuals (physiological or neurological) can affect their movement capacity and consequently movement patterns (Nathan *et al.*, 2008; Pittman *et al.*, 2014). When considering infection as an internal state, disease can alter host movements (Binning *et al.*, 2017). Infected individuals may have lowered body condition either when resources are allocated for immune responses or are lost to the pathogen (Lochmiller and Deerenberg, 2000; Lafferty and Shaw, 2013; Dougherty *et al.*, 2018). Additionally, host manipulation via chemical or physical modification can affect an individual's capacity for locomotion (van Dijk *et al.*, 2015; Welicky and Sikkel, 2015). Infected individuals can also modify their movement behavior as a response to infection. In some ectothermic vertebrates, movement to warmer places can increase body temperature and cause a "behavioral fever" to help combat infections (Rakus *et al.*, 2017). These mechanisms can potentially increase or decrease an individual's movement patterns and result in population-wide consequences. For example, queen snakes, *Regina septemvittata,* infected with snake fungal disease had reduced emigration and immigration rates and infected grousewinged backswimmers, *Notonecta undulata*, by *Hydrachnidia* mites had reduced dispersal ability (Baines *et al.*, 2020; McKenzie *et al.*, 2021). Although movement is crucial in understanding disease dynamics, there are few studies that incorporate both due to the difficulty of obtaining movement data of individuals and tracking disease across time. In the few studies of movement and wildlife disease, birds and mammals are well studied while taxa such as amphibians are still lacking (Dougherty *et al.*, 2018).

Amphibians are among the most at-risk taxa with a third of the world's species declining due to multiple factors such as habitat loss, climate change, and disease (Stuart *et al.*, 2004; Adams *et al.*, 2013; Grant *et al.*, 2016). One such disease, chytridiomycosis caused by the fungal pathogen *Batrachochytrium dendrobatidis* (hereafter, "*Bd*"), has been directly or indirectly responsible for the decline of over 500 amphibian species worldwide (Ben C. Scheele *et al.*, 2019). *Bd* can be transmitted either through direct contact between individuals or through environmental transmission with the motile stage and can persist in aquatic environments from two weeks to several years (Longcore *et al.*, 1999; Johnson and Speare, 2003; Mosher *et al.*,

2018). In amphibian populations with chytridiomycosis, symptoms include lethargy, abnormal posture, and the loss of right reflex in anurans, all of which affect movement ability (Voyles *et al.*, 2011). *Bd*'s ability to persist in the environment along with pond-breeding amphibians reliance on clusters of aquatic habitats that can occur in close proximity of one another, makes it important to investigate the connectivity of ponds through individual movement to understand potential drivers of disease spread (Semlitsch, 2008; Heard *et al.*, 2012; Pittman *et al.*, 2014).

Eastern red-spotted newts (hereafter, "newts") are a common and highly mobile species that can potentially facilitate the movement and spread of *Bd* among aquatic and terrestrial habitats. Newts occupy a variety of habitats that range from ephemeral pools to more permanent bodies of water across the eastern United States (Gates and Thompson, 1982; Gabor and Nice, 2004). In populations where breeding migration occurs, newts vary in how far and when they migrate (differential migration) and in the proportion of the population that migrates (partial migration) in and out of aquatic habitats (Hurlbert, 1963; Grayson and Wilbur, 2009). Newts are also known to have high prevalence and low intensities of *Bd* infections (Rothermel *et al.*, 2008, 2016; Groner and Relyea, 2010; Raffel *et al.*, 2010, Chapter 1). These characteristics may allow for increased contact rate between infected newts and other susceptible amphibian hosts as well as environmental shedding of *Bd* in the aquatic and terrestrial environment. While the annual migrations of newts are well studied (Hurlbert, 1963; Gill, 1978a; b), there are few studies on the interpatch movement of *N. viridescens* during breeding season. If movement of individuals among ponds does occur, the rates of newt movements may be enough to spread disease between ponds in close proximity.

Although annual migrations of amphibians have been documented (Semlitsch, 2008; Bailey and Muths, 2019), the few studies on the connectivity of patches and populations through the movement of individuals in consideration of disease have focused on more mobile and larger taxa (Tracey *et al.*, 2014; Borg *et al.*, 2017; Tardy *et al.*, 2018). In this study, we investigated the connectivity of a network of ponds by examining interpatch movements of newts, the displacement of an individual from one pond to another. We focused on three objectives: 1) to estimate the proportion of interpatch movements of adult newts, 2) to determine whether the infection state of newts as well as other individual characteristics and timing affects their propensity to move among ponds, and 3) to determine whether the decision to move affects the

infection state of individuals that do move wetlands (Figure 2.1). We predicted that movement probability will be greater among ponds that are closer to one another. Furthermore, we predicted that infected newts that move will either lower or clear their infections and that susceptible newts that move will be less likely to become infected. We also predicted that infected newts were more likely to move to help combat infections via migratory recovery. Finally, we predicted that male newts will be more mobile due to density-dependent factors and larger individuals more mobile because of reduced movement costs.

METHODS

Study Area

We studied movement and *Bd* infection status of newts in a network of twelve ponds in central Pennsylvania that varied in size, hydrology, and amphibian community. The overall network of twelve ponds can be sub-divided into three smaller clusters of ponds with the shortest distance between ponds within a cluster being forty meters and longest distance between ponds in different clusters being 582 meters (Figure 2.2). The maximum area at peak inundation of the ponds ranged from 125 m^2 to 1869 m^2. Of the twelve ponds, eight are ephemeral ponds that completely dry in mid-to-late summer in every year while four are semi-permanent, drying in some years and not in others. Another eleven ponds occur within the same area but we never detected newts within them despite repeated surveys. All of these unoccupied sites were characterized by short hydroperiods (generally drying earlier in the summer than the other ephemeral wetlands where newts occurred). The local abundances of newts in occupied ponds vary among ponds and changed within seasons. In general, newts became active in ponds and were regularly observed soon after ice melted each spring. Numbers observed stayed steady until declining later in the summer as ponds began to approach drying out. Other amphibian species that occur in the ponds include *Ambystoma jeffersonianum, Ambystoma maculatum, Hyla chrysoscelis, Lithobathes clamitans, Lithobates sylvatica*, and *Pseudacris crucifer*.

Data Collection

We repeatedly sampled each pond multiple times across the active season annually from 2018 to 2021, although sampling effort differed between the ponds based on inundation and availability. We began sampling as soon as ponds cleared of ice and snow in March and continued until mid to late summer when most of the ponds are completely dry in August, and newts were rare in samples from ponds that still contained water. We attempted to sample ponds weekly and continued to do so as long as they remained inundated and newts were available for capture. During these surveys, newts were captured, marked, and released. To observe how individual infections change within a season, we also conducted *Bd* surveys where newts were also sampled for *Bd* presence during three to four separate week-long sessions each season. Start and end dates for each year varied according to weather, pond type, and availability. We sampled three ponds in 2018 for a total of thirteen days and all twelve ponds in 2019 for a total of forty-nine days, in 2020 for a total of fifty-six days, and in 2021 for a total of twenty-nine days.

We captured and processed newts individually to avoid cross-contamination. Newts were captured by dragging a dipnet along the edges of a pond, and once captured, were held individually in a plastic bag. We used ultraviolet flashlights while newts were in the plastic bags to identify previously marked individuals through Visual Implant Elastomer (VIE) marks. When identified as a recaptured individual, another researcher confirmed VIE marks to reduce identification error. Once identified as a recaptured or new individual, during our *Bd* sampling surveys, unique newts were then swabbed once using a sterile, rayon-tipped dry swab (MW-113). We used new gloves for each animal and swabbed newts five times each at the inner thigh region, inner arm region, alongside the stomach, under the chin, alongside the back, and on both sides of the tail for a total of thirty-five times. Unique newts caught a second time in the same week were not resampled, but if the same animal was caught multiple times within a year on separate weeks, we collected samples during each encounter.

In addition to sampling newts for *Bd*, we also measured length, determined their sex, and gave newly caught individuals a unique mark. We measured snout-vent-length (SVL; mm) for newts. Males were determined by assessing physical characteristics such as darker and swollen cloaca, larger tail fin and hindlegs, and nuptial pads on the hind legs that occur earlier in the breeding season. Upon initial capture, newly caught newts were marked with VIE, which have

been shown to not affect individual survival or movements (Northwest Marine Technology, Shaw Island, Washington USA; Sapsford *et al.*, 2014). Each unique individual was given a unique six-color combination consisting of four colors (blue, orange, red, and yellow) immediately behind the front legs, immediately in front of the back legs, and immediately behind the back legs at the base of the tail. The colors used for the two tail marks were kept unique to a pond to clearly identify the pond an individual was first caught in as well as minimize the likelihood of misidentifying a movement among ponds. Animals were released at approximately the same capture location.

Bd Sampling

We used quantitative polymerase chain reaction (qPCR) to quantify *Bd* zoospores in our swab samples and determined individual infection status (positive if *Bd* was detected in the sample) and infection intensity (estimated *Bd* zoospore copies per swab given an individual was positive; Boyle *et al.*, 2004; Hyatt *et al.*, 2007; Rebollar *et al.*, 2017). We extracted DNA from swabs as described by Hyatt et al. (2007) except that 125 µl of PrepMan® Ultra Sample Preparation Reagent (Applied Biosystems, Foster City, CA) and 100 mg of zirconium/silica beads (Biospec Products, Bartlesville, OK) were used so that the entire swab was immersed during the procedure, and the bead-beating steps were conducted using a FastPrep®-24 homogenizer (MP Biomedicals, Santa Ana, CA). We ran reactions on the 7500 fast real-time PCR system (Applied Biosystems, Foster City, CA) using QuantiFast Probe RT-PCR mastermix kit with ROX dye (Qiagen, Valencia, CA) and BSA as per the kit instructions. We used five microliters of the PrepMan® solution containing the extracted DNA as template for the PCR. We included a negative extraction control and a standard curve run in duplicate on each PCR plate. The standard curve consisted of five different concentrations of the target sequence for *Bd* included from commercially synthesized single gene block (gBlock, Integrated DNA Technologies, Coralville, IA). The concentrations of the standards occurred at ten-fold dilutions ranging from 110-1,100,000 copies (0.5 fg – 5000 fg DNA) per reaction. The threshold for signal detection was set at 5% of the maximum fluorescence of the standards run for that assay. We calculated the efficiency of each run using standard curve amplification and repeated PCR plates with an efficiency of less than 90% or greater than 110%.

Statistical Analysis

Movement Rates – We used capture-mark-recapture (CMR) sampling and a multi-state multi-period stopover model, developed by Worthington et al. (2019) and modified by Davis et al. (*in review*; 2020), to estimate adult newt interpatch movements. We fit the among-season movement model from Davis et al. (*in review*, Davis 2020), where site fidelity is assumed to be constant among ponds and cumulative movement rates represent the total movement from the beginning of one year to the beginning of the next. We were interested specifically in two parameters estimated by the model: 1) the annual proportion of animals in a given pond that moved to another pond within our network each year and 2) the relative probability of movement to a new pond as a function of a distance based on a distance-dependent dispersal kernel. We fit the model using a dataset that consisted of multiple captured individuals, both swabbed and unswabbed, across our four years of sampling. We used a Gaussian kernel for our distance-dependent dispersal function (Fujiwara *et al.*, 2006) to describe the probabilities of an individual dispersing from one pond to another. The function follows the form of a half-normal distribution, with relative probabilities governed by the estimated σ for the function. Unlike Davis et al. (*in review*; Davis 2020), whom fit their model to data for *A. maculata* which are known to skip returning to breeding ponds in some years, we did not allow for temporary emigration within years. Furthermore, we assumed all individuals were present at the beginning of the year but that individuals could leave the population available for capture as the season went on. Additionally, we fixed survival rate to be constant for all observations and allowed for detection rates to vary among years. By accounting for incomplete detection, we were able to generate true estimates of overall movement probabilities and connectivity for out populations.

Relationships between movement and infection state – To address our other two objectives, understanding how infection state was related to the probability of moving and how moving affected future infection states, we limited data to individuals caught and sampled for *Bd* at least two times. We separated data into within-year recaptures and between-years recaptures, allowing us to isolate short-term and long-term movement-infection interactions. We paired captures of the same unique individual to obtain an initial capture and an end capture and these pairs served as the sample unit for all analyses (hereafter, "capture pair"). Infection status and infection intensity were measured on each sampling day in a capture pair to determine if

infection states changed between captures. Because of our CMR sampling method, we defined movement as the same unique individual captured at different ponds between the two sampling dates in a capture pair. For within-year analyses, for each individual we selected only the capture pair with the largest gap in days between captures to increase our chance of observing movement. If an individual made within-year movements in multiple years, we only selected the capture pair in the first year. For between-year movements, we only included capture pairs with a one-year gap between captures and included all the capture pairs for the same unique individual if they made multiple between-year movements across different years.

When fitting models, we controlled for additional factors that might affect movement and infection state interactions. For within-year analyses, we calculated the number of days between captures to account for the length of time between observations. We also considered the initial capture Julian day and the end Julian day as potential covariates to standardize for seasonal variation in movement probabilities. For each capture in our capture pairs, we included two measurements of disease: 1) infection status (positive or negative for infection) and infection intensity (severity of infection in a positive individual). To account for seasonality of infection, we used residuals from a previous study for our infection intensity measurements (Chapter 1). Lastly, we included individual sex and SVL to determine if either affected movement rates of newts. We fit generalized linear mixed models to estimate relationships, using a logit-link function and binomial distribution for movement probability and probability of infection and an identity-link function and Gaussian distribution for *Bd* intensity residuals. We selected among different model parameterizations based on AIC. All analyses were conducted using R (R Core Team, 2021) with the package, lme4 (v.1.1-26, Bates, Douglas).

We first analyzed our data to determine if newt movement between ponds was influenced by infection status or intensity. We considered four different datasets for models. These differed in whether data were for movements within- or between-year movements and the explanatory variable for infection state used to predict movement (infected or not; or infection intensity of infected individuals). For our within-year dataset, our full model included one of the infection measurements, initial capture Julian day, gap between captures, sex, and SVL as fixed effects and pond as a random effect to account for multiple sampling from the same ponds. Between-year models were similar except we excluded gap between captures since we only selected one-

year gap pairs and included unique individual as another random effect. We then considered all combinations of removing one or both individual-level covariates to see which model best fit our datasets. For our Julian day covariates, we considered both linear and quadratic relationship.

Next, we wanted to examine how infection state could be affected by movement. Again, we had four different datasets for each infection measurement and movement type. Our full within-year infection status models included movement, initial infection status, end Julian day, gap between captures, sex, and SVL as fixed effects with pond as a random effect. Our full between-year model did not include gap between captures, but did include both initial and end Julian day and unique individual as a random effect. For our infection intensity model, we did not include Julian day since we used residuals from a previous model that accounted for Julian day already. Our full within-year infection intensity model included movement, initial infection intensity, gap between captures, sex, and SVL with pond as a random effect. The full between-year infection intensity model consisted of the same covariates except the removal of gap between captures and the addition of unique individual as a random effect. We again compared all combinations of models with or without the individual-level covariates while considering linear and quadratic relationships to find the best fit model for movement effects on infection state (Table 2.1).

RESULTS

Movement Rates

4,818 unique newts were used in our mark-recapture analysis. Adult newts exhibited high site fidelity (proportion remaining in the same pond from one year to the next being 0.904; SE = 0.0003) with the remaining ~10% of animals making interpatch movements to a different pond. Our results show that movement rates were higher between ponds that were closer in proximity and, therefore, within the same cluster. Our estimate of σ for the half-normal dispersal kernel was 0.25 km (Figure 2.3; 2.4). This is consistent with our raw data, where we observed that 85%

of movements (246 out of 288) were among ponds within 200 m of each other, 2% (7 out of 288) between 200 and 400 m, and 12% (35 out of 288) from 400 to 600 m. From our model, the individual pair of ponds with the highest estimated movement rates were P1 and P2, even though the distance between these two ponds were not shortest distance (143m) with 3% of newts predicted to move from P1 to P2 each year and 1.8% from P2 to P1 each year (Figure 2.3). In general, our model predicted that most movements were among ponds in the smaller clusters, although among cluster movements are non-negligible (Figure 2.4). The lowest rates of movement occurred between our longest distance ponds (482 – 582m) and were all less than 0.2%.

Relationships between movement and infection state

We captured and swabbed 564 unique individuals more than once within a breeding season and 225 unique individuals between one year (Table 1.2). Out of the 564 within-year capture pairs, 30 pairs showed movement with seven initially positive individuals. We observed 250 between-year capture pairs (some individuals made multiple movements between one year and the next) and found that 39 pairs showed movement. 31 of the 39 between-year capture pairs were initially positive.

Effect of infection status on movement – In general, we found that infected individuals were less likely to make within-year movements than healthy conspecifics, although confidence intervals included 0. In contrast, infection status had no relationship to the probability of between-year movements. Among models we fit for our within-year dataset, the best fit model included a quadratic effect of initial Julian day, a linear effect of SVL, and the gap between captures (Table 2.1). Infected newts had a lower probability of moving with an estimated effect size of 0.565. However, the confidence interval for the effect had a significant overlap with 0 (CI: -1.711 – 0.580; p = 0.334). Additionally, the model suggests that larger individuals had a higher probability of moving (coef. = 0.443; CI: 0.012 – 0.873; p = 0.044) and that smaller gaps between captures trended towards a higher probability of movement (coef. = -0.27; CI: -0.67 – 0.12; p = 0.173). Our best fit model for infection status effect on between-year movement included a linear effect of the start Julian day and sex. Infection status was unrelated to between-year movements (coef. = -0.006; CI: -1.034 – 1.023; p = 0.992), while earlier start Julian days

resulted in a higher probability of movement between years (coef. = -0.418; CI: -0.79 – -0.05; p = 0.027). Males, on average, tended to be less likely to move ponds between years; although the confidence interval of the effect still included 0 (coef. = -0.734; CI: -1.581 – 0.114; p = 0.090; Table 2.1).

Effect of infection intensity on movement – Our results suggest that infection intensity of individual newts has little effect on whether they moved among ponds both within- and between-years. Our best fit model for within-year movement and infection intensity included a quadratic effect of start Julian day, linear effect of SVL, and gap between captures and suggests little relationship between movement and infection intensity (coef. = 0.095; CI: -0.232 – 0.422; p = 0.570; Table 2.1). Similar to the relationship between size and within-year movements in the infection status model, larger individuals tended to be more likely to move (coef. = 0.737; CI: -0.256 – 1.729; p = 0.146). Furthermore, the longer the gap between captures in a capture pair, the less likely an individual would move (coef. = -1.992; CI: -3.539 – - 0.444; p = 0.012). For our between-year movement and intensity, the best fit model included a linear effect for initial Julian day and a linear effect for sex (Table 2.1). Again, intensity was unrelated to between-year movements (-0.003; CI: -0.220 – 0.214; p = 0.928). Males tended to be less likely to move between years than females (-0.868' CI: -1.870 – 0.134; p = 0.090), and starting Julian day was unrelated to between-year movements (coef. = 0.371; CI: -0.893 – 0.151; p =0.164).

Effect of movement on infection status – Individuals that make within-year movements tend to be less likely to be positive for *Bd* compared to those that did not move, and this trend is also seen with between-year movements. The best fit model when considering movement on infection status included a quadratic effect for the ending Julian day and a linear effect for sex, SVL, starting infection status, and the gap between captures (Table 2.1). Individuals that move were more likely to be negative when captured the second time (coef. = 1.121; CI: -2.184 – -0.058; p = 0.039; Figure 2.5b). This was after controlling for initial infection state, with individuals that were infected to start being more likely to be infected when they were recaptured whether they moved or not (0.848; CI: 0.182 – 1.513; p = 0.013). Our best fit model also suggests that longer gaps between captures results in higher probability of individual's being positive with the second capture (0.385; CI: 0.072 – 0.697; p = 0.016), while larger individuals were less likely to be positive (-0.362; CI: -0.625 – -0.099; p = 0.007). When considering

between-year movements, the best fit model did not include sex or SVL but included the starting status of individuals and a quadratic effect for both starting and ending Julian. There was only a weak negative relationship between among-year movement and ending infection state with wide overlap in the confidence interval with 0 (-0.358; CI: -1.470 – 0.754; p = 0.528) (Table 2.1). Whether an individual was infected or not was not related to the ending status the next year (coef. = 0.24; CI: -0.818 – 1.291; p = 0.661).

Effect of movement on infection intensity – Similar to our infection status results, within-year movements resulted in lower infection intensities while between-year movements had less of an effect on intensities. Our best fit model for within-year movement effects on infection intensity did not include sex or SVL but did include the gap between captures and the starting intensities of individuals (Table 2.1). The model suggests that individuals that moved had a lower infection intensity than those that did not move (coef. = -1.933; CI: -3.652 – -0.214 p = 0.028; Figure 2.5a). Again, their starting infection intensity did affect their ending intensity (coef. = 0.207; CI: 0.120 – 0.294; p < 0.001); however, the gap between captures was unrelated (coef. = -0.15; CI: -0.422 – 0.105; p = 0.239). With between-year movements, the best model excluded SVL but included individual starting intensities and sex. The best model suggested movement as unrelated when considering infection intensity from one year to the next (-0.331; CI: -1.666 – 1.005, p = 0.628) (Table 2.1). Starting intensities tend to result in higher ending intensities and males were more likely to have higher intensities, although confidence intervals contained 0 (coef. = 0.19; CI: -0.010 – 0.389; p = 0.066 and coef. = 0.85; CI: -0.02 – 1.72; p = 0.057, respectively).

DISCUSSION

We set out to determine the movement ecology underlying disease transmission networks in a chytrid-amphibian metapopulation. We demonstrate that movements among populations are frequent. In addition, we found that although infection state does not predict the probability newts move, newts that move were more likely to eliminate or reduce infection intensity are

moving. Our results suggest that interpatch connectivity for this host-pathogen system depends not only on rates of movement, but also on the behavioral effects of movement on infection persistence.

Our study demonstrates that ponds are interconnected through the movements of a widespread and common species that are relatively resistant to *Bd* infections. Although we could not estimate movement rates separately for within- and between-year movements, our model integrated both movement types. Our results are consistent with another study in the same network of ponds that focused on adult breeding dispersal of spotted salamanders (*A. maculatum*; Davis et al., *in review*). In contrast, another study on *N. viridescens* observed the lack of movements between ponds and may be attributed to site differences since the sampling effort and maximum distance between ponds were similar (< ~1 km; Gill, 1978a). Within our system, we observed higher exchanges of individuals among close proximity ponds than further distant ponds, but longer distance dispersal can occur, which is supported by other studies investigating distance effect on movement rates and with spotted salamander movements in the same network of ponds (Smith and Green, 2005; Bar-David *et al.*, 2007; Sinsch, 2014, Davis et al., *in review*). The longer the distance an individual needs to travel, the more costly the movement is (i.e. desiccation risk for amphibians; Pittman *et al.*, 2014; Rittenhouse *et al.*, 2015). Additionally, directionality of movements resulted in different movement rates and suggest differences in habitat characteristics can drive those movement rates. Previous research have shown that hydroperiod, population density, and habitat quality can influence movement between wetlands (Tournier *et al.*, 2017; Cayuela *et al.*, 2019; Barrile *et al.*, 2021). Because newts can have a high prevalence for infection at low intensities, their movements among the ponds may facilitate the transmission of disease to other populations and communities (Chapter 1). To better understand how newts may be spreading disease, we must also understand how movement and disease interact.

Studies have shown that the movement of individuals can be affected by infections across multiple host taxa and pathogens. In laboratory experiments, lobsters (*Panulirus argus* Latreille) infected with *Panulirus argus* Virus 1 moved less than healthy conspecifics and became sedentary as the infection increased while movement capacity of *Lithobates pipiens* infected with *Bd* was lower for infected individuals in performance experiments (Behringer *et al.*, 2008;

Chatfield *et al.*, 2013). Empirical studies that tracked movements in French grunts infected with *Anilocra haemuli*, pool frogs (*Pelophylax lessonae*) infected with *Bd*, and mallards (*Anas platyrhynchos*) infected with avian influenza virus showed that movements were decreased in infected individuals (van Dijk *et al.*, 2015; Welicky and Sikkel, 2015; Kärvemo *et al.*, 2020). These reductions in movements may be attributed to lower body conditions from infection. Kopecký et al. (2010) found that the body condition of male *Mesotriton alpestris* that changed wetlands was higher than those that stayed. Additionally, *Bd* exposure trials with infected frogs resulted in lower body condition from weight loss (Retallick and Miera, 2007). Another explanation may be that the costs of movement while infected is greater than staying in place and dealing with infection. Movements from one location to another are physiologically costly and moving while infected can result in mortality (Altizer *et al.*, 2011; Shepard *et al.*, 2013). While confidence intervals for our estimates all included zero, the general trend for our results were in the direction of healthier individuals moving more than infected individuals, but if infected, higher infected individuals moved more. This study was limited to the subset of individuals that were recaptured in our ponds and cannot rule out that differences in the observed populations occurred because of mortality associated with movements (e.g., if higher mortality occurred in infected individuals that moved than those that did not move). Future work should measure infections on individuals as they are leaving and entering ponds to improve our understanding of how infection affects movement. Despite this, our results do suggest that infected individuals, even if they move less frequently, still do make regular interpatch movements that may facilitate pathogen transmission to new populations.

In contrast to infection affecting movement, we did find strong and consistent relationship on how movement affects infection. Within-year movements are associated with lower infections, which may indicate the importance of movements in seasonal infection dynamics. Conversely, between-year movements were unrelated to infection and may suggest other mechanisms that drive between-year infection patterns or that effects of movement on infection dynamics are transient and dissipate with time. Individuals that moved within-years were less likely to be positive and had lower infection intensities if they were initially positive. Although we could not measure infections while newts were traveling between ponds, this period away from the aquatic environment may itself facilitate reductions in infection load. By leaving the aquatic environment, newts are leaving ideal conditions for *Bd*, since *Bd* is reliant on

moisture and low temperatures to grow and survive (Piotrowski *et al.*, 2004; Berger *et al.*, 2005). In infection experiments with adult alpine newt (*Ichthyosaura alpestris*), individuals that left the aquatic environment were more likely to recover from infection or reduce their infection intensity (Daversa, Manica, *et al.*, 2018). With between-year infections, movements from one year to the next did not affect infection status or intensity. Our population of newts likely return to terrestrial habitat post-breeding season, and may be able to clear infections via migratory recovery before returning to the ponds the next breeding season; therefore, affecting infection levels the first time they were caught the following year. In our system, infection levels are cyclical and low early in the season when newts are returning to the ponds (Chapter 1). Additionally, the day of capture the following year in a capture pair is highly significant in determining infection status, further supporting the idea that within-year infection dynamics are more important in determining the current infection state of individuals compared to previous infections from the prior year. Other studies have also found migratory recovery post-breeding migration (Kinney *et al.*, 2011; Daversa, Monsalve-Carcaño, *et al.*, 2018).

Interestingly, within-year movement rates were better explained by individual size and between-year movements by sex. Larger individuals may have better body condition and have lower costs of movement such as lower dehydration risk and higher locomotor capabilities (Watling and Braga, 2015). This hypothesis is supported by multiple amphibian studies including *Lithobates sylvatica*, *Triturus cristatus*, *Lithobathes clamitans*, and *Aneides aeneus* (Mazerolle, 2001; Denoël *et al.*, 2018; Searcy *et al.*, 2018; John *et al.*, 2019). While size was important for within-year movements, sex was more important in determining the probability we observed between-year movements. Our results show that males were less likely to move to a different pond from one year to the next, which may be explained by local mate competition (Perrin and Mazalov, 2000). In addition to a male-biased sex ratio, males arrive earlier to the ponds before females (Bloch and Grayson, 2010; Grayson *et al.*, 2012). Males may remain closer to ponds during post-breeding season and have higher between-year site fidelity to maximize breeding opportunities (Johnson *et al.*, 2007; Cayuela *et al.*, 2019). Females may be choosier where they go from year to year and may travel further from ponds than males, which may result in more between-year movement. Additionally, Grayson et al. (2012) reported changes in female behavior and body condition based on male mating harassment in male-biased environments and can potentially influence how females are selecting ponds between years. A previous study on

spotted salamanders (*A. maculatum*) in the same network of ponds as our study found that female spotted salamanders had higher site fidelity (Davis et al., *in review*). Other studies have shown that females travel more (Johnson *et al.*, 2007), males had higher site fidelity (Vasconcelos and Calhoun, 2004), males travel more (Denoël *et al.*, 2018), or that there were no differences between sexes (Kopecký *et al.*, 2010).

Host movements have been recognized as crucial for understanding how infectious diseases spread and persist in the landscape as well as in populations; yet the challenges of tracking individuals and disease across time and space have made it difficult to investigate such relationships (Sinsch, 2014; Dougherty *et al.*, 2018; Muths *et al.*, 2018; Bailey and Muths, 2019). Our study demonstrates the connectivity of wetlands through newt movement both between years and within breeding seasons and is not limited to juvenile dispersal. More broadly, our study supports the growing literature on the relationships between infectious disease and host movement patterns (Dougherty *et al.*, 2018). Infections can impact host behavior and movement capabilities, but hosts can also alter disease risk through their movement decisions. While our study was limited to examining movement between captures, different sampling methods could help determine infections as individuals move in and out of ponds. Additionally, investigating within pond movements and microhabitat usage may give further insights to how finer scale movements can affect infections. By determining how movements affect infections and vice versa, we can improve our understanding of how pathogens can be transmitted into populations and habitats.

REFERENCES

Adams, A.J., Kupferberg, S.J., Wilber, M.Q., Pessier, A.P., Grefsrud, M., Bobzie, S., *et al.* 2017. Extreme drought, host density, sex, and bullfrogs influence fungal pathogen infection in a declining lotic amphibian. *Ecosphere*, **8**.

Adams, M.J., Miller, D.A.W., Muths, E., Corn, P.S., Grant, E.H.C., Bailey, L.L., *et al.* 2013. Trends in Amphibian Occupancy in the United States. *PLoS One*, **8**: 6–10.

Altizer, S., Bartel, R., Han, B.A., Altizer, S., Bartel, R. and Han, B.A. 2011. Animal Migration and Infectious Disease Risk. *Science (80-.).*, **331**: 296–302.

Altizer, S., Dobson, A., Hosseini, P., Hudson, P. and Pascual, M. 2006. Seasonality and the dynamics of infectious diseases. 467–484.

Ando, K., Hammar, S. and Grumet, R. 2009. Age-related resistance of diverse Cucurbit fruit to infection by phytophthora capsici. *J. Am. Soc. Hortic. Sci.*, **134**: 176–182.

Bailey, L.L. and Muths, E. 2019. Integrating amphibian movement studies across scales better informs conservation decisions. *Biol. Conserv.*, **236**: 261–268. Elsevier.

Baines, C.B., Diab, S. and McCauley, S.J. 2020. Parasitism risk and infection alter host dispersal. *Am. Nat.*, **196**: 119–131.

Bar-David, S., Segev, O., Peleg, N., Hill, N., Templeton, A.R., Schultz, C.B., *et al.* 2007. Long-distance movements by fire salamanders (Salamandra infraimmaculata) and implications for habitat fragmentation. *Isr. J. Ecol. Evol.*, **53**: 143–159.

Barrile, G.M., Walters, A., Webster, M. and Chalfoun, A.D. 2021. Informed breeding dispersal following stochastic changes to patch quality in a pond-breeding amphibian. *J. Anim. Ecol.*, **90**: 1878–1890.

Behringer, D.C., Butler, M.J. and Shields, J.D. 2008. Ecological and physiological effects of PaV1 infection on the Caribbean spiny lobster (Panulirus argus Latreille). *J. Experiemental Mar. Biol. Ecol.*, **359**: 26–33.

Beldomenico, P.M. and Begon, M. 2010. Disease spread, susceptibility and infection intensity: vicious circles? *Trends Ecol. Evol.*, **25**: 21–27.

Berger, L., Hyatt, A.D., Speare, R. and Longcore, J.E. 2005. Life cycle stages of the amphibian chytrid Batrachochytrium dendrobatidis. *Dis. Aquat. Organ.*, **68**: 51–63.

Berger, L., Speare, R., Daszak, P., Green, D.E., Cunningham, A.A., Goggin, C.L., *et al.* 1998. Chytridiomycosis causes amphibian mortality associated with population declines in the rain forests of Australia and Central America. *Proc. Natl. Acad. Sci. U. S. A.*, **95**: 9031–9036.

Berger, L., Speare, R., Hines, H.B., Marantelli, G., Hyatt, A.D., Donald, K.R.M.C., *et al.* 2004. Effect of season and temperature on mortality in amphibians due to chytridiomycosis. *Aust. Vet. J.*, **82**: 434–439.

Binning, S.A., Shaw, A.K. and Roche, D.G. 2017. Parasites and host performance: Incorporating infection into our understanding of animal movement. *Integr. Comp. Biol.*, **57**: 267–280.

Blehert, D.S., Hicks, A.C., Behr, M., Meteyer, C.U., Brenda, M., Buckles, E.L., *et al.* 2009. Bat White-Nose Syndrome: An Emerging Fungal Pathogen? *Science (80-.).*, **323**: 227.

Bloch, A.M. and Grayson, K.L. 2010. Reproductive costs of migration for males in a partially migrating, pond-breeding amphibian. *Can. J. Zool.*, **88**: 1113–1120.

Boots, M. and Bowers, R.G. 2004. The evolution of resistance through costly acquired immunity. *Proc. R. Soc. B Biol. Sci.*, **271**: 715–723.

Borg, N.J., Mitchell, M.S., Lukacs, P.M., Mack, C.M., Waits, L.P. and Krausman, P.R. 2017. Behavioral connectivity among bighorn sheep suggests potential for disease spread. *J. Wildl. Manage.*, **81**: 38–45.

Boulinier, T., Kada, S., Ponchon, A., Dupraz, M., Dietrich, M., Gamble, A., *et al.* 2016. Migration, Prospecting, Dispersal? What Host Movement Matters for Infectious Agent Circulation? *Integr. Comp. Biol.*, **56**: 330–342.

Bowne, D.R., Bowers, M.A. and Hines, J.E. 2006. Connectivity in an agricultural landscape as reflected by interpond movements of a freshwater turtle. *Conserv. Biol.*, **20**: 780–791.

Boyle, D.G., Boyle, D.B., Olsen, V., Morgan, J.A.T. and Hyatt, A.D. 2004. Rapid quantitative detection of chytridiomycosis (Batrachochytrium dendrobatidis) in amphibian samples using real-time Taqman PCR assay. *Dis. Aquat. Organ.*, **60**: 141–148.

Brannelly, L.A., Hunter, D.A., Lenger, D., Scheele, B.C., Skerratt, L.F. and Berger, L. 2015. Dynamics of Chytridiomycosis during the Breeding Season in an Australian Alpine Amphibian. *PLoS One*, **10**: 1–15.

Brannelly, L.A., Martin, G., Llewelyn, J., Skerratt, L.F. and Berger, L. 2018. Age- and size-dependent resistance to chytridiomycosis in the invasive cane toad Rhinella marina. *Dis. Aquat. Organ.*, **131**: 107–120.

Brannelly, L.A., Ohmer, M.E.B., Saenz, V. and Richards-Zawacki, C.L. 2019. Effects of hydroperiod on growth, development, survival and immune defences in a temperate amphibian. *Funct. Ecol.*, **33**: 1952–1961.

Burrow, A.K., Rumschlag, S.L. and Boone, M.D. 2017. Host size influences the effects of four isolates of an amphibian chytrid fungus. *Ecol. Evol.*, **7**: 9196–9202.

Casadevall, A. and Pirofski, L. anne. 2018. What is a host? Attributes of individual susceptibility. *Infect. Immun.*, **86**: 1–12.

Cayuela, H., Schmidt, B.R., Weinbach, A., Besnard, A. and Joly, P. 2019. Multiple density- -dependent processes shape the dynamics of a spatially structured amphibian population. *J. Anim. Ecol.*, 164–177.

Chatfield, M.W.H., Brannelly, L.A., Robak, M.J., Freeborn, L., Lailvaux, S.P. and Richards-Zawacki, C.L. 2013. Fitness consequences of infection by batrachochytrium dendrobatidis in northern leopard frogs (Lithobates pipiens). *Ecohealth*, **10**: 90–98.

Daszak, P., Cunningham, A.A. and Hyatt, A.D. 2000. Emerging infectious diseases of wildlife - Threats to biodiversity and human health. *Science (80-.).*, **287**: 443–449.

Daversa, D.R., Fenton, A., Dell, A.I., Garner, T.W.J. and Manica, A. 2017. Infections on the move: How transient phases of host movement influence disease spread. *Proc. R. Soc. B Biol. Sci.*, **284**.

Daversa, D.R., Manica, A., Bosch, J., Jolles, J.W. and Garner, T.W.J. 2018. Routine habitat switching alters the likelihood and persistence of infection with a pathogenic parasite. *Funct. Ecol.*, **32**: 1262–1270.

Daversa, D.R., Monsalve-Carcaño, C., Carrascal, L.M. and Bosch, J. 2018. Seasonal migrations, body temperature fluctuations, and infection dynamics in adult amphibians. *PeerJ*, **2018**: 1–17.

Davis, C.L., Teitsworth, E.W. and Miller, D.A.W. 2018. Combining Data Sources to Understand Drivers of Spotted Salamander (Ambystoma maculatum) Population Abundance. *J. Herpetol.*, **52**: 116–126.

Denoël, M., Dalleur, S., Langrand, E., Besnard, A. and Cayuela, H. 2018. Dispersal and alternative breeding site fidelity strategies in an amphibian. *Ecography (Cop.).*, **41**: 1543–1555.

Denoël, M. and Lehmann, A. 2006. Multi-scale effect of landscape processes and habitat quality on newt abundance: Implications for conservation. *Biol. Conserv.*, **130**: 495–504.

Dougherty, E.R., Seidel, D.P., Carlson, C.J., Spiegel, O. and Getz, W.M. 2018. Going through the motions: incorporating movement analyses into disease research. *Ecol. Lett.*, **21**: 588–604.

Dube, D., Kim, K., Alker, A.P. and Harvell, C.D. 2002. Size structure and geographic variation in chemical resistance of sea fan corals Gorgonia ventalina to a fungal pathogen. *Mar. Ecol. Prog. Ser.*, **231**: 139–150.

Fujiwara, M., Anderson, K.E., Neubert, M.G. and Caswell, H. 2006. On the estimation of dispersal kernels from individual mark-recapture data. *Environ. Ecol. Stat.*, **13**: 183–197.

Gabor, C.R. and Nice, C.C. 2004. Genetic Variation among Populations of Eastern Newts , Notophthalmus viridescens : A Preliminary Analysis Based on Allozymes. *Her*, **60**: 373–386.

Gahl, M.K., Longcore, J.E. and Houlahan, J.E. 2011. Varying Responses of Northeastern North American Amphibians to the Chytrid Pathogen Batrachochytrium dendrobatidis. *Conserv. Biol.*, **26**: 135–141.

Garner, T.W.J., Walker, S., Bosch, J., Leech, S., Rowcliffe, J.M., Cunningham, A.A., *et al.* 2009. Life history tradeoffs influence mortality associated with the amphibian pathogen Batrachochytrium dendrobatidis. *Oikos*, **118**: 783–791.

Gates, J.E. and Thompson, E.L. 1982. Small Pool Habitat Selection by Red-Spotted Newts in Western Maryland. *J. Herpetol.*, **16**: 7–15.

Gill, D.E. 1978a. Effective Population Size and Interdemic Migration Rates in a Metapopulation of the Red-Spotted Newt, Notophthalmus viridescens (Rafinesque). *Evolution (N. Y).*, **32**: 839.

Gill, D.E. 1978b. The Metapopulation Ecology of the Red-Spotted Newt, Notophthalmus viridescens (Rafinesque). *Ecol. Monogr.*, **48**: 145–166.

Grant, E.H.C., Miller, D.A.W., Schmidt, B.R., Adams, M.J., Amburgey, S.M., Chambert, T., *et al.* 2016. Quantitative evidence for the effects of multiple drivers on continental-scale amphibian declines. *Sci. Rep.*, **6**: 1–9.

Grassly, N.C. and Fraser, C. 2006. Seasonal infectious disease epidemiology. *Proc. R. Soc. B Biol. Sci.*, **273**: 2541–2550.

Grayson, K.L., De Lisle, S.P., Jackson, J.E., Black, S.J. and Crespi, E.J. 2012. Behavioral and physiological female responses to male sex ratio bias in a pond-breeding amphibian. *Front. Zool.*, **9**.

Grayson, K.L. and Wilbur, H.M. 2009. Sex- and context-dependent migration in a pond-breeding amphibian. *Ecology*, **90**: 306–312.

Grogan, L.F., Robert, J., Berger, L., Skerratt, L.F., Scheele, B.C., Castley, J.G., *et al.* 2018. Review of the amphibian immune response to chytridiomycosis, and future directions. *Front. Immunol.*, **9**: 1–20.

Groner, M.L. and Relyea, R.A. 2010. Batrachochytrium dendrobatidis is Present in Northwest Pennsylvania , USA , with High Prevalence in Notophthalmus viridescens. *Herpetol. Rev.*, **41**: 462–465.

Heard, G.W., Scroggie, M.P. and Malone, B.S. 2012. Classical metapopulation theory as a useful paradigm for the conservation of an endangered amphibian. *Biol. Conserv.*, **148**: 156–166. Elsevier Ltd.

Hudson, M.A., Griffiths, R.A., Martin, L., Fenton, C., Adams, S.L., Blackman, A., *et al.* 2019. Reservoir frogs: Seasonality of Batrachochytrium dendrobatidis infection in robber frogs in Dominica and Montserrat. *PeerJ*, **2019**: 1–21.

Hurlbert, S.H. 1963. The Breeding Migrations and Interhabitat Wandering of the Vermilion-spotted Newt Notophthalmus Viridescens (Rafinesque). *Ecol. Monogr.*, **39**: 465–488.

Hyatt, A.D., Boyle, D.G., Olsen, V., Boyle, D.B., Berger, L., Obendorf, D., *et al.* 2007. Diagnostic assays and sampling protocols for the detection of Batrachochytrium dendrobatidis. *Dis. Aquat. Organ.*, **73**: 175–192.

John, R.R., Gitzen, R.A. and Guyer, C. 2019. Overnight Movements of Green Salamanders (Aneides aeneus) in Northern Alabama. *J. Herpetol.*, **53**: 158–164.

Johnson, J.R., Knouft, J.H. and Semlitsch, R.D. 2007. Sex and seasonal differences in the spatial terrestrial distribution of gray treefrog (Hyla versicolor) populations. *Biol. Conserv.*, **140**: 250–258.

Johnson, M.L. and Speare, R. 2003. Survival of Batrachochytrium dendrobatidis in water:

Quarantine and disease control implications. *Emerg. Infect. Dis.*, **9**: 922–925.

Joly, P. 2019. Behavior in a Changing Landscape: Using Movement Ecology to Inform the Conservation of Pond-Breeding Amphibians. *Front. Ecol. Evol.*, **7**: 1–17.

Kärvemo, S., Wikström, G., Widenfalk, L.A., Höglund, J. and Laurila, A. 2020. Chytrid fungus dynamics and infections associated with movement distances in a red-listed amphibian. *J. Zool.*, **311**: 164–174.

Kiesecker, J.M. and Skelly, D.K. 2001. Effects of disease and pond drying on gray tree frog growth, development, and survival. *Ecology*, **82**: 1956–1963.

Kilpatrick, A.M., Briggs, C.J. and Daszak, P. 2009. The ecology and impact of chytridiomycosis : an emerging disease of amphibians. *Trends Ecol. Evol.*, **25**: 109–118.

Kinney, V.C., Heemeyer, J.L., Pessier, A.P. and Lannoo, M.J. 2011. Seasonal pattern of batrachochytrium dendrobatidis infection and mortality in lithobates areolatus: Affirmation of vredenburg's "10,000 zoospore rule." *PLoS One*, **6**: 0–10.

Kopecký, O., Vojar, J. and Denoël, M. 2010. Movements of Alpine newts (Mesotriton alpestris) between small aquatic habitats (ruts) during the breeding season. *Amphib. Reptil.*, **31**: 109–116.

Korfel, C.A. and Hetherington, T.E. 2014. Temperature alone does not explain patterns of Batrachochytrium dendrobatidis infections in the green frog Lithobates clamitans. *Dis. Aquat. Organ.*, **109**: 177–185.

Kriger, Kerry M and Hero, J. 2007. The chytrid fungus Batrachochytrium dendrobatidis is non-randomly distributed across amphibian breeding habitats. *Divers. Distrib.*, **13**: 781–788.

Kriger, Kerry M. and Hero, J.M. 2007. Large-scale seasonal variation in the prevalence and severity of chytridiomycosis. *J. Zool.*, **271**: 352–359.

Kriger, K.M., Pereoglou, F. and Hero, J.M. 2007. Latitudinal variation in the prevalence and intensity of chytrid (Batrachochytrium dendrobatidis) infection in eastern Australia. *Conserv. Biol.*, **21**: 1280–1290.

Lafferty, K.D. and Shaw, J.C. 2013. Comparing mechanisms of host manipulation across host and parasite taxa. *J. Exp. Biol.*, **216**: 56–66.

Lenker, M.A., Savage, A.E., Becker, C.G., Rodriguez, D. and Zamudio, K.R. 2014. Batrachochytrium dendrobatidis infection dynamics vary seasonally in upstate New York, USA. *Dis. Aquat. Organ.*, **111**: 51–60.

Lips, K.R., Brem, F., Brenes, R., Reeve, J.D., Alford, R.A., Voyles, J., *et al.* 2006. Emerging infectious disease and the loss of biodiversity in a Neotropical amphibian community. *Proc. Natl. Acad. Sci. U. S. A.*, **103**: 3165–3170.

Lochmiller, R.L. and Deerenberg, C. 2000. Trade-Offs in Evolutionary Immunology : Just What Is the Cost of Immunity? *Oikos*, **88**: 87–98.

Longcore, J.E., Pessier, A.P., Nichols, D.K., Longcore, J.E., Pessier, A.P., Nichols, D.K., *et al.* 1999. Batrachochytrium dendrobatidis gen. et sp. nov., a chytrid pathogenic to amphibians.

Mycologia, **91**: 219–227.

Mazerolle, M.J. 2001. Amphibian Activity , Movement Patterns , and Body Size in Fragmented Peat Bogs. *J. Herpetol.*, **35**: 13–20.

McKenzie, J.M., Price, S.J., Connette, G.M., Bonner, S.J. and Lorch, J.M. 2021. Effects of snake fungal disease on short-term survival, behavior, and movement in free-ranging snakes. *Ecol. Appl.*, **31**: 1–11.

McLean, R.G., Ubico, S.R., Docherty, D.E., Hansen, W.R., Sileo, L. and McNamara, T.S. 2001. West Nile virus transmission and ecology in birds. *Ann. N. Y. Acad. Sci.*, **951**: 54–57.

Morin, P.J. 1981. Predatory salamanders reverse the outcome of competition among three species of anuran tadpoles. *Science (80-.).*, **212**: 1286–1288.

Mosher, B.A., Huyvaert, K.P. and Bailey, L.L. 2018. Beyond the swab: ecosystem sampling to understand the persistence of an amphibian pathogen. *Oecologia*, **188**: 319–330. Springer Berlin Heidelberg.

Muths, E., Bailey, L.L., Lambert, B.A. and Schneider, S.C. 2018. Estimating the probability of movement and partitioning seasonal survival in an amphibian metapopulation. *Ecosphere*, **9**: 1–15.

Nathan, R., Getz, W.M., Revilla, E., Holyoak, M., Kadmon, R., Saltz, D., *et al.* 2008. A movement ecology paradigm for unifying organismal movement research. *Proc. Natl. Acad. Sci. U. S. A.*, **105**: 19052–19059.

Ocock, J.F., Rowley, J.J.L., Penman, T.D., Rayner, T.S. and Kingsford, R.T. 2013. Amphibian chytrid prevalence in an amphibian community in arid Australia. *Ecohealth*, **10**: 77–81.

Park, A.W. 2012. Infectious disease in animal metapopulations: The importance of environmental transmission. *Ecol. Evol.*, **2**: 1398–1407.

Perrin, N. and Mazalov, V. 2000. Local competition, inbreeding, and the evolution of sex-biased dispersal. *Am. Nat.*, **155**: 116–127.

Petersen, C.E., Lovich, R.E., Phillips, C.A., Dreslik, M.J. and Lannoo, M.J. 2016. Prevalence and Seasonality of the Amphibian Chytrid Fungus Batrachochytrium dendrobatidis Along Widely Separated Longitudes Across the United States. *Ecohealth*, **13**: 368–382. Springer US.

Piotrowski, J.S., Annis, S.L. and Longcore, J.E. 2004. Physiology of Batrachochytrium dendrobatidis, a chytrid pathogen of amphibians. *Mycologia*, **96**: 9–15.

Pittman, S.E., Osbourn, M.S. and Semlitsch, R.D. 2014. Movement ecology of amphibians: A missing component for understanding population declines. *Biol. Conserv.*, **169**: 44–53. Elsevier Ltd.

Pullen, K.D., Best, A.M. and Ware, J.L. 2010. Amphibian pathogen Batrachochytrium dendrobatidis prevalence is correlated with season and not urbanization in central Virginia. *Dis. Aquat. Organ.*, **91**: 9–16.

Raffel, T.R., Michel, P.J., Sites, E.W. and Rohr, J.R. 2010. What Drives Chytrid Infections in

Newt Populations ? Associations with Substrate , Temperature , and Shade. *Ecohealth*, **7**: 526–536.

Rakus, K., Ronsmans, M. and Vanderplasschen, A. 2017. Behavioral fever in ectothermic vertebrates. *Dev. Comp. Immunol.*, **66**: 84–91. Elsevier Ltd.

Real, L.A. and Biek, R. 2007. Spatial dynamics and genetics of infectious diseases on heterogeneous landscapes. *J. R. Soc. Interface*, **4**: 935–948.

Rebollar, E.A., Woodhams, D.C., LaBumbard, B., Kielgast, J. and Harris, R.N. 2017. Prevalence and pathogen load estimates for the fungus Batrachochytrium dendrobatidis are impacted by ITS DNA copy number variation. *Dis. Aquat. Organ.*, **123**: 213–226.

Retallick, R.W.R. and Miera, V. 2007. Strain differences in the amphibian chytrid Batrachochytrium dendrobatidis and non-permanent, sub-lethal effects of infection. *Dis. Aquat. Organ.*, **75**: 201–207.

Rittenhouse, T.A.G., Semlitsch, R.D. and Thompson, F.R. 2015. Survival Costs Associated with Wood Frog Breeding Migrations : Effects of Timber Harvest and Drought Published by : Ecological Society of America Linked references are available on JSTOR for this article : You may need to log in to JSTOR to access the lin. *Ecology*, **90**: 1620–1630.

Roche, B., Dobson, A.P., Guégan, J.F. and Rohani, P. 2012. Linking community and disease ecology: The impact of biodiversity on pathogen transmission. *Philos. Trans. R. Soc. B Biol. Sci.*, **367**: 2807–2813.

Rollins-Smith, L.A. 1998. Metamorphosis and the amphibian immune system. *Immunol. Rev.*, **166**: 221–230.

Rothermel, B.B., Miller, D.L., Travis, E.R., McGuire, J.L.G., Jensen, J.B. and Yabsley, M.J. 2016. Disease dynamics of red-spotted newts and their anuran prey in a montane pond community. *Dis. Aquat. Organ.*, **118**: 113–127.

Rothermel, B.B., Walls, S.C., Mitchell, J.C., Jr, C.K.D., Irwin, L.K., Green, D.E., *et al.* 2008. Widespread occurrence of the amphibian chytrid fungus Batrachochytrium dendrobatidis in the southeastern USA. *Dis. Aquat. Organ.*, **82**: 3–18.

Ruggeri, J., De Carvalho-E-silva, S.P., James, T.Y. and Toledo, L.F. 2018. Amphibian chytrid infection is influenced by rainfall seasonality and water availability. *Dis. Aquat. Organ.*, **127**: 107–115.

Ryce, E.K.N., Zale, A. V., MacConnell, E. and Nelson, M. 2005. Effects of fish age versus size on the development of whirling disease in rainbow trout. *Dis. Aquat. Organ.*, **63**: 69–76.

Sapsford, S.J., Alford, R.A. and Schwarzkopf, L. 2013. Elevation , Temperature , and Aquatic Connectivity All Influence the Infection Dynamics of the Amphibian Chytrid Fungus in Adult Frogs. *PLoS One*, **8**: 1–13.

Sapsford, S.J., Roznik, E.A., Alford, R.A. and Schwarzkopf, L. 2014. Visible implant elastomer marking does not affect short-term movements or survival rates of the treefrog litoria rheocola. *Herpetologica*, **70**: 23–33.

Scheele, Ben C, Pasmans, F., Skerratt, L.F., Berger, L., Martel, A., Beukema, W., *et al.* 2019. Amphibian fungal panzootic causes catastrophic and ongoing loss of biodiversity. **1463**: 1459–1463.

Scheele, Ben C., Pasmans, F., Skerratt, L.F., Berger, L., Martel, A., Beukema, W., *et al.* 2019. Amphibian fungal panzootic causes catastrophic and ongoing loss of biodiversity. *Science (80-.).*, **1463**: 1459–1463.

Scholthof, K.G. 2007. The disease triangle : pathogens , the environment and society. **5**: 152–156.

Searcy, C.A., Gilbert, B., Krkošek, M., Rowe, L. and McCauley, S.J. 2018. Positive correlation between dispersal and body size in green frogs (Rana clamitans) naturally colonizing an experimental landscape. *Can. J. Zool.*, **96**: 1378–1384.

Searle, C.L., Gervasi, S.S., Hua, J., Hammond, J.I., Relyea, R.A., Olson, D.H., *et al.* 2011. Differential Host Susceptibility toBatrachochytrium dendrobatidis, an Emerging Amphibian Pathogen. *Conserv. Biol.*, **25**: 965–974.

Searle, C.L., Mendelson, J.R., Green, L.E. and Duffy, M.A. 2013. Daphnia predation on the amphibian chytrid fungus and its impacts on disease risk in tadpoles. *Ecol. Evol.*, **3**: 4129–4138.

Semlitsch, R.D. 2008. Differentiating Migration and Dispersal Processes for Pond-Breeding Amphibians. *J. Wildl. Manage.*, **72**: 260–267.

Semlitsch, R.D. 2000. Principles for Management of Aquatic-Breeding Amphibians. *J. Wildl. Manage.*, **64**: 615–631.

Shepard, E.L.C., Wilson, R.P., Rees, W.G., Grundy, E., Lambertucci, S.A. and Vosper, S.B. 2013. Energy landscapes shape animal movement ecology. *Am. Nat.*, **182**: 298–312.

Sinsch, U. 2014. Movement ecology of amphibians: From individual migratory behaviour to spatially structured populations in heterogeneous landscapes1,2. *Can. J. Zool.*, **92**: 491–502.

Skerratt, L.F., Berger, L., Speare, R., Cashins, S., McDonald, K.R., Phillott, A.D., *et al.* 2007. Spread of chytridiomycosis has caused the rapid global decline and extinction of frogs. *Ecohealth*, **4**: 125–134.

Smith, M.A. and Green, D.M. 2005. Dispersal and the metapopulation paradigm in amphibian ecology and conservation: Are all amphibian populations metapopulations? *Ecography (Cop.).*, **28**: 110–128.

Snodgrass, J.W., Komoroski, M.J., Bryan, A.L. and Burger, J. 2000. Relationships among isolated wetland size, hydroperiod, and amphibian species richness: Implications for wetland regulations. *Conserv. Biol.*, **14**: 414–419.

Sonn, J.M., Utz, R.M. and Richards-Zawacki, C.L. 2019. Effects of latitudinal, seasonal, and daily temperature variations on chytrid fungal infections in a North American frog. *Ecosphere*, **10**.

Steiner, C.F. 2004. Daphnia dominance and zooplankton community structure in fishless ponds.

J. Plankton Res., **26**: 799–810.

Stuart, S.N., Chanson, J.S., Cox, N.A., Young, B.E., Rodrigues, A.S.L., Fischman, D.L., *et al.* 2004. Status and trends of amphibian declines and extinctions worldwide. *Science (80-.).*, **306**: 1783–1786.

Tardy, O., Massé, A., Pelletier, F. and Fortin, D. 2018. Interplay between contact risk, conspecific density, and landscape connectivity: An individual-based modeling framework. *Ecol. Modell.*, **373**: 25–38. Elsevier.

Terrell, K.A., Quintero, R.P., Murray, S., Kleopfer, J.D., Murphy, J.B., Evans, M.J., *et al.* 2013. Cryptic impacts of temperature variability on amphibian immune function. *J. Exp. Biol.*, **216**: 4204–4211.

Tøttrup, A.P., Thorup, K., Rainio, K., Yosef, R. and Lehikoinen, E. 2008. Avian migrants adjust migration in response to environmental conditions en route. 685–688.

Tournier, E., Besnard, A., Tournier, V. and Cayuela, H. 2017. Manipulating waterbody hydroperiod affects movement behaviour and occupancy dynamics in an amphibian. *Freshw. Biol.*, **62**: 1768–1782.

Tracey, J.A., Bevins, S.N., Vandewoude, S. and Crooks, K.R. 2014. An agent-based movement model to assess the impact of landscape fragmentation on disease transmission. *Ecosphere*, **5**: 1–24.

Trenham, P.C., Koenig, W.D. and Shaffer, H.B. 2001. Spatially Autocorrelated Demography and Interpond Dispersal in the Salamander Ambystoma californiense. *Ecology*, **82**: 3519–3530.

van Dijk, J.G.B., Kleyheeg, E., Soons, M.B., Nolet, B.A., Fouchier, R.A.M. and Klaassen, M. 2015. Weak negative associations between avian influenza virus infection and movement behaviour in a key host species, the mallard Anas platyrhynchos. *Oikos*, **124**: 1293–1303.

Van Rooij, P., Martel, A., Haesebrouck, F. and Pasmans, F. 2015. Amphibian chytridiomycosis: A review with focus on fungus-host interactions. *Vet. Res.*, **46**: 1–22. BioMed Central.

Van Sluys, M. and Hero, J.M. 2009. How does chytrid infection vary among habitats? the case of Litoria wilcoxii (Anura, Hylidae) in SE Queensland, Australia. *Ecohealth*, **6**: 576–583.

VanderWaal, K.L. and Ezenwa, V.O. 2016. Heterogeneity in pathogen transmission: mechanisms and methodology. *Funct. Ecol.*, **30**: 1606–1622.

Vasconcelos, D. and Calhoun, A. 2004. Movement Patterns of Adult and Juvenile Rana sylvatica (LeConte) and Ambystoma maculatum (Shaw) in Three Restored Seasonal Pools in Maine. *J. Herpetol.*, **38**: 551–561.

Voyles, J., Rosenblum, E.B. and Berger, L. 2011. Interactions between Batrachochytrium dendrobatidis and its amphibian hosts : a review of pathogenesis and immunity. *Microbes Infect.*, **13**: 25–32. Elsevier Masson SAS.

Vredenburg, V.T., Knapp, R.A., Tunstall, T.S. and Briggs, C.J. 2010. Dynamics of an emerging disease drive large-scale amphibian population extinctions. *Proc. Natl. Acad. Sci. U. S. A.*, **107**: 9689–9694.

Watling, J.I. and Braga, L. 2015. Desiccation resistance explains amphibian distributions in a fragmented tropical forest landscape. *Landsc. Ecol.*, 1449–1459. Springer Netherlands.

Welicky, R.L. and Sikkel, P.C. 2015. Decreased movement related to parasite infection in a diel migratory coral reef fish. *Behav. Ecol. Sociobiol.*, **69**: 1437–1446.

Whiles, M.R., Lips, K.R., Pringle, C.M., Kilham, S.S., Bixby, R.J., Brenes, R., *et al.* 2006. The effects of amphibian population declines on the structure and function of neotropical stream ecosystems. *Front. Ecol. Environ.*, **4**: 27–34.

Worthington, H., McCrea, R., King, R. and Griffiths, R. 2019. Estimating abundance from multiple sampling capture-recapture data via a multi-state multi-period stopover model. *Ann. Appl. Stat.*, **13**: 2043–2064.

Zipkin, E.F., DiRenzo, G. V., Ray, J.M., Rossman, S. and Lips, K.R. 2020. Tropical snake diversity collapses after widespread amphibian loss. *Science (80-.).*, **367**: 814–816.

Chapter 2 Tables

Table 2.1. Summary table for adult *N. viridescens* movements in our within-year capture pair dataset and between-year capture pair dataset. Movements were defined as re-capturing a unique individual in a pond different from their pond from the previous capture. Between-year captures are described as the last capture in a previous year and the first time the same individual was caught in the current year. We only sampled from three ponds in 2018 and broadened our sampling efforts to twelve ponds the following years.

Movement-type	Year	Total	Moved	Ponds Sampled
Within-year	2018	96	7	3
	2019	186	8	12
	2020	170	10	12
	2021	112	5	12
Between-year	2018-2019	47	6	
	2019-2020	103	20	
	2020-2021	100	13	

Table 2.2. Best fit models for response variable of interest. Analyses were performed using generalized linear mixed models, and best fit models were selected based on AIC. Estimates, standard error, and confidence intervals reported are for our parameter of interest (**bolded**).

Movement Type	Response	Model	Estimate	Std. Error	95% CI
Within-year	Movement	**Start Status** + Start Julian + Start Julian² + Gap + SVL + (1|Start Site)	-0.565	0.584	[-1.711 - 0.580]
	Movement	**Start Intensity** + Start Julian + Start Julian² + Gap + SVL + (1|Start Site)	0.095	0.167	[-0.232 - 0.422]
	Ending Infection Status	**Movement** + Start Status + End Julian + End Julian² + Gap + SVL + Sex + (1|Start Site)	**-1.121***	0.542	[-2.184 - -0.058]
	Ending Infection Intensity	**Movement** + Start Intensity + Gap + (1|Start Site)	**-1.933***	0.877	[-3.652 - -0.214]
Between-year	Movement	**Start Status** + Start Julian + Sex + (1|Start Site) + (1|Individual)	-0.006	0.525	[-1.034 - 1.023]
	Movement	**Start Intensity** + Start Julian + Sex + (1|Start Site) + (1|Individual)	-0.003	0.111	[-0.220 - 0.214]
	Ending Infection Status	**Movement** + Start Status + Start Julian + Start Julian² + End Julian + End Julian² + (1|Start Site) + (1|Individual)	-0.358	0.567	[-1.470 - 0.754]
	Ending Infection Intensity	**Movement** + Start Intensity + Sex + (1|Start Site) + (1|Individual)	-0.331	0.681	[-1.666 – 1.005]

Chapter 2 Figures

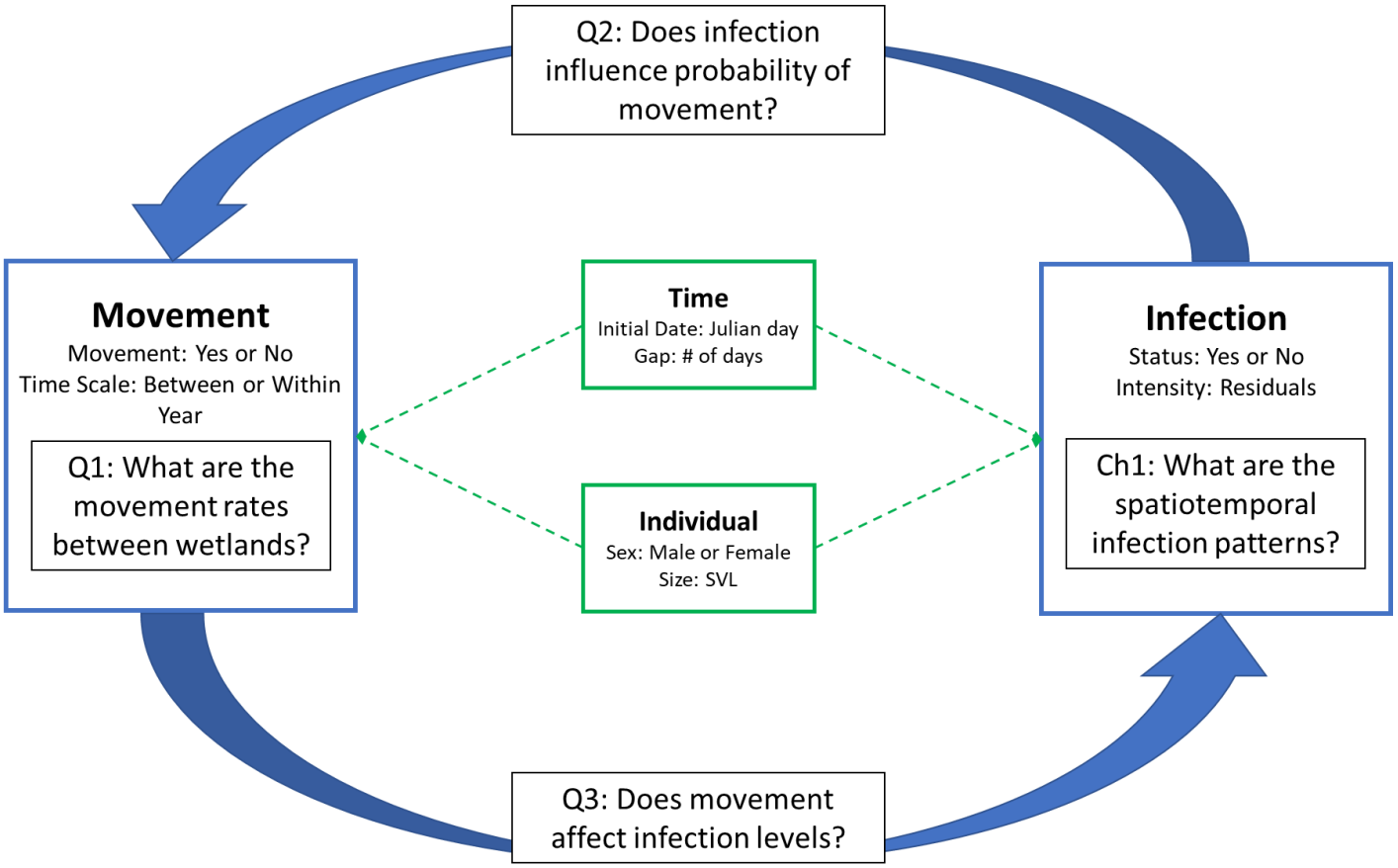

Figure 2.1. Relationship between movement and infection. Feedback loop between movement and infection where movements can result in increases or decreases in infection levels and infection can alter movement capabilities and behavior. We also consider how variation in time and individual characteristics can affect both movement and infection patterns.

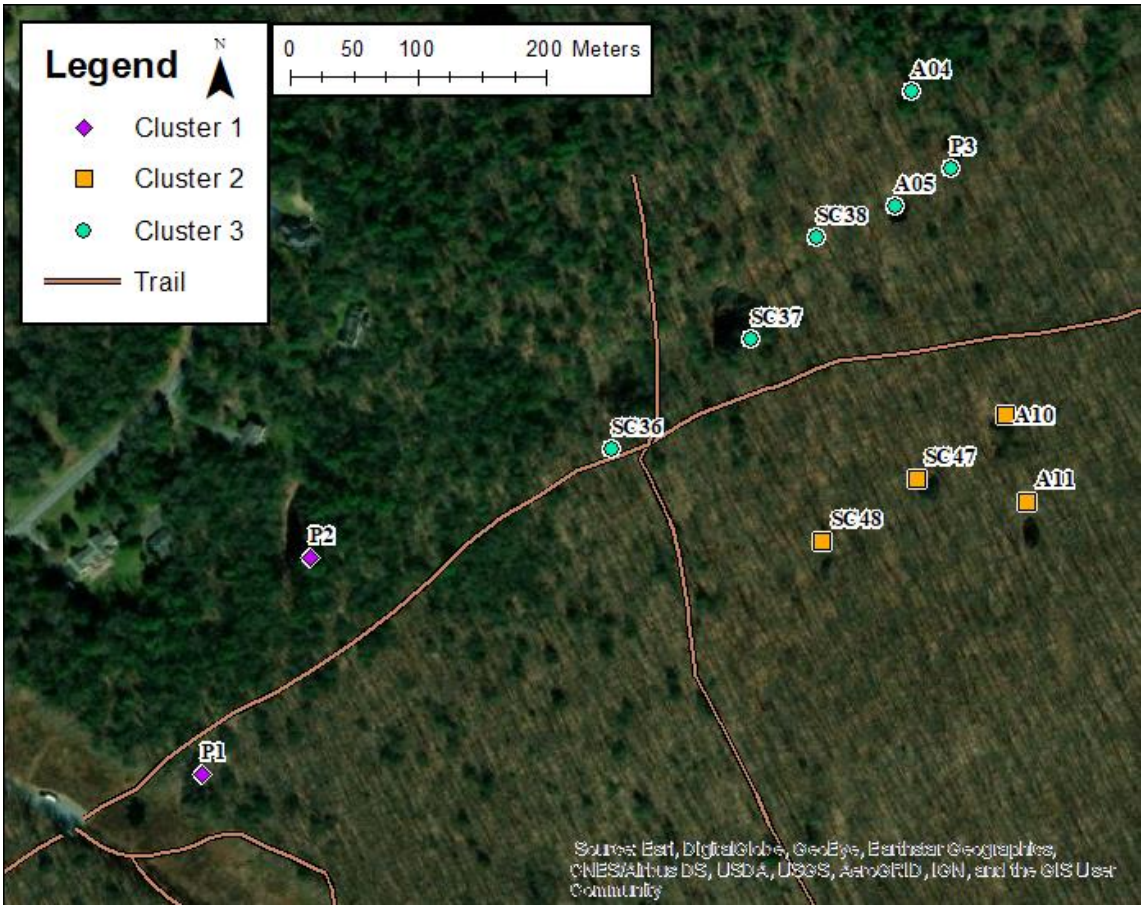

Figure 2.2. Study site map. Locations of the twelve ponds in central Pennsylvania, PA, where we conducted capture-mark-recapture surveys of *Notophthalmus viridescens* from 2018 to 2021. There are three distinct clusters of ponds with eight ephemeral ponds and four semi-permanent ponds. Other ponds within this area were either unable to be sampled or did not contain newts.

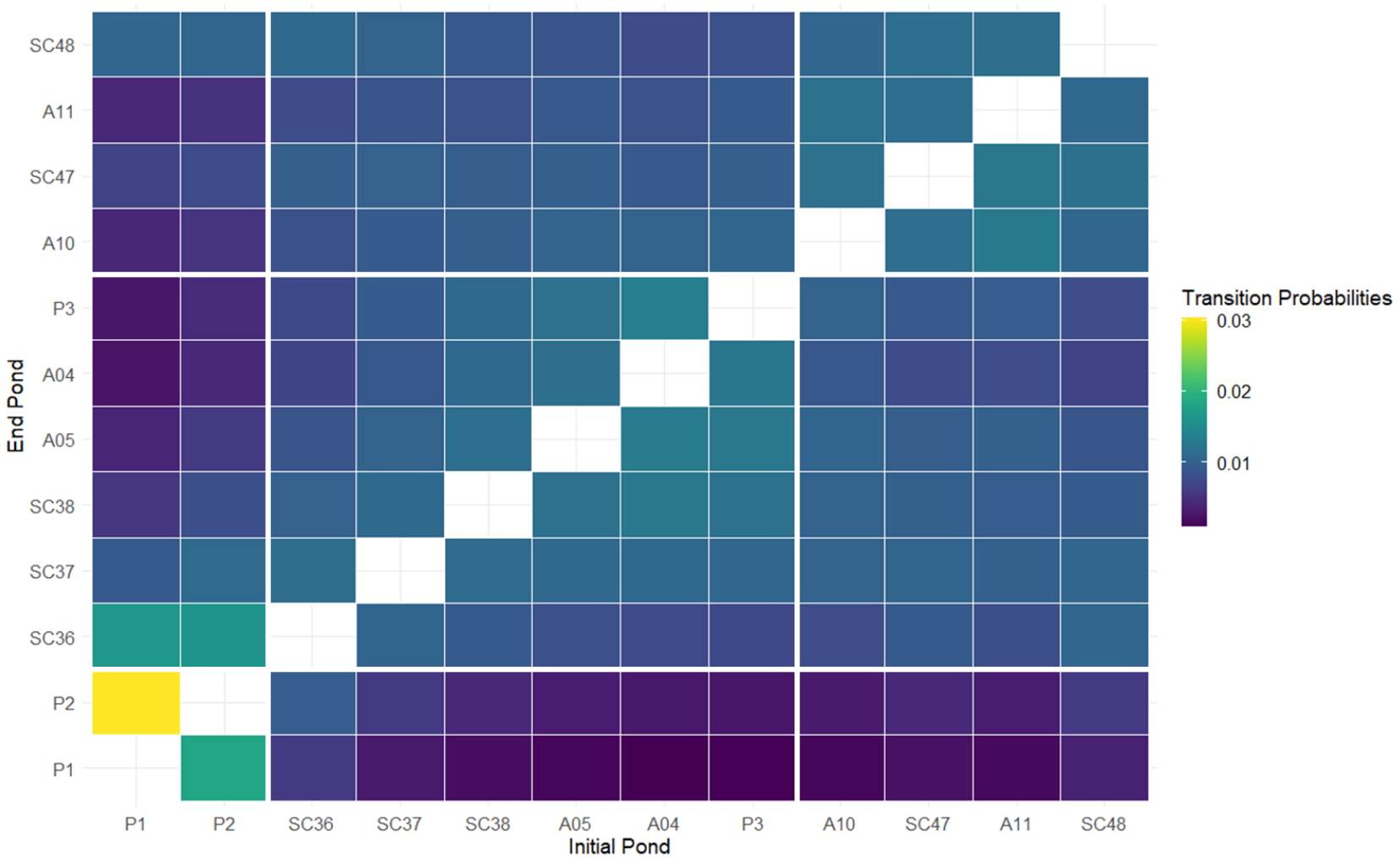

Figure 2.3. Transition probability matrix between the twelve ponds. Mean estimates for movement of individuals between the twelve ponds in central Pennsylvania. High probability movements were more likely to occur within the same cluster of ponds. Site fidelity (0.90) was held constant for all ponds.

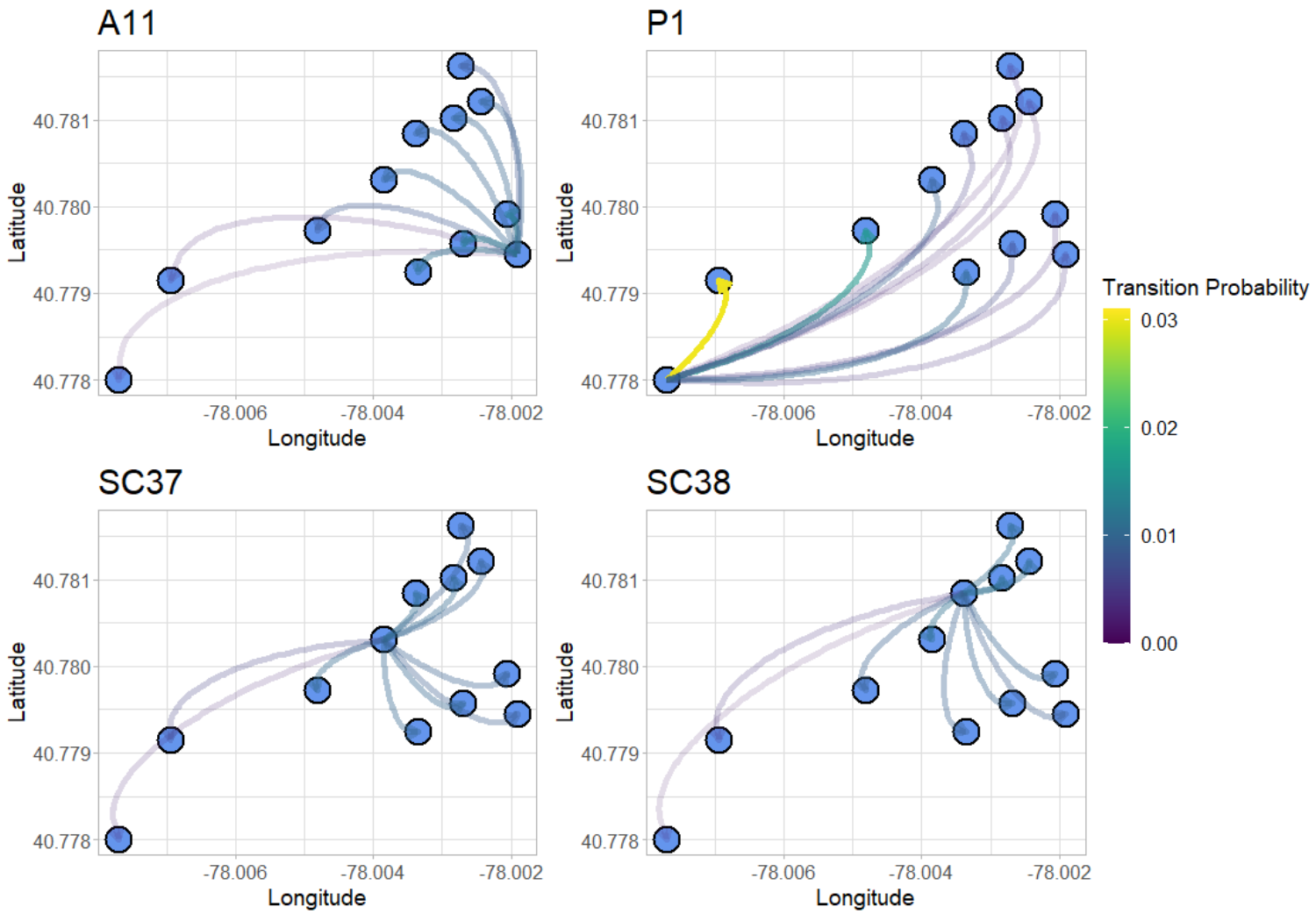

Figure 2.4. Transition probability map. Mean estimates for site fidelity and movement probabilities between the twelve ponds in central Pennsylvania with the initial ponds being the four most productive and sampled ponds.

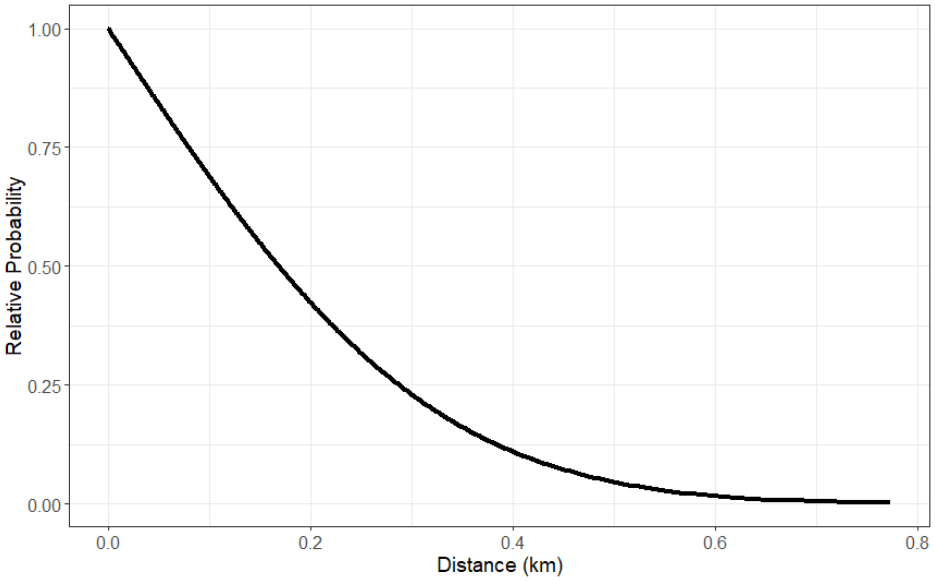

Figure 2.5. Distance kernel for movement between two ponds. Mean estimates for probability of movement between two ponds as a function of the distance between them.

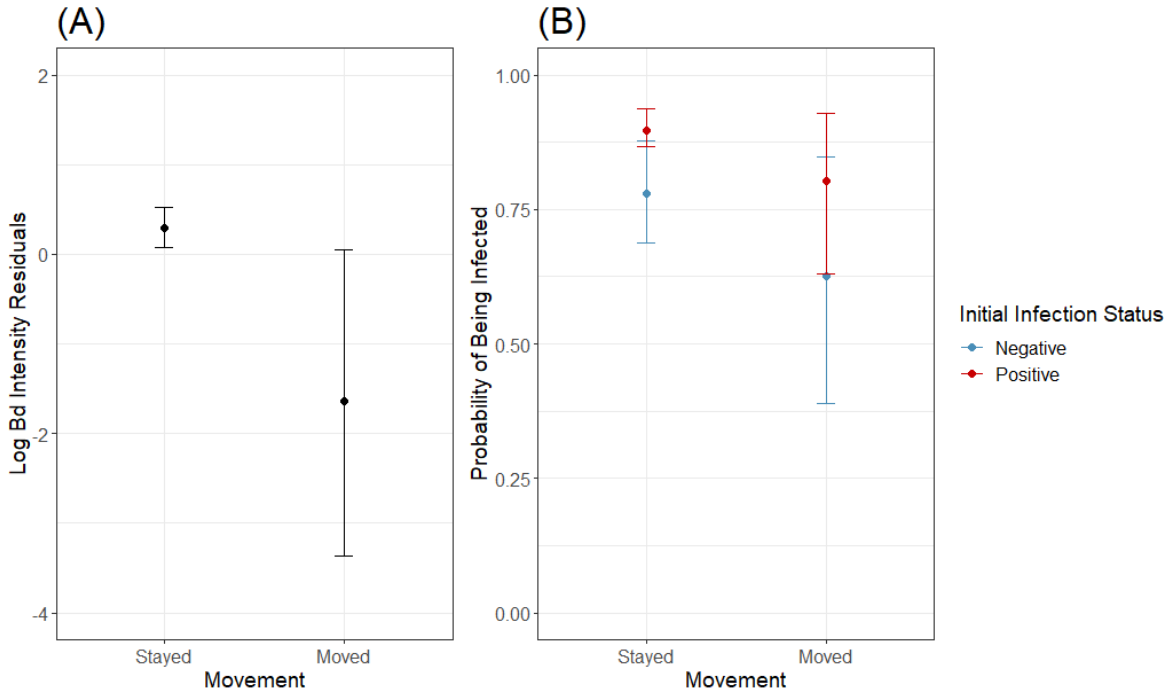

Figure 2.6. Estimated means and 95% bootstrap confidence intervals for within-year movements on (A) infection intensity and (B) infection status. (A) Infected individuals that moved ponds within a year decreased infection intensity (coef. = -1.933; CI: -3.652 – -0.214 p = 0.028). (B) Regardless of starting infection state, individuals that moved were less likely to be infected (coef. = 1.121; CI: -2.184 – -0.058; p = 0.039).

Appendix A: Chapter 2 – Model results when selecting best fit models for our generalized linear mixed model analyses

Table 2A.1. Starting infection status and within-year movement. We included pond as a random effect to account for differences between ponds. We selected the best fit model based on lowest AICc value.

Response	Model	df	Log likelihood	AICc	ΔAICc	Akaike weight
Within-year Movement	**Start Status + Start Julian + Gap + SVL**	**6**	**-80.959**	**174.1**	**0**	**0.394**
	Start Status + Start Julian + Start Julian² + Gap + SVL	7	-80.897	176.0	1.93	0.15
	Start Status + Start Julian + Gap + Sex + SVL	7	-80.938	176.1	2.01	0.144
	Start Status + Start Julian + Gap	5	-83.049	176.2	2.14	0.135
	Start Status + Start Julian + Start Julian² + Gap + Sex + SVL	8	-80.880	178.0	3.95	0.055
	Start Status + Start Julian + Start Julian² + Gap	6	-82.970	178.1	4.02	0.053
	Start Status + Start Julian + Gap + Sex	6	-83.035	178.2	4.15	0.049
	Start Status + Start Julian + Start Julian² + Gap + Sex	7	-82.952	180.1	6.04	0.019

Table 2A.2. Starting infection intensity and within-year movement. We included pond as a random effect to account for differences between ponds. We selected the best fit model based on lowest AICc value.

Response	Model	df	Log likelihood	AICc	ΔAICc	Akaike weight
Within-year Movement	**Start Residual + Start Julian + Start Julian² + Gap + SVL**	**7**	**-24.342**	**63.0**	**0**	**0.346**
	Start Residual + Start Julian + Start Julian² + Gap	6	-25.463	63.1	0.17	0.317
	Start Residual + Start Julian + Start Julian² + Gap + Sex + SVL	8	-24.315	65.0	2.03	0.125
	Start Residual + Start Julian + Start Julian² + Gap + Sex	7	-25.447	65.2	2.21	0.114
	Start Residual + Start Julian + Gap + SVL	6	-27.537	67.3	4.32	0.040
	Start Residual + Start Julian + Gap	5	-28.820	67.8	4.82	0.031
	Start Residual + Start Julian + Gap + Sex + SVL	7	-27.536	69.4	6.39	0.014
	Start Residual + Start Julian + Gap + Sex	6	-28.728	69.7	6.70	0.012

Table 2A.3. Starting infection status and between-year movement. We included pond as a random effect to account for differences between ponds and individual as a random effect to account for multiple sampling of same unique individuals. We selected the best fit model based on lowest AICc value.

Response	Model	df	Log likelihood	AICc	ΔAICc	Akaike weight
Between-year Movement	**Start Status + Start Julian + Sex**	**6**	**-88.818**	**190.0**	**0**	**0.277**
	Start Status + Start Julian	5	-90.185	190.6	0.63	0.202
	Start Status + Start Julian + Start Julian² + Sex	7	-88.398	191.3	1.28	0.147
	Start Status + Start Julian + Start Julian²	6	-89.831	192.0	2.03	0.101
	Start Status + Start Julian + Sex + SVL	7	.88.778	192.0	2.04	0.100
	Start Status + Start Julian + SVL	6	-90.098	192.5	2.56	0.077
	Start Status + Start Julian + Start Julian² + Sex + SVL	8	-88.313	193.2	3.24	0.055
	Start Status + Start Julian + Start Julian² + SVL	7	-89.680	193.8	3.84	0.041

Table 2A.4. Starting infection intensity and between-year movement. We included pond as a random effect to account for differences between ponds and individual as a random effect to account for multiple sampling of same unique individuals. We selected the best fit model based on lowest AICc value.

Response	Model	df	Log likelihood	AICc	ΔAICc	Akaike weight
Between-year Movement	**Start Residual + Start Julian + Sex**	**6**	**-69.942**	**152.3**	**0**	**0.276**
	Start Residual + Start Julian + Start Julian² + Sex	7	-69.277	153.1	0.81	0.184
	Start Residual + Start Julian	5	-71.437	153.2	0.87	0.179
	Start Residual + Start Julian + Start Julian²	6	-70.897	154.2	1.91	0.106
	Start Residual + Start Julian + Sex + SVL	7	-69.939	154.4	2.14	0.095
	Start Residual + Start Julian + Start Julian² + Sex + SVL	8	-69.277	155.3	2.98	0.062
	Start Residual + Start Julian + SVL	6	-71.436	155.3	2.99	0.062
	Start Residual + Start Julian + Start Julian² + SVL	7	-70.898	156.4	4.06	0.036

Table 2A.5. Within-year movement and ending infection status. We included pond as a random effect to account for differences between ponds. We selected the best fit model based on lowest AICc value.

Response	Model	df	Log likelihood	AICc	ΔAICc	Akaike weight
Ending infection status	**Movement + Start Status + Start Julian + Start Julian² + Gap + Sex + SVL**	**9**	**-193.513**	**405.4**	**0**	**0.504**
	Movement + Start Status + Start Julian + Start Julian² + Gap + SVL	8	-194.751	405.8	0.41	0.410
	Movement + Start Status + Start Julian + Start Julian² + Gap	7	-197.925	410.1	4.70	0.048
	Movement + Start Status + Start Julian + Start Julian² + Gap + Sex	8	-197.130	410.5	5.17	0.038
	Movement + Start Status + Start Julian + Gap + SVL	7	-233.103	480.4	75.06	0.000
	Movement + Start Status + Start Julian + Gap + Sex + SVL	8	-232.318	480.9	75.54	0.000
	Movement + Start Status + Start Julian + Gap	6	-238.105	488.4	83.01	0.000
	Movement + Start Status + Start Julian + Gap + Sex	7	-237.747	489.7	84.34	0.000

Table 2A.6. Between-year movement and ending infection status. We included pond as a random effect to account for differences between ponds and individual as a random effect to account for multiple sampling of same unique individuals. We selected the best fit model based on lowest AICc value.

Response	Model	df	Log likelihood	AICc	ΔAICc	Akaike weight
Ending infection status	**Movement + Start Status + Start Julian + Start Julian² + End Julian + End Julian²**	**9**	**-96.580**	**211.9**	**0**	**0.555**
	Movement + Start Status + Start Julian + Start Julian² + End Julian + End Julian² + SVL	10	-96.551	214.0	2.11	0.193
	Movement + Start Status + Start Julian + Start Julian² + End Julian + End Julian² + Sex	10	-96.579	214.1	2.17	0.188
	Movement + Start Status + Start Julian + Start Julian² + End Julian + End Julian² + Sex + SVL	11	-96.550	216.2	4.30	0.065
	Movement + Start Status + Start Julian + End Julian	7	-114.104	242.7	30.76	0.000
	Movement + Start Status + Start Julian + End Julian + Sex	8	-114.098	244.8	32.88	0.000
	Movement + Start Status + Start Julian + End Julian + SVL	8	-114.103	244.8	32.89	0.000
	Movement + Start Status + Start Julian + End Julian + Sex + SVL	9	-114.098	246.9	35.03	0.000

Table 2A.7. Within-year movement and ending infection intensity. We included pond as a random effect to account for differences between ponds. We selected the best fit model based on lowest AICc value.

Response	Model	df	Log likelihood	AICc	ΔAICc	Akaike weight
Ending infection intensity	**Movement + Start Intensity + Gap**	**6**	**-708.575**	**1429.4**	**0**	**0.403**
	Movement + Start Intensity + Gap + SVL	7	-707.682	1429.7	0.30	0.347
	Movement + Start Intensity + Gap + Sex + SVL	8	-707.574	1431.6	2.18	0.135
	Movement + Start Intensity + Gap + Sex	7	-708.782	1431.9	2.50	0.115

Table 2A.8. Between-year movement and ending infection intensity. We included pond as a random effect to account for differences between ponds and individual as a random effect to account for multiple sampling of same unique individuals. We selected the best fit model based on lowest AICc value.

Response	Model	df	Log likelihood	AICc	ΔAICc	Akaike weight
Ending infection intensity	**Movement + Start Intensity + Sex**	**7**	**-240.615**	**496.3**	**0**	**0.567**
	Movement + Start Intensity	6	-242.556	497.9	1.60	0.255
	Movement + Start Intensity + Sex + SVL	8	-240.979	499.4	3.05	0.123
	Movement + Start Intensity + SVL	7	-242.941	501.0	4.65	0.055

Appendix B: Chapter 2 – Additional figures from movement and infection state model results

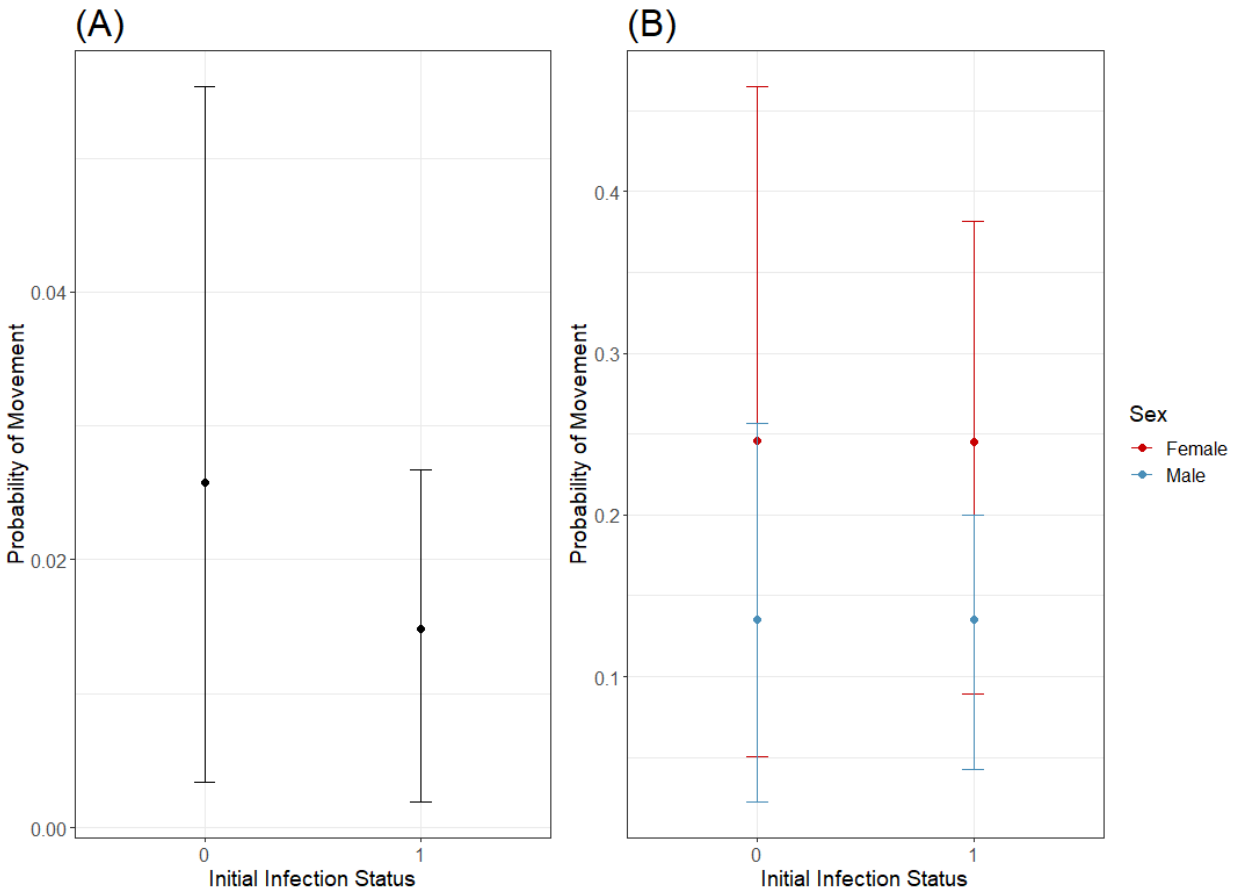

Figure 2B.1. Estimated means and 95% bootstrap confidence intervals for initial infection status on (A) within-year movements and (B) between-year movements. (A) Although non-significant, infected individuals are less likely to move. (B) Females are more likely to make between-year movements, but there is no difference between infected and non-infected individuals.

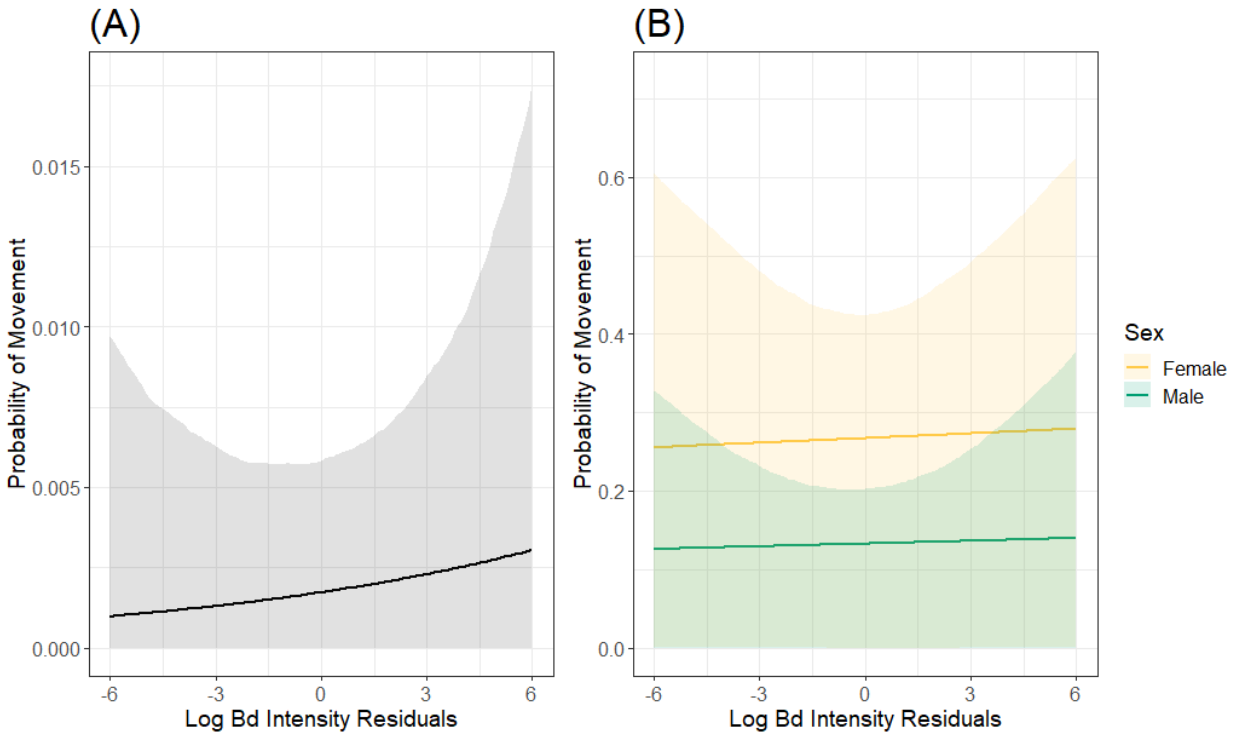

Figure 2B.2 Estimated means and 95% bootstrap confidence intervals for initial infection intensity on (A) within-year movements and (B) between-year movements. (A) Although non-significant, infected individuals with higher infection intensities are more likely to make within-year movements. (B) Infection intensity does not greatly influence between-year movements, but males are less likely to switch ponds between years.

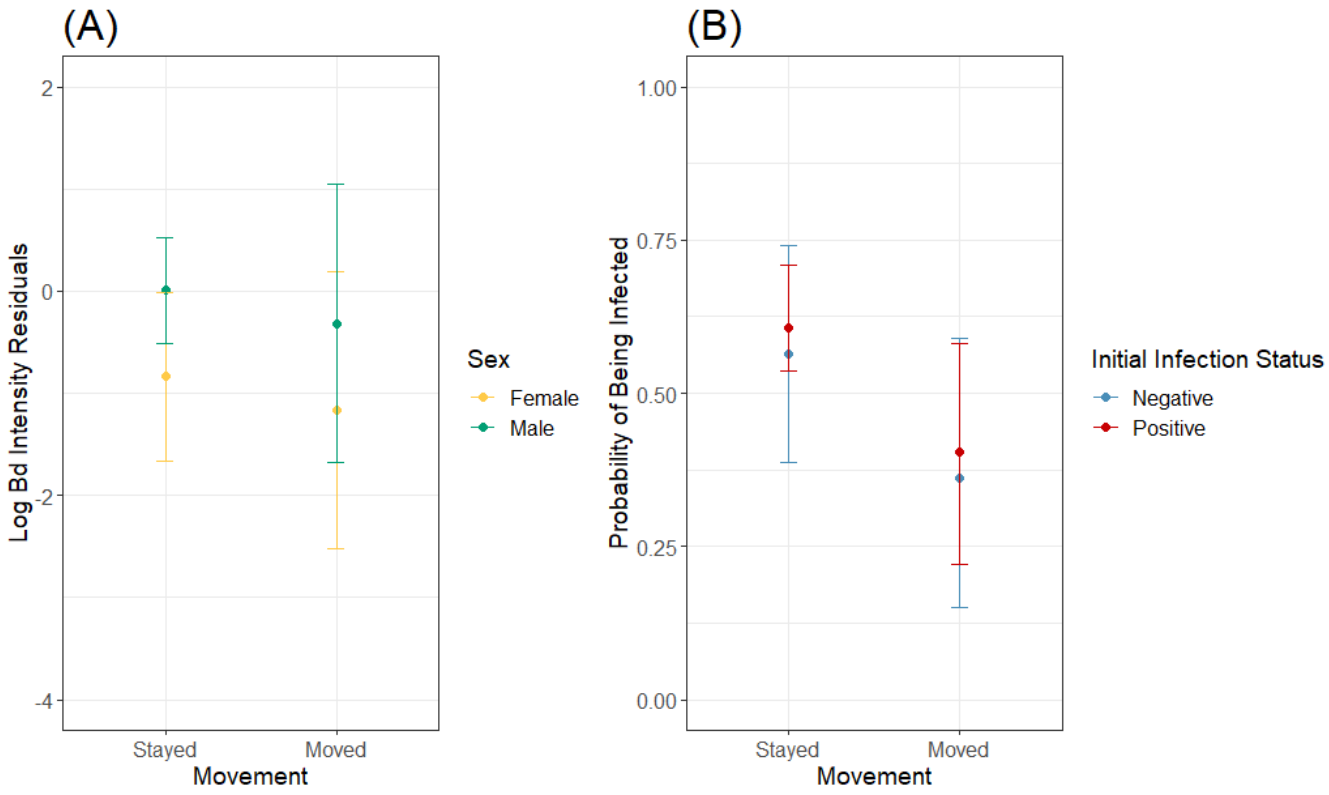

Figure 2B.3 Estimated means and 95% bootstrap confidence intervals for between-year movements on (A) infection intensity and (B) infection status. (A) Between-year movement did not have a relationship with ending infection intensity. (B) Although non-significant, mean probability of being infected was lower if an individual made between-year movements.

Appendix C: Chapter 2 – Infection status histories

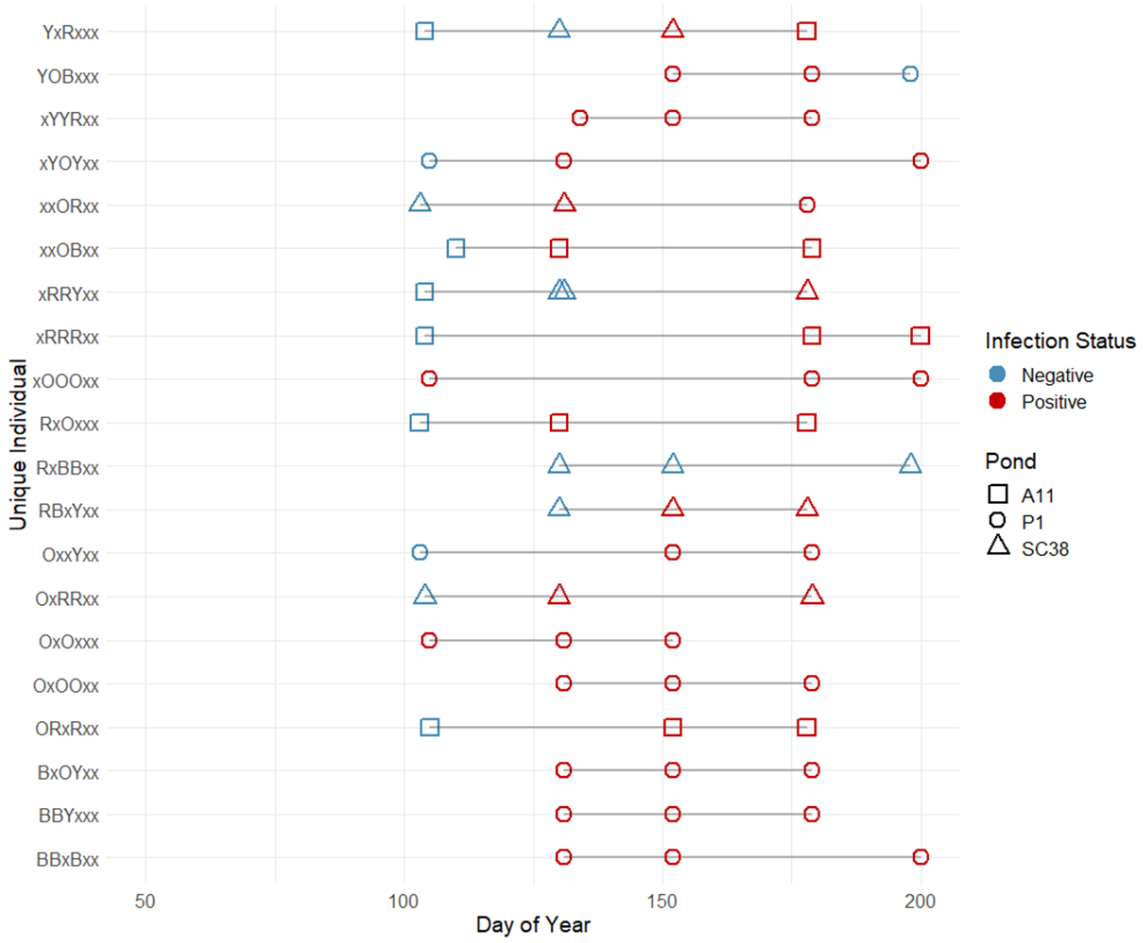

Figure 2C.1. Infection histories for unique individuals with at least three swabbed captures in 2018. We sampled three ponds up to thirteen days this season.

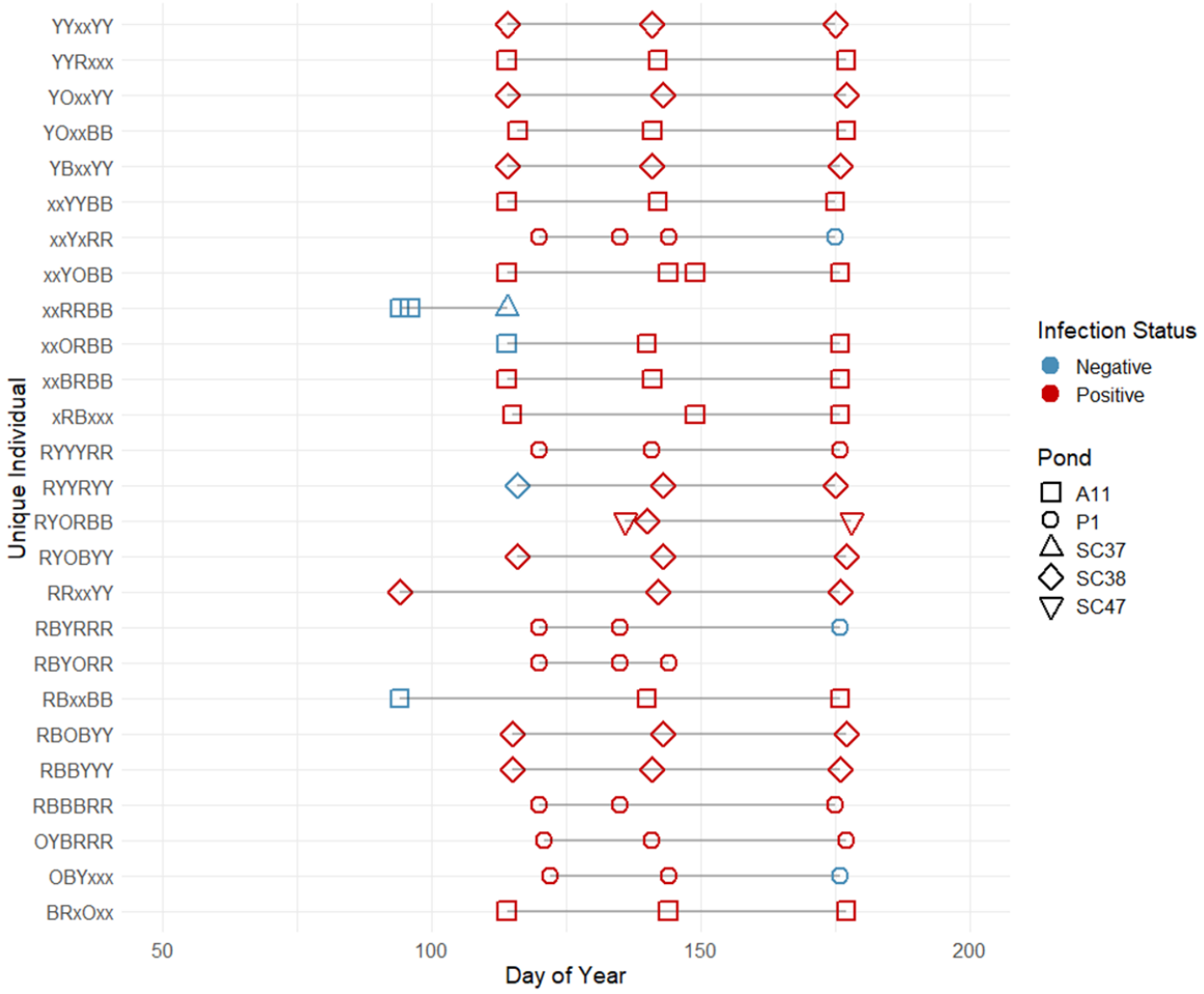

Figure 2C.2. Infection histories for unique individuals with at least three swabbed captures in 2019. We sampled all twelve ponds up to forty-nine days this season.

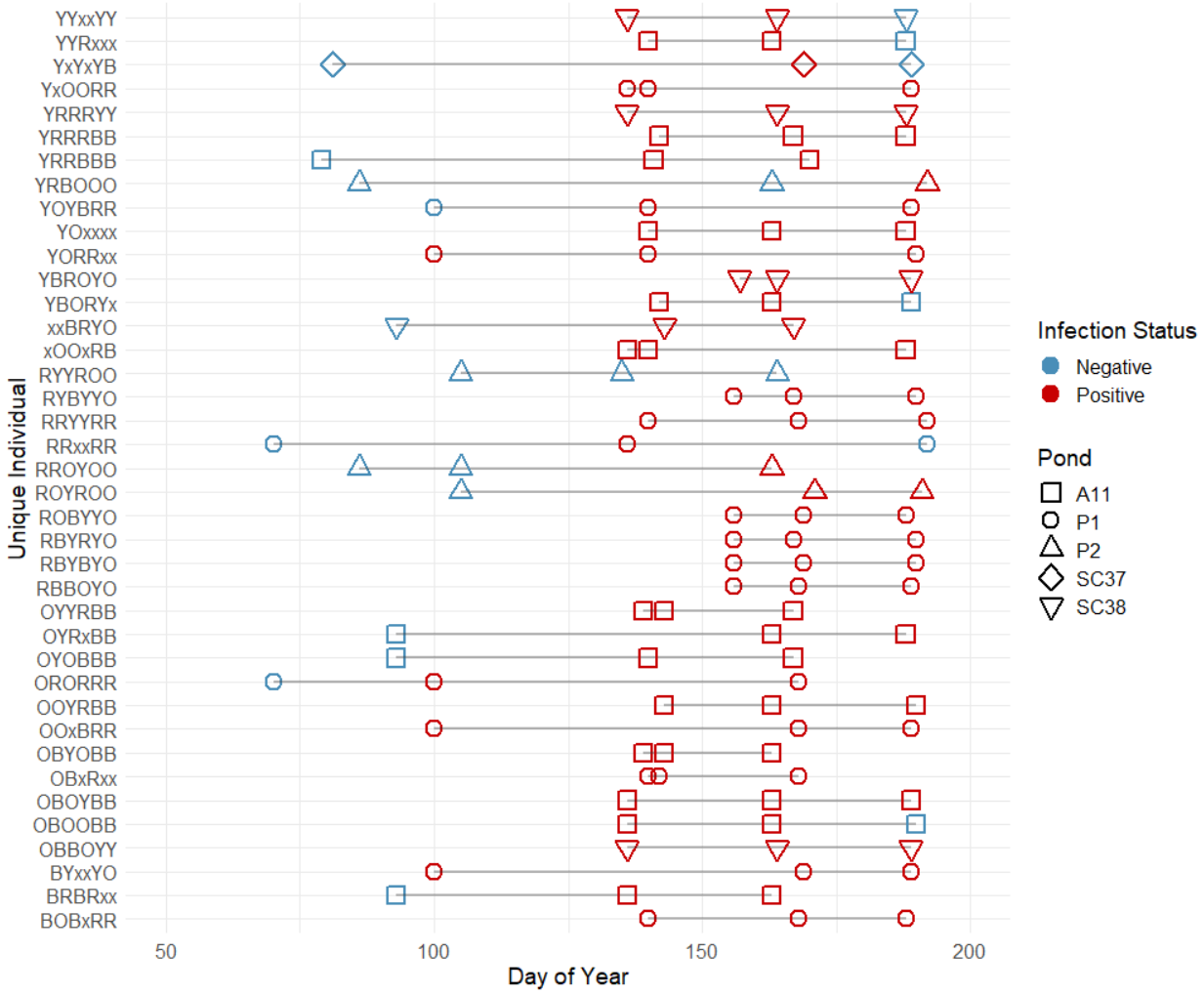

Figure 2C.3. Infection histories for unique individuals with at least three swabbed captures in 2020. We sampled all twelve ponds up to fifty-six days this season.

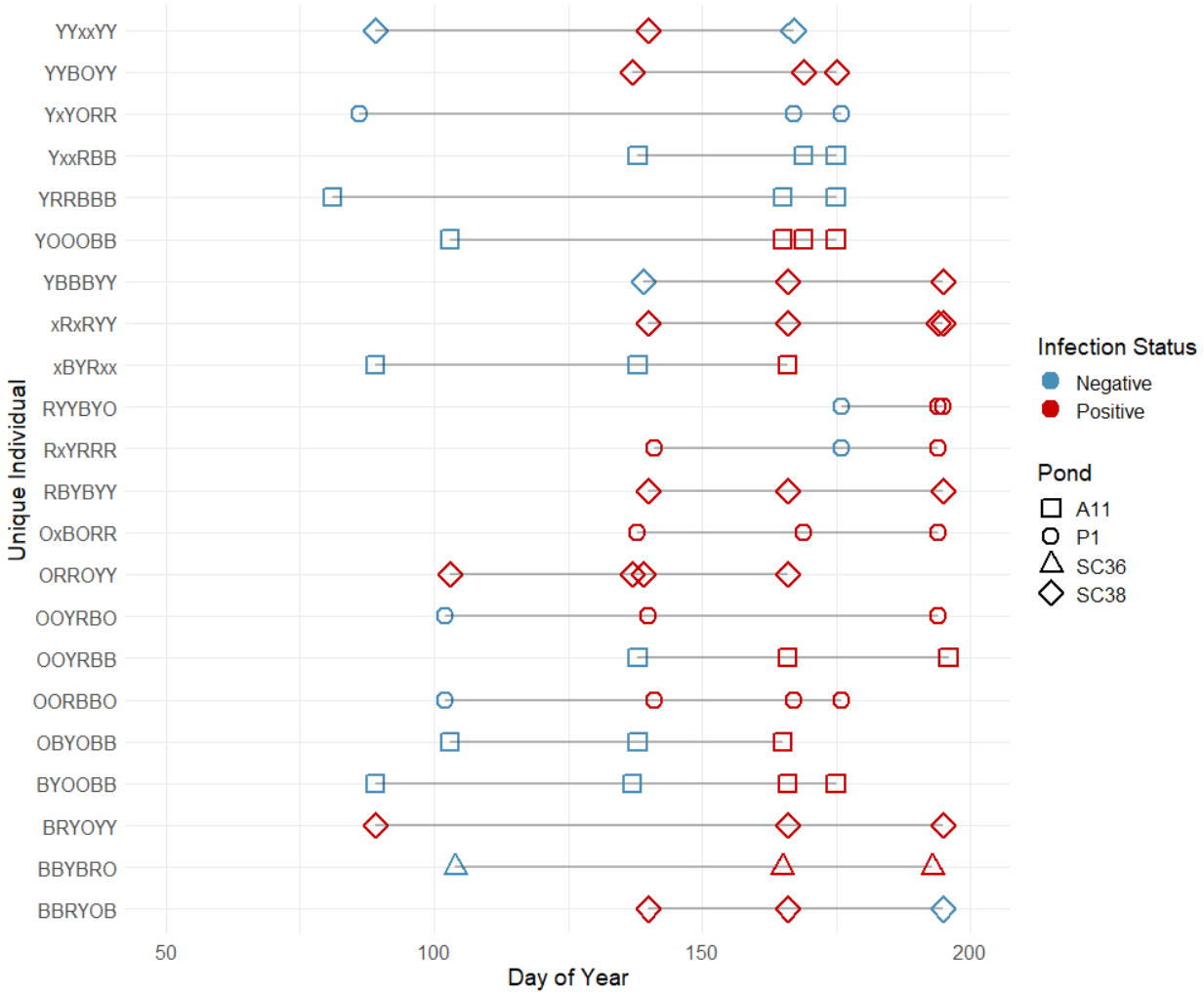

Figure 2C.4. Infection histories for unique individuals with at least three swabbed captures in 2021. We sampled all twelve ponds up to fifty-six days this season.